C 51.17/12:991/5

Tech Notes

MAY 1991

PB91-925905

PENNSYLVANIA STATE
UNIVERSITY

MAY 21 1991

DOCUMENTS-COLLECTION
U.S. Depository Copy

Technology fact sheets from Federal laboratories

NTIS

U.S. DEPARTMENT OF COMMERCE
National Technical Information Service
Center for the Utilization of Federal Technology

U.S. DEPARTMENT OF COMMERCE
Robert A. Mosbacher, Secretary of Commerce

National Technical Information Service
Joseph F. Caponio, Director

ISSN 0889-8464

COPYRIGHT WARNING
International Copyright © National Technical Information Service, 1991. All portions of this publication are protected against copying or other reproduction outside of the United States under the provisions of Article II of the Universal Copyright Convention. United States copyright is not asserted under the United States Copyright Law, Title 17, United States Code.

The Secretary of Commerce has determined that the publication of this periodical is necessary in the transaction of the public business required by law of this department. Use of funds for printing this periodical has been approved by the Director of the Office of Management and Budget through 1991.

Tech Notes

Highlighting Selected U.S. Government Technology & Resources

May 1991

Contents

Agriculture & Food 360

Computers 364

Electrotechnology 371

Energy 388

Engineering 389

Environmental Science & Technology 403

Manufacturing, Machinery & Tools 405

Materials 413

Medicine & Biology 424

Natural Resources Technology & Engineering 434

Physical Sciences 438

Transportation & Components 443

Workshop are presen36

Published monthly by the National Technical Information Service (NTIS), Tech Notes bring together individual one- to two-page fact sheets prepared by Federal agencies, their laboratories, or contractors. These fact sheets highlight current Federal technology determined to have commercial or practical application. Topics cover new processes, materials, techniques, software, instrumentation, and resources.

Some of the current sources are the Department of the Navy, Department of the Army, NASA, Department of Energy, Environmental Protection Agency, Department of the Interior, and the Department of Agriculture.

Special assistance is provided by the Federal Laboratory Consortium.

Change of address or questions concerning subscriptions should be sent to:
Subscriptions Department
National Technical Information Service
Springfield, VA 22161
(703) 487-4630

Suggestions, comments, or questions concerning Tech Notes should be directed to:
Tech Notes Editor
Room 300B F
National Technical Information Service
Springfield, VA 22161
(703) 487-4805

How to Use Tech Notes

Every Tech Notes fact sheet lists a source for additional information. The source of this information may be a special support package from the originating agency, a personal contact, a licensing opportunity, or a backup report available from NTIS.

Each fact sheet also is perforated to allow for easy removal for those subscribers who may wish to keep a special fact sheet file or route to others in their organization

Sources of Further Backup Information

Below are two representative examples of how each Tech Note fact sheet provides you with a source of further information. In most cases, this information is provided directly by the agency or its laboratory. However, there are cases where NTIS is the source for backup documentation. In these cases, use the order form at the end.

Examples:

significant distance from the endwalls. Therefore, a radial variation in efficiency should be used when designing small stators.
Project Officer Jeffrey E. Haas
(216) 433-4000.

FOR ADDITIONAL INFORMATION

You can learn more about this technology by ordering the NTIS report(s):
Cold-Air Performance of Compressor Drive Turbine
Order number: AD-A101066/NAA
Price code: A02
Order from:
National Technical Information Service
5285 Port Royal Road
Springfield, VA 22161
(703) 487-4650

158

Agency contact who can supplement the information contained in the backup report.

NTIS Order Number*

NTIS Price Code*

* See the order form and price code table at the end of the issue.

Suggested applications include other kinds of refrigerators, heat engines, thermal instrumentation, and heat switches.
This work was done by Emanuel Tward of Caltech for NASA's Jet Propulsion Laboratory.
NPO-15479/TN

FOR ADDITIONAL INFORMATION
Contact: Director, Technology Transfer Division, P.O. Box 8587, BWI Airport, MD 21240: (301) 621-0100 Ext.241.
REFER TO THE NUMBER LISTED AT THE END OF THE ARTICLE

178

Agency reference number

Source of more information about the technology described in the fact sheet

Page number

Tech Notes Title List for May 1991

Agriculture & Food

0360 Edible Fruit Coating

0361 Detecting Natural Flavors

0362 Production of Fructose

0363 Ultrasound Processing of Soybean Oil

Other Items of Interest

0437 Microcomputer Weather Model

Computers

0364 Simple Method to Interface Database Developed

0365 Use of IRDS Standard in CALS Publication Issued

Software

0366 Estimating the Cost of Developing Software—The SOFTCOST program combines diverse mathematical models that represent aspects of the development task.

0367 General-Purpose Ada Software Packages—A collection of subprograms brings to Ada many features from other programming languages.

0368 Programs for Modeling Fault-Tolerant Computing Systems—One program uses a Pade approximation; the other uses a Taylor-series solution technique.

0369 S-Chart - Scheduling-Chart Program—An easy-to-use program turns out time-line graphics of high quality.

0370 YAMM - Yet Another Menu Manager—Alimentary connotations notwithstanding, this is about software for the management of software.

Electrotechnology

0371 CMOS Analog Four-Quadrant Multiplier Invented

0372 Electronic Noise-Reducing System (Licensing Opportunity)

0373 New EMPF Electronics Manufacturing Learning Center

0374 Improving Contracts to High-T(c) Superconductors

0375 Test Chamber Performance Enhanced

0376 Time and Frequency User's Manual Updated

0377 Real-Time, Ultra-High-Resolution Image Projection Display Using Laser-Addressed Liquid-Crystal Light Valve

0378 Heterojunction-Internal-Photoemission Infrared Detectors—A new type of photodetector would add options for the design of imaging devices. (Licensing Opportunity)

0379 Meissner-Effect Stepping Motor—Weight, cost, and maintenance would be reduced.

0380 Long-Lifetime Laser Materials for Effective Diode Pumping—Long quantum lifetimes reduce the number of diodes required to pump. (Licensing Opportunity)

0381 Multistage Estimation of Frequency and Phase—Each stage would refine the estimate further. (Licensing Opportunity)

Testing & Instrumentation

0382 Multiple-Quantum-Well Intersubband Infrared Detector—Bandwidth and detectivity would be increased. (Licensing Opportunity)

0383 Self-Oscillating Inductive Boost Regulator—Features include optical coupling and rapid response.

0384 Simultaneous Detection and Estimation Amid Strong Dynamical Effects—The effective signal-to-noise ratio is several decibels greater than in previous schemes. (Licensing Opportunity)

0385 Status of Imaging Radar Polarimetry—Topics include theory, equipment, and experimental data.

0386 Method of Measuring Magnetic Effects Due to Eddy Currents (Licensing Opportunity)

Energy

0388 Reinforced Positive Filler Paste for Lead/Acid Batteries—Lead-coated glass fibers would extend the battery life. (Licensing Opportunity)

Engineering

0389 Robots Readied for Mapping, Removing Radioactive Wastes

0390 During a Fire, Brightness is Best for Exit Signs

0391 Design and Testing of a Balanced Air Regulator for Deep-Sea and Scuba Divers

0392 Evaporation Duct Height Calculations

0393 Naval Systems and Sciences Laboratory

0394 Test Bed for Telerobots—A versatile system keeps up with new technology.

0395 Splicing Wires Permanently With Explosives—The technique produces superior, reliable splices. (Licensing Opportunity)

0396 Making Large Suction Panels for Laminar-Flow Control—Perforated titanium panels are used to identify and resolve issues related to manufacture.

Software

0397 Program Analyzes Errors in STAGS—This program assists in scrutiny of the output of the STAGS finite-element program for plates.

0398 Program Generates Images of Solid Surfaces—Various shapes can be constructed and viewed from several perspectives.

Engineering (Cont.)

Testing & Instrumentation

0399 Optimum Flow Noise Cancelling Hydrophone Module (Licensing Opportunity)

0400 Nondestructive Testing of Concrete with Ultrasonic Pulse-Echo

0401 Apparatus for Tests of Percussion Primers—Tests are conducted under realistic conditions. (Licensing Opportunity)

0402 Electro-optical Position-Measuring System—A nonintrusive system determines positions of models within the test section of a wind tunnel.

Other Items of Interest

0403 Design, Construction, and Evaluation of Clay Liners for Waste Management Facilities

0407 Eliminating Unbonded Edges in Explosive Bonding—A notch in the flyer plate eases removal of unbonded material. (Licensing Opportunity)

0410 Improved Computation of Dynamic Stresses—The cost of computation is reduced.

0411 Model of Bearing With Hydrostatic Damper—The model accurately represents the nonlinear aspects of the dynamics.

0414 Navy Studies Feasibility of BZS for Marine Timber Preservation

0443 Predictions of Drag in Viscous Transonic Flow—Results from the Viscous Transonic Airfoil Workshop are presented.

Environmental Science & Technology

0403 Design, Construction, and Evaluation of Clay Liners for Waste Management Facilities

0404 Treating Wastewater With Immobilized Enzymes—Urea and other contaminants are removed. (Licensing Opportunity)

Manufacturing, Machinery & Tools

0405 The One Part - One Part Number - One Drawing Standardization System

0406 Superplastic Forming/Diffusion Bonding For Low-Cost Advanced Titanium Missile Inlets

0407 Eliminating Unbonded Edges in Explosive Bonding—A notch in the flyer plate eases removal of unbonded material. (Licensing Opportunity)

0408 Electrical-Discharge Machining With Additional Axis—Benefits include enhanced flexibility of operation and reduced cost of machining.

0409 Fast, Nonspattering Inert-Gas Welding—A conceptual technique would combine the best features of three previous arc-welding methods. (Licensing Opportunity)

0410 Improved Computation of Dynamic Stresses—The cost of computation is reduced.

0411 Model of Bearing With Hydrostatic Damper—The model accurately represents the nonlinear aspects of the dynamics.

0412 Plasma Spraying Reclaims Compressor Housings—Metal coats are deposited on worn and pitted areas.

Other Items of Interest

0373 New EMPF Electronics Manufacturing Learning Center

0423 Preventing Vapor Deposition of the Backs of Substrates—This technique has been applied in the selective deposition of silicon on silicon carbide. (Licensing Opportunity)

Materials

0413 Model of Fiber Use Developed

0414 Navy Studies Feasibility of BZS for Marine Timber Preservation

0415 Space-Grown Protein Crystals Examined

0416 Materials for Magnetic Fusion Energy

0417 New Superconductor Polymer Composites Developed

0418 Lightweight Substrates for Mirrors—Layered structures would be made of carbon/carbon material.

0419 Polyphenylquinoxalines via Aromatic Nucleophilic Displacement—A new reaction sequence costs less and provides for a variety of molecular structures. (Licensing Opportunity)

0420 Radiographic Detection of Voids in SIC and SIN Ceramics—Projection radiography provides greater sensitivity of detection.

Testing & Instrumentation

0421 New Technique Measures Fiber Matrix in Composites (Licensing Opportunity)

0422 Measuring Adhesion and Friction Forces—The Cavendish balance is adapted to a new purpose.

0423 Preventing Vapor Deposition of the Backs of Substrates—This technique has been applied in the selective deposition of silicon on silicon carbide. (Licensing Opportunity)

Other Items of Interest

0374 Improving Contracts to High-T(c) Superconductors

0380 Long-Lifetime Laser Materials for Effective Diode Pumping—Long quantum lifetimes reduce the number of diodes required to pump. (Licensing Opportunity)

0400 Nondestructive Testing of Concrete with Ultrasonic Pulse-Echo

0406 Superplastic Forming/Diffusion Bonding For Low-Cost Advanced Titanium Missile Inlets

Medicine & Biology

0424 Anesthetic Compound

0425 Defining Human Factors

0426 Ergonomics Databases

0427 Statistical Methods for Estimating Risk for Exposure Above the Reference Dose

0428 California DNA Crime Laboratory Opens

0429 Scheiner-Principle Pocket Optometer for Self Evaluation and Biofeedback Accommodation Training

0430 Scanning Tunneling Microscopy

Software

0431 Subjective Workload Assessment Technique

0432 Membrane Bioreactor With Pressure Cycle—Inhibitory reaction products and gradients of concentration are removed. (Licensing Opportunity)

0433 Rotationally Actuated Prosthetic Hand—A simple mechanism is powered by rotation of the forearm. (Licensing Opportunity)

Other Items of Interest

0434 Prosthetic Hand Lifts Heavy Loads—Features include ruggedness, simplicity, and relatively low cost. (Licensing Opportunity)

Natural Resources Technology & Engineering

0434 Prosthetic Hand Lifts Heavy Loads—Features include ruggedness, simplicity, and relatively low cost. (Licensing Opportunity)

0435 Estimating the SNR of AVIRIS Data—Improved estimates of noise are better suited to the needs of investigators.

0436 Measuring Wildfires From Aircraft and Satellites—Remote sensing systems yield a wealth of data.

Software

0437 Microcomputer Weather Model

Physical Sciences

0438 Recovery of Carboxylic Acids from Solvents (Licensing Opportunity)

0439 Adhesion Between Particles and Surfaces in a Vacuum—Factors that could affect contamination are studied.

0440 Monolithic Unidirectional Nonplanar Ring Laser—A design concept provides for narrow-linewidth operation in relatively inexpensive Nd:glass. (Licensing Opportunity)

0441 Real-Gas Properties of Air and Air-Plus-Hydrogen Mixtures—Properties related to chemical reactivity are calculated from first principles.

Testing & Instrumentation

0442 Wavefront Dividing Infrared Interferometer

Other Items of Interest

0415 Space-Grown Protein Crystals Examined

0419 Polyphenylquinoxalines via Aromatic Nucleophilic Displacement—A new reaction sequence costs less and provides for a variety of molecular structures. (Licensing Opportunity)

0422 Measuring Adhesion and Friction Forces—The Cavendish balance is adapted to a new purpose.

Transportation & Components

0443 Predictions of Drag in Viscous Transonic Flow—Results from the Viscous Transonic Airfoil Workshop are presented.

Agriculture & Food

0360 Edible Fruit Coating

0361 Detecting Natural Flavors

0362 Production of Fructose

0363 Ultrasound Processing of Soybean Oil

Other Items of Interest

0437 Microcomputer Weather Model

Edible Fruit Coating

An edible, inexpensive coating that can be easily applied to fresh fruit and vegetables retards ripening without reducing quality. ARS scientists added an emulsifier to a commercially available, vegetable-oil-based coating. As a result of the emulsifier, which disperses fat globules in water, the new coating increased shelf life of tomatoes, Florida-grown carambola and oranges. Scientists have successfully treated other fruits and vegetables. The coating allows produce to be stored at 70 degrees F, room temperature. Juice from coated oranges, stored for 8 to 10 days, contained up to 14 times more of the usual flavor volatiles. Patent application will be filed. (PATENT)

Citrus and Subtropical Products Research Lab,
Winter Haven, FL
Myrna O. Nisperos-Carriedo, (813) 293-4133

Detecting Natural Flavors

Detecting phony flavors, priced and sold as all-natural products, could be easier now. A new technique easily separates key flavor compounds of apples, pineapples and strawberries into two distinctive forms—one natural and the other a tip-off to synthetic flavorings. Similar analyses might be done by food manufacturers on dozens of fruits that contain the two flavor forms, called enantiomers. Samples are injected into a special column, lined with molecules called beta-cyclodextrin, that is used in a capillary gas chromatograph. Because enantiomers can differ drastically in aroma, potency and other characteristics, the technique could also be used to ensure products such as perfumes, medicines and lures for insect control contain the desired enantiomer.

Food Quality Research,
Western Regional Research Center, Albany, CA
Gary R. Takeoka, (415) 559-5668

Idaho National Engineering Laboratory

Production of Fructose

Fructose is a natural sweetener that is sweeter than the sugar (sucrose) produced from sugar beets and sugar cane. A new method to produce fructose has been developed jointly at the INEL and the University of Idaho. This method produces fructose using enzymatic procedures with beet sugar as the raw material; cane sugar may also be used. The process could have significant cost advantages over competitor processes. For instance, crystalline fructose is currently expensive to produce (approximately $1.00/lb). The INEL method could greatly reduce processing costs for production of pure fructose and provide an effective method to make fructose from beet sugar.

In this invention, raw beet sugar is taken from the press. Beet sugar molasses can also be used as the source of sucrose. The beet juice, with pulp removed, may be inoculated directly with a microorganism known to produce levan, a fructose polymer, from sucrose. Additional nutrients such as a nitrogen source, cofactors, or minerals may be added, if necessary. The levan solution is concentrated using ultrafiltration. After further purification, the levan is hydrolyzed using the enzyme levan hydrolase or dilute acid. The fructose formed is concentrated using reverse osmosis, evaporation, or chromatographic techniques in accordance with process economics. In this manner, a solution of pure fructose is obtained. The fructose can then be crystallized to produce pure crystalline fructose.

A patent entitled "Production of Substantially Pure Fructose" has been issued on the INEL process. For more information, contact Joanne Kapp at (208) 526-2892.

Ultrasound Processing of Soybean Oil

"Tuning up" crude soybean oil with sound waves can produce a better salad dressing. The new oil processing method uses ultrasound—very high frequency sound waves—to get rid of gummy impurities. It could replace today's more complicated and costly processing. With the new technique, soybean "crude" is sound-vibrated at 20,000 times per second in a mix of water and citric acid. With all the shaking going on, tiny bubbles continuously form and pop, creating mini-sites of extreme heat where flavor-damaging gum compounds cluster. The gums—fatty acids and phospholipids—are easily spun away with a centrifuge. What's left is a partially processed oil for further refining into a flavorful soy oil. Taste panelists couldn't distinguish the refined oil from the conventionally processed kind.

Food Quality and Safety,
Northern Regional Research Center, Peoria, IL
Timothy L. Mounts, (309) 685-4011, Ext. 555

Computers

0364 Simple Method to Interface Database Developed

0365 Use of IRDS Standard in CALS Publication Issued

Software

0366 Estimating the Cost of Developing Software—The SOFTCOST program combines diverse mathematical models that represent aspects of the development task.

0367 General-Purpose Ada Software Packages—A collection of subprograms brings to Ada many features from other programming languages.

0368 Programs for Modeling Fault-Tolerant Computing Systems—One program uses a Pade approximation; the other uses a Taylor-series solution technique.

0369 S-Chart - Scheduling-Chart Program—An easy-to-use program turns out time-line graphics of high quality.

0370 YAMM - Yet Another Menu Manager—Alimentary connotations notwithstanding, this is about software for the management of software.

Simple Method to Interface Database Developed

A human computer interface to a database has been developed that can accept typed English sentence questions from a human user and translate them into Structured Query Language (SQL) format database requests. To perform tests and evaluation of the Natural Language (NL) interface and to provide a complete usable product, a database and software to interface the database with the NL program was needed.

The Naval Ocean Systems Center (NOSC), San Diego, California, has documented computer software, which interfaces a database management system (DBMS) to a program that generates database requests. The software described controls the passing of (SQL) commands into ORACLE and the capture of its output for return to the program that made the request. The software was designed for a DBMS running on a UNIX computer to be accessed by a program on the same or a remote computer. This remote computer can be running any hardware or operating system that has File Transfer Protocol (FTP) connection with the UNIX machine.

The software approach presented provides a simple, robust way to interface a database to another computer program. It is an excellent approach for a development environment where transaction records are needed and several second delays in data exchange are acceptable. The simplicity of the code accommodates maintenance and flexibility to work with different application programs and database managers. Also, it achieves robustness via simplicity, which makes it a candidate software for a deliverable system, again where a several second delay is acceptable.

For Additional Information:

Backup material on this effort is available from:

Navy Domestic Technology Fact Sheet Reader Reply Service
Code E211
Naval Surface Weapons Center
Dahlgren, VA 22448-5000
(703) 663-8921

Refer to 150603/TN

NIST Technology Update
National Institute of Standards & Technology
U.S. Department of Commerce, Gaithersburg, MD 20899

Use of IRDS Standard in CALS Publication Issued

Use of the IRDS Standard in CALS (NISTIR 89-4169), a paper authored by David K. Jefferson and Cita M. Furlani, shows how the Information Resource Dictionary System (IRDS) can fulfill critical design and operational requirements for CALS (Computer-aided Acquisition and Logistic Support program of the Department of Defense) Phase II. The authors provide examples as well as a schedule to illustrate that the IRDS and other data management standards will be available when needed to meet the immediate requirements of CALS. An architecture is presented to show additional standards required to achieve longer-range goals of distributed database, and development tasks are recommended.

FOR ADDITIONAL INFORMATION: Available from the National Technical Information Service, Springfield, Va. 22161. Order by PB#90-130295 for $23 prepaid.

Estimating the Cost of Developing Software

The SOFTCOST program combines diverse mathematical models that represent aspects of the development task.

The early estimation of required resources and of a schedule for the development and maintenance of software is usually the least precise aspect of the life cycle of software. However, it is desirable to make some sort of an orderly and rational attempt at estimation in order to plan and organize an implementation effort. The Software Cost Estimation Model program, SOFTCOST, was developed to provide a consistent automated resource-and-schedule mathematical model that is more formalized than the often-used guesswork model based on experience, intuition, and luck.

SOFTCOST was developed after the evaluation of a number of existing cost-estimation programs indicated that there was a need for a cost-estimation program that has a wide range of applicability and adaptability to diverse kinds of software. SOFTCOST combines several software-cost models found in the open literature into one comprehensive set of algorithms that compensate for nearly 50 implementation factors relative to size of the task, inherited baseline, organizational and system environment, and difficulty of the task.

SOFTCOST produces mean and variance estimates of software size, implementation productivity, recommended staff level, probable duration, amount of computer resources required, and amount and cost of software documentation. Since the confidence level for a project using mean estimates is small, the user is given the opportunity to enter risk-biased values for effort, duration, and staffing, to achieve higher confidence levels. SOFTCOST then produces a program evaluation and review technique/critical path method (PERT/CPM) file with subtask efforts, durations, and precedences defined so as to produce the work-breakdown structure (WBS) and schedule that are characterized by the requested overall effort and duration.

The SOFTCOST program operates in an interactive environment, prompting the user for all of the required input. The program builds the supporting PERT data base in a file for later generation or revision of reports. The PERT schedule and the WBS schedule can be printed and stored in a file for later use.

The SOFTCOST program is written in Microsoft BASIC for interactive execution and has been implemented on an IBM PC-XT/AT computer operating under MS-DOS 2.1 or higher with 256K bytes of memory. SOFTCOST was originally developed for the Zylog Z80 system running under CP/M in 1981. It was converted to run on the IBM PC-XT/AT in 1986.

This program was written by Robert C. Tausworthe of **NASA's Jet Propulsion Laboratory.** *NPO-17936/TN*

FOR ADDITIONAL INFORMATION

CONTACT

COSMIC®
112 Barrow Hall
University of Georgia
Athens, GA 30602

(404) 542-3265

General-Purpose Ada Software Packages

A collection of subprograms brings to Ada many features from other programming languages.

The General-Purpose Ada Packages computer program contains 10 families of subprograms. The families bring to Ada many features from HAL/S, PL/I, FORTRAN, and other languages. These families are as follows: string subprograms (INDEX, TRIM, LOAD, etc.); scalar subprograms (MAX, MIN, REM, etc.); array subprograms (MAX, MIN, PROD, SUM, GET, and PUT); numerical subprograms (EXP, CUBIC, etc.); service subprograms (DATE_TIME function, etc.); linear-algebra subprograms; Runge–Kutta integrators; and three text input/output families of software packages.

In two cases, a family consists of a single nongeneric package. In all other cases, a family comprises a generic package and its instances for a selected group of scalar types. All generic packages are designed to be easily instantiated for the types declared in the user's facility. Most packages have widespread applicability, although some are oriented for avionics applications. All are designed to facilitate writing new software in Ada.

Several of the packages use conventions introduced by other programming languages. A package of string subprograms is based on HAL/S (a language designed for the avionics software in the Space Shuttle) and PL/I. Packages of scalar and array subprograms are taken from HAL/S or generalized current Ada subprograms. A package of Runge–Kutta integrators is patterned after a built-in MAC (MIT Algebraic Compiler) integrator. Those packages modeled after HAL/S make it easy to translate existing HAL/S software to Ada.

The source code is available as ASCII text files on two 360K, 5.25-in. (13.3-cm) floppy disks written on an IBM/AT personal computer running under PC DOS, v. 3.1. The size of the largest file is 44,032 bytes. The software was developed by use of VAX Ada, v. 1.5 under DEC VMS, v. 4.5. It should be portable to any validated Ada compiler, and it should be executable either interactively or in batch. The software was developed in 1989.

This program was written by Allan R. Klumpp of Caltech for **NASA's Jet Propulsion Laboratory.**
NPO-17983/TN

FOR ADDITIONAL INFORMATION

CONTACT
COSMIC®
112 Barrow Hall
University of Georgia
Athens, GA 30602

(404) 542-3265

Programs for Modeling Fault-Tolerant Computing Systems

One program uses a Pade approximation; the other uses a Taylor-series solution technique.

The Pade Approximation with Scaling, (PAWS) and Scaling Taylor Exponential Matrix (STEM) computer programs are software tools for design and validation. These programs provide a flexible, user-friendly, language-based interface for the input of Markov mathematical models that describe the behaviors of fault-tolerant computer systems. Markov models can include both the recovery from faults via reconfiguration and the behaviors of such systems when faults occur. PAWS and STEM produce exact solutions of the probability of system failure and provide a conservative estimate of the number of significant digits in the solution.

The calculation of the probability of entering a death state of a Markov model, i.e., the state that represents the failure of a system, requires the solution of a set of coupled differential equations. Because of the large disparity between the rates of arrivals of faults and recoveries of the system, models of fault-tolerant architectures inevitably lead to numerically stiff differential equations. PAWS uses a Pade approximation as a solution technique; STEM uses a Taylor-series solution technique. Both programs can solve numerically stiff models. PAWS and STEM possess complementary properties with regard to their input space; and additional strength of these programs is that they accept input compatible to the Semi-Markov Unreliability Range Evaluator (SURE) program (COSMIC program number LAR-13789).

The mathematical approach chosen to solve a reliability problem may vary with the size and nature of the problem. Although different solution techniques are used in different programs, it is possible to have a common input language.

The Systems Validation Methods group at NASA Langley Research Center has created a set of programs that form the basis for a "reliability analysis" workstation. The components are as follows: SURE itself, the PAWS/STEM reliability-analysis programs based upon the SURE input language, and the Abstract Semi-Markov Specification Interface to SURE Tool (ASSIST) program (COSMIC program number LAR-14193). ASSIST automatically generates Markov/semi-Markov model descriptions in the SURE input language from an abstract language.

PAWS and STEM are written in PASCAL and FORTRAN for interactive execution and have been implemented on a DEC VAX computer operating under VMS 4.7 with a virtual-memory requirement of approximately 292K of 8-bit bytes. For graphical output, the graphics library TEMPLATE is required. However, both PAWS and STEM can be used without graphical input. PAWS and STEM were developed in 1988.

This program was written by Ricky W. Butler of **Langley Research Center.** *LAR-14165/TN*

FOR ADDITIONAL INFORMATION

CONTACT

COSMIC®
112 Barrow Hall
University of Georgia
Athens, GA 30602

(404) 542-3265

S-Chart — Scheduling-Chart Program

An easy-to-use program turns out time-line graphics of high quality.

The Schedule Chart Program (S-Chart) produces quickly, through an array of simple menu choices, high-quality Gantt-type scheduling and production time-line charts with minimal data-entry requirements. The software produces high-quality charts (20-, 40-, and 80-day options) in 10 to 20 minutes, including startup, entry of data, and printing. Reprints take less than 1 minute. Some of the more significant features are as follows: speed and ease of use with menu-driven selections from start to finish; storage and catalogs of all sets of data for rapid access and manipulation; compact program to permit storage of dozens of sets of data on the program disk; and creation of ASCII text files of graphs for rapid printing. The final product of the plotting routine is an extended ASCII character file, which shows the scheduled and actual work dates of the events. This file may be printed from the program or from DOS, or imported to a word processor for customizing.

S-Chart is not intended to take the place of commercial scheduling/project-management software. It is, however, a simple, somewhat limited Gantt-chart-plotting and scheduling/tracking program with an emphasis on the straightforward entry of data. There is no complex building of relationships between the scheduled events. Dates are entered as dates, not as algebraic functions.

All the files of S-Chart, except for the graph picture and the stand-alone executable, were written in a code that is 100 percent compatible with dBASE III. The executable was created with CLIPPER, and the graph picture files are written in ASCII code. S-Chart was implemented on a IBM PC-series computer under DOS and requires 215K bytes of memory. The program was developed in 1988.

This program was written by Eric R. Klinkner of Rockwell International Corp. for **Marshall Space Flight Center.**

Inquiries concerning rights for the commercial use of this invention should be addressed to the Patent Counsel, Marshall Space Flight Center. Refer to MFS-29531/TN.

FOR ADDITIONAL INFORMATION

CONTACT

COSMIC®
112 Barrow Hall
University of Georgia
Athens, GA 30602

(404) 542-3265

YAMM—Yet Another Menu Manager

Alimentary connotations notwithstanding, this is about software for the management of software.

One of the most time-consuming, yet necessary, tasks of writing any piece of interactive software is the development of a software interface with the user. The Yet Another Menu Manager (YAMM) computer program is an application-independent menuing package of software designed to remove much of the difficulty and save much of the time inherent in the implementation of the front ends of large packages of software. Written in C for a UNIX-based operating system, YAMM provides a complete menuing front end for a wide variety of applications, with provisions for independence from specific types of terminals, configurations that meet the specific needs of users, and dynamic creation of menu trees.

An application program running under the menu package consists of two parts: a description of the menu configuration and the body of application code. The menu configuration is used at run time to define the menu structure and any nonstandard keyboard mappings and terminal capabilities. Menu definitions define specific menus within the menu tree. The names used in a definition may be either referenced to application functions or the names of other menus defined within the menu configuration. Application parameters are entered by use of data-entry screens, which allow for required and optional parameters, tables, and lists of legal values. Both automatic andapplication-specific checking for errors are available. Help is available for both menu operation and specific applications.

The YAMM program was written in C for execution on a Sun Microsystems workstation running SunOS, based on the Berkeley (4.2bsd) version of UNIX. During development, YAMM has been used on both 68020 and SPARC architectures, running SunOS versions 3.5 and 4.0. YAMM should be portable to most other UNIX-based systems. It requires a control memory of approximately 232K bytes. YAMM was developed in 1988.

This program was written by Alan S. Mazer and Richard J. Weidner of Caltech for **NASA's Jet Propulsion Laboratory.** *NPO-17769/TN*

FOR ADDITIONAL INFORMATION

CONTACT

COSMIC®
112 Barrow Hall
University of Georgia
Athens, GA 30602

(404) 542-3265

Electrotechnology

0371 CM0S Analog Four-Quadrant Multiplier Invented

0372 Electronic Noise-Reducing System (Licensing Opportunity)

0373 New EMPF Electronics Manufacturing Learning Center

0374 Improving Contracts to High-T(c) Superconductors

0375 Test Chamber Performance Enhanced

0376 Time and Frequency User's Manual Updated

0377 Real-Time, Ultra-High-Resolution Image Projection Display Using Laser-Addressed Liquid-Crystal Light Valve

0378 Heterojunction-Internal-Photoemission Infrared Detectors—A new type of photodetector would add options for the design of imaging devices. (Licensing Opportunity)

0379 Meissner-Effect Stepping Motor—Weight, cost, and maintenance would be reduced.

0380 Long-Lifetime Laser Materials for Effective Diode Pumping—Long quantum lifetimes reduce the number of diodes required to pump. (Licensing Opportunity)

0381 Multistage Estimation of Frequency and Phase—Each stage would refine the estimate further. (Licensing Opportunity)

Testing & Instrumentation

0382 Multiple-Quantum-Well Intersubband Infrared Detector—Bandwidth and detectivity would be increased. (Licensing Opportunity)

0383 Self-Oscillating Inductive Boost Regulator—Features include optical coupling and rapid response.

0384 Simultaneous Detection and Estimation Amid Strong Dynamical Effects—The effective signal-to-noise ratio is several decibels greater than in previous schemes. (Licensing Opportunity)

0385 Status of Imaging Radar Polarimetry—Topics include theory, equipment, and experimental data.

0386 Method of Measuring Magnetic Effects Due to Eddy Currents (Licensing Opportunity)

NAVY
Domestic Technology Transfer Fact Sheet

CMOS Analog Four-Quadrant Multiplier Invented

The Naval Ocean Systems Center (NOSC), San Diego, California, has invented a four-quadrant multiplier that provides a simple four-terminal transistor circuit that achieves four-quadrant multiplication and requires no-bias voltages to actuate the transistors. The inputs, V_1 and V_2, can be applied directly to the transistors. The simplified circuit makes the invention suitable for use in large arrays expected to be found in artificial neural networks.

Analog multiplier circuits form important building blocks for devices such as adaptive filters, function generators, and modulators. In the emerging field of artificial neural networks, implementation of useful network structures in analog integrated circuitry will, in many cases, require large arrays of multipliers. Some designs for analog four-quadrant multiplication MOS circuitry existing to date are based upon the characteristics of MOS transistors in saturation.

For Additional Information:

Backup material on this effort is available from:

Navy Domestic Technology Fact Sheet Reader Reply Service
Code E211
Naval Surface Weapons Center
Dahlgren, VA 22448-5000
(703) 663-8921

Refer to 150706/TN

U.S. Navy Fact Sheet

Licensing Opportunity

Naval Underwater Systems Center

Electronic Noise-Reducing System

This method and apparatus reduces noise from a near-field noise source present together with signals from a far-field source. An adaptive shaping filter and a summer, in conjunction with a directional reference sensor and a primary sensor, have at least a common sensing element. The direction reference sensor, situated between the near-field noise source and the far-field signal source, rejects the broadband signal but accepts the broadband noise and feeds this noise into a reference channel of the adaptive filter. The primary sensor accepts both the far-field signal and near-field noise with equal sensitivity. The primary sensor feeds into the primary channel of the adaptive filter. The adaptive filter system subtracts the noise in the reference channel from the signal-plus-noise in the primary channel, thus producing an output having a greatly improved signal-to-noise ratio.

Patent Number 4,589,137

FOR ADDITIONAL INFORMATION: Margaret M. McNamara (Code 105), Naval Underwater Systems Center, New London, CT 06320-5594; (203)440-4590.

New EMPF Electronics Manufacturing Learning Center

A new Electronics Manufacturing Learning Center (EMLC) has opened in Indianapolis. The EMLC is operated by Indiana University-Purdue University at Indianapolis (IUPUI) as part of the Electronics Manufacturing Productivity Facility (EMPF) under a cooperative agreement between the Naval Avionics Center, the Naval Weapons Support Center Crane, and IUPUI. The cooperative agreement is authorized by the Federal Technology Transfer Act of 1986. The Learning Center will offer state-of-the-art training in electronics manufacturing with emphasis on skill courses, seminars, and workshops tied directly to applied research.

The learning center represents a synergism between DOD, industry, and academia and provides a forum for technology transfer and technology sharing. In addition to the special offerings that will be based on ongoing research, the EMLC provides solder technology training that was previously offered through the Naval Avionics Center's Solder Technology Training Center, including courses based on MIL-STD-2000. All courses comply with best manufacturing practices and DOD specifications and are designed to ensure the transfer of emerging electronics manufacturing technology to private industry, government, and academia.

Researchers at the EMPF are reviewing current projects to identify topics for future seminars and workshops. Potential seminar topics include plated hole rework and repair (depot level), surface mount technology rework and repair (depot level), alternative flux and assembly materials, CFC alternatives, point-to-point soldering, fine-pitch surface mount technology manufacturing, and Total Quality Management (TQM) technology (using instrumentation techniques, automated data collection, and empirical modeling for Statistical Process Control and TQM).

Potential workshop topics include conformal coatings application and repair, flexible interfaces from control system to subsystems, chip-on-board technology, tape automated bonding, and depot repair.

The EMLC is now accepting applications for the following skill courses:

The MIL-STD-2000 Training course provides advanced training in all aspects of hand and machine soldering. The course provides specialized knowledge in government specifications, soldering technology, and approved processes/procedures required for contractors to establish their own training programs or otherwise implement the requirements of government specifications.

The Instructor Training course is targeted at instructors and those who develop training plans for industrial training. Topics include training plan generation, developing objectives, planning motivation techniques, and how to manage students of varying backgrounds.

Rework/Repair Training deals with the rework/repair techniques as applied to government specifications. The primary emphasis is on correct methods of rework to eliminate repairs. The student will use both wicking braid and vacuum extraction methods of removing solder from the solder connections. Methods of repair are discussed, from how common repairs are performed, to the reliability of the electronic assembly based on the type of repair used. Conformal coating removal and replacement are also discussed and performed.

In Printed Wiring Technology Training, military specifications and how they relate to printed wiring board design are the major topics. The lecture series will cover MIL-STD-2000, MIL-STD-275, MIL-P-55110, MIL-STD-2118, and MIL-P-50884 specifications. Other topics

include printed wiring board design, military requirements, how design influences assembly operations, and common mistakes made in design.

The design and assembly of cables and harnesses is discussed in Cables and Harnesses Training. The student will use MIL-STD-2000 and MIL-C-45224 specifications in the lecture series. Hands-on experience in the assembly of harnesses will include the use of lacing and tie wraps.

Surface Mount Technology Training will examine military requirements for surface mount technology. The course includes hands-on experience with infrared and vapor phase soldering equipment. The main emphasis is process control in the assembly of printed wiring assemblies.

All courses run for five days (40 classroom hours), except for the MIL-STD-2000 Training course, which runs two weeks (80 classroom hours), and Printed Wiring Technology Training, which consists of three days (24 classroom hours).

For scheduling information or to enroll in an Electronics Manufacturing Learning Center course, call Kitty Hughes at (317) 274-5059. For further information on the content of skill courses, call Gordon Morris at (317) 353-3910. If you would like to learn more about the EMLC program and future seminars and workshops, call Dr. Larita Killian at (317) 351-4242.

Federal laboratory resource

NIST Technology Update

National Institute of Standards & Technology
U.S. Department of Commerce, Gaithersburg, MD 20899

Improving Contracts to High-T(c) Superconductors

A broad-based method for making vastly improved electrical contacts to high-critical-temperature (high-T_c) superconductors is the subject of a new patent. Jack W. Ekin of the NIST Boulder Laboratories and Armand J. Panson and Betty A. Blankenship of the Westinghouse Science & Technology Center in Pittsburgh, Pa., developed techniques for making ultra-low-resistivity contacts for various kinds of high-T_c ceramic oxide superconductors. Contact resistivity using these methods is less than a billionth of that of conventional indium-solder contacts. The work removes a serious obstacle to the commercial application of high-temperature superconductors in both large-scale and thin-film devices. The technology is available for licensing under U.S. patent number 4,963,523, "High-T_c Superconducting Unit Having Low Contact Surface Resistivity and Method of Making."

FOR ADDITIONAL INFORMATION: Interested parties should contact Bruce Mattson, A343 Physics Bldg., NIST, Gaithersburg, Md. 20899; (301)975-3084. Reprints of papers describing the techniques are available from Jack Ekin, Div. 724.05, NIST, Boulder, Colo. 80303.

NIST Technology Update

National Institute of Standards & Technology
U.S. Department of Commerce, Gaithersburg, MD 20899

Test Chamber Performance Enhanced

NIST has enhanced the performance of its anechoic test chamber to extend to the millimeter wave region. The frequency range now extends to 40 GHz from 18 GHz. The chamber, a large shielded, metal-clad room covered with radio-frequency (rf) absorbers, is used to establish standard electromagnetic (EM) fields and to calibrate antennas, EM probes, and rf radiation hazard monitors. The chamber is available for use by industry and government agencies. A new publication, *Generating Standard Reference Electromagnetic Fields in the NIST Anechoic Chamber, 0.2 to 40 GHz* (NIST TN 1335), describes the chamber in detail.

FOR ADDITIONAL INFORMATION: A copy of the report is available from NTIS, Springfield, VA 22161; (703)487-4600.

NTIS order number: PB90-221797/NAC
Price code: A03

NIST Technology Update

National Institute of Standards & Technology
U.S. Department of Commerce, Gaithersburg, MD 20899

Time and Frequency User's Manual Updated

NIST has just published a new edition of its popular *Time and Frequency User's Manual*. Written for readers at all levels of understanding, this edition contains updated information about time and frequency services available from NIST, other federal agencies, and other countries. The carefully indexed publication will be useful to technicians, experimenters, calibration laboratories, and scientists since it covers most aspects of receiving and using time and frequency calibration signals, the history of time services, foreign transmitters, satellite services, and calibration methods.

FOR ADDITIONAL INFORMATION: A copy of the report is available from NTIS, Springfield, VA 22161; (703)487-4600.

NTIS order number: PB91-107532/NAC
Price code: A08

U.S. Navy Fact Sheet

Naval Ocean Systems Center

Real-Time, Ultra-High-Resolution Image Projection Display Using Laser-Addressed Liquid-Crystal Light Valve

A wide screen display enables a number of viewers the simultaneous viewing of rapidly updated data in real time at video rates. A beam of coherent radiation from a laser is modulated at video rates in an acousto-optic modulator. The modulated beam is fed to an X scanner that imparts an acousto-optic displacement of the modulated beam in the X direction. A Y scanner is aligned to receive the X-scanned modulated beam and imparts an acousto-optic reciprocal displacement of the beam so that the video modulated beam is displaced in both the X and Y directions. A liquid-crystal light valve is disposed to receive the X- and Y-displaced modulated beam so that it scans the surface of the light valve to stimulate the photosensor layers within. This causes the impression of a replica voltage pattern on a birefringent liquid crystal in the valve. A high-intensity lamp projects a high-intensity incoherent light beam onto the liquid- crystal light valve through a polarizing biprism. Since the birefringent liquid crystal has been modulated by the X- and Y-scanned modulated coherent beam, a corresponding image is reflected from the birefringent liquid crystal and onto the screen. The acousto-optic modulation X scan and Y scan occur at much higher rates and with greater control than conventional arrangements so that the resolution of about 2000 lines at a video rate is possible. The real-time display provides a number of viewers with a more realistic image so that responsive decisions and actions may be taken.

Patent Number 4,611,245

FOR ADDITIONAL INFORMATION: Dr. Richard November (Code 0144), Naval Ocean Systems Center, San Diego, CA 92152-5000; (619)553-2103.

NASA Tech Brief
National Aeronautics and Space Administration
NASA's Jet Propulsion Laboratory, Pasadena, California

Licensing Opportunity

Heterojunction-Internal-Photoemission Infrared Detectors

A new type of photodetector would add options for the design of imaging devices.

Heterojunction-internal-photoemission (HIP) infrared photodetectors have been proposed for incorporation into planar arrays in imaging devices that are required to function well at wavelengths from 8 to 17 μm and at temperatures above 65 K. The ability to fabricate specially tailored heterostructures containing elements from groups III and V of the periodic table has opened up the possibility of making these and other new optoelectronic devices. The proposed photodetectors could be built into integrated circuits that also include silicon multiplexer/readout circuits.

Detection would occur via photoemission of electrons over heterojunction barriers. In a representative detector of this type, the heterojunction would be incorporated into an appropriately doped structure. The heterojunction could be formed, for example, between heavily electron-donor-doped (n^+) $In_xGa_{1-x}As$ and GaAs (see figure). By selection of the composition x one could set the height, ϕ, of the energy barrier for electrons and make it correspond to the cutoff wavelength, λ_c, according to $\lambda_c = hc/\phi$, where h is Planck's constant and c is the speed of light. For operation in the long-wavelength infrared region of interest, one would typically choose $x \approx 0.1$.

Unlike some quantum-well infrared detectors, the proposed devices could detect radiation that impinged perpendicularly to the plane of the heterojunction. Incident photons would excite free electrons from the occupied energy states of the degenerate n^+ $In_xGa_{1-x}As$ layer to the higher energy states in the continuum of the conduction energy band. If the distance between a photoexcited electron and the barrier were of the order of a mean free path for inelastic scattering and the electron were excited with an energy $> \phi$, then there would be a high probability that the electron would cross the barrier and be collected.

The undoped GaAs layer adjacent to the heterojunction would constitute a barrier region with a built-in electrostatic field that would terminate at an interface with an n^+ GaAs layer. The electrons that cross the barrier would be swept by this field into the n^+ GaAs layer, where they would be collected. This effect would be identical to the photovoltaic effect in p/n-junction or Schottky-barrier devices. Therefore, with the addition of suitable contacts, photodetectors of this type could be operated as photovoltaic detectors, and imaging arrays of them could provide direct outputs to multiplexer/readout circuits, without having to apply bias voltages to the arrays.

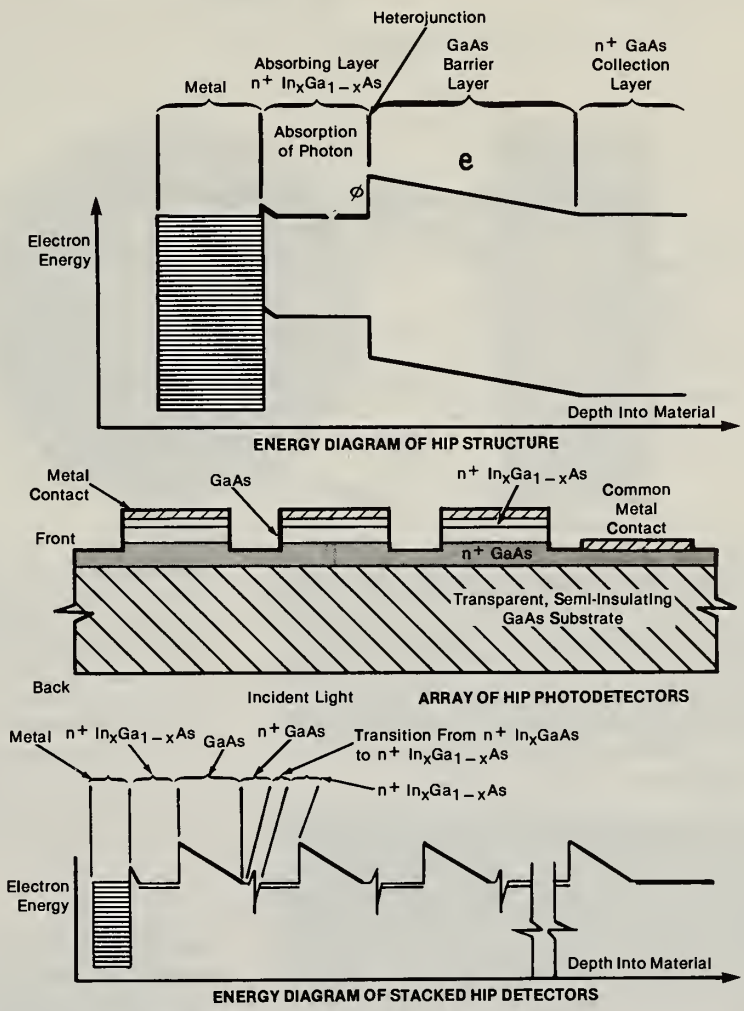

In an HIP Infrared Photodetector, photoexcited electrons would cross an energy barrier at a heterojunction and be swept toward a collection layer. An array of such detectors could be made by etching mesa structures. HIP layers could be stacked to increase quantum efficiency.

It would be relatively easy to form the electrical contact between the $In_xGa_{1-x}As$ layer and an outer metal layer, especially if the composition x were increased near the metal/semiconductor interface to make an ohmic contact of low resistance. The thickness of the n^+ $In_xGa_{1-x}As$ layer should be kept approximately at the electron-scattering mean free path to maximize the quantum efficiency. An array of mesa picture-element detectors could be etched by standard photolithography, as shown in the middle of the figure. In this configuration, radiation may be incident from the back side of the transparent, semi-insulating GaAs substrate and be reflected from the front metal contacts, thus providing two passes through the absorbing n^+ $In_xGa_{1-x}As$ layer. The common contact to the GaAs n layer could be placed at a peripheral point from the front

side.

The quantum efficiency of an HIP infrared detector would be limited by the thinness of a single n^+ $In_xGa_{1-x}As$ absorbing layer. With suitable doping and matching of layers, detectors could be stacked to increase quantum efficiency, as shown at the bottom of the figure.

This work was done by Joseph Maserjian of **NASA's Jet Propulsion Laboratory**. *Center for Space Microelectronics Technology.*

Inquiries concerning rights for the commercial use of this invention should be addressed to the Patent Counsel, NASA Resident Office-JPL. Refer to NPO-17879/TN.

Jet Propulsion Lab.
NASA Resident Office
Technology Utilization Officer: Gordon S. Chapman
Mail Stop 180-801
4800 Oak Grove Drive
Pasadena, CA 91109
(818) 354-4849
Patent Counsel: Paul F. McCaul
Mail Code 180-801
4800 Oak Grove Drive
Pasadena, CA 91109
(818) 354-2734

Technology Utilization Mgr. for JPL: Norman L. Chalfin
Mail Stop 156-211
4800 Oak Grove Drive
Pasadena, CA 91109
(818) 354-2240

FOR ADDITIONAL INFORMATION: *Contact: Director, Technology Transfer Division, P.O. Box 8757, BWI Airport, MD 21240; (301) 621-0100 Ext. 241*

REFER TO THE NUMBER LISTED AT THE END OF THIS ARTICLE

NASA Tech Brief
National Aeronautics and
Space Administration
Marshall Space Flight Center, Alabama

Meissner-Effect Stepping Motor

Weight, cost, and maintenance would be reduced.

A proposed stepping motor would derive torque from the diamagnetic repulsion produced by the Meissner effect — the exclusion of a magnetic field from the interior of a superconductor. The design of the motor would take advantage of silver-doped YB_2Cu_3O and other compounds that have recently been discovered to be superconductive at temperatures as high as that of liquid nitrogen.

The motor (see figure) would include a rotor and a stator in a nonmagnetic housing. The rotor would include a shaft mounted on bearings in the housing and restrained axially by retaining rings. The stator would include electromagnets spaced equally around the circumference and joined at the periphery by a magnetically soft cylinder that would conduct magnetic return flux between them. The rotor body, made of nonmagnetic material, would be mounted on the shaft and would include passages for liquid nitrogen, which would be used to cool it to the temperature required for superconductivity. The outer surface of the rotor body would be a cusped cylinder covered by a superconductive skin.

Figure 2 illustrates the principle of operation. In the top part of this figure, the peaks of the cusps (called "nodes") are positioned between electromagnets C and electromagnets A. Only electromagnets A are energized. Because of the Meissner effect, the magnetic flux of each energized electromagnet is confined to the right of the nearby node. The resulting gradient of magnetic pressure pushes the rotor toward the left.

In the middle part of the Figure 2, the rotor has moved so that the nodes now face the midpoints of unenergized electromagnets C. The fluxes from energized magnets A to unenergized magnets C now pass symmetrically through the bottoms of the valleys between the nodes, and consequently exert no net magnetic force to the right or left. However, because the fluxes from energized magnets A to unenergized magnets C are confined by the Meissner effect to the right of the nodes, there is still a net magnetic force on the rotor toward the left.

If electromagnets A were to remain energized, eventually the rotor would reach the position shown at the bottom of Figure 2. This is a magnetic-equilibrium position because the symmetry of the magnetic fields on all cusps results in zero net magnetic force to the right or left. If it were desired to continue the movement to the left, then electromagnets C would have to be turned on, while electromagnets A would have to be turned off. Similarly, it would be necessary to turn on electromagnets B and turn off electromagnets C to produce motion past the next equilibrium position. Repetition of this cycle would result in continuous motion to the left. Of course, the sequence could be reversed to obtain motion to the right. Modern electronic rotor-position sensors and commutation circuitry would be used to switch the electromagnets on and off at the required positions and times.

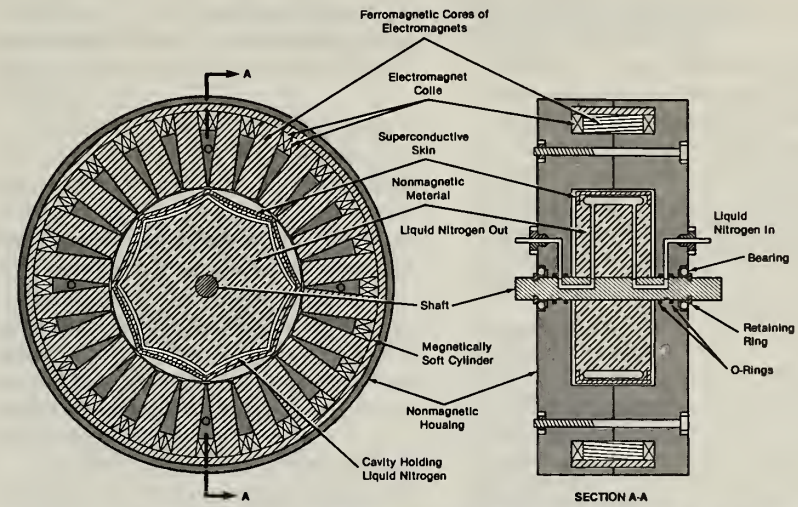

Figure 1. The **Skin of the Rotor** would be cooled below its superconducting-transition temperature by liquid nitrogen. O-Rings would prevent leaks of liquid nitrogen from the rotor.

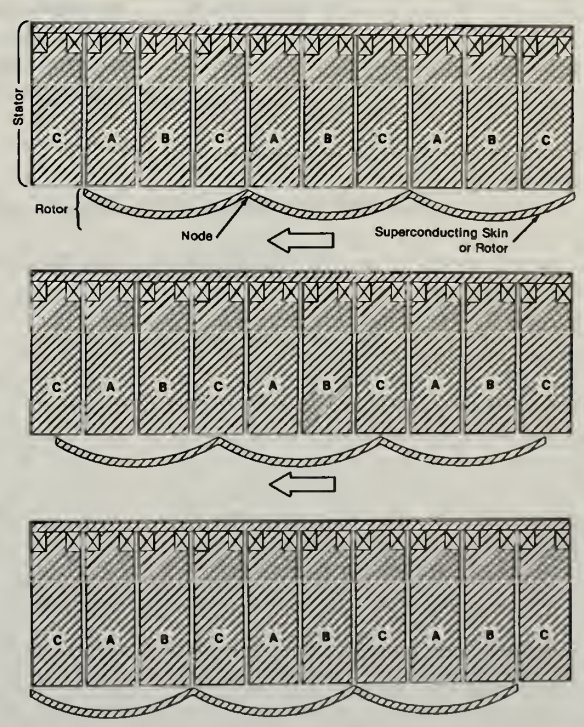

Figure 2. This **Simplified, Flattened View** of the rotor illustrates the principle of operation. One out of every three adjacent magnets is switched on at a given time. The asymmetry of the magnetic field on the superconducting skin of the rotor results in a net magnetic force to the right or left.

The stator of the proposed motor would weigh less and cost less than a conventional stepping motor does because it would not contain the usual heavy metallic, magnetic housing. The rotor would cost less, both to build and to maintain, because it would not contain an arcing commutator. The use of the Meissner effect to produce magnetic force and torque would promote high energy efficiency.

This work was done by Glen Robertson of **Marshall Space Flight Center.** *MFS-28409/TN*

FOR ADDITIONAL INFORMATION: *Contact: Director, Technology Transfer Division, P.O. Box 8757, BWI Airport, MD 21240; (301) 621-0100 Ext. 241*

REFER TO THE NUMBER LISTED AT THE END OF THIS ARTICLE

NASA Tech Brief
National Aeronautics and
Space Administration
Langley Research Center, Hampton, Virginia

Licensing Opportunity

Long-Lifetime Laser Materials for Effective Diode Pumping

Long quantum lifetimes reduce the number of diodes required to pump.

While Nd lasers have proved to be quite useful, they would be even more so if they could be pumped by laser diodes. Pumping by laser diodes has been demonstrated with such common Nd laser materials as neodymium:yttrium aluminum garnet (Nd:YAG) and Nd:$YLiF_4$, but such materials as Nd:LaF_3, Nd:$NaF{\bullet}9YF_3$, and possibly Nd:YF_3 could be more useful because of the long lifetimes of their upper laser energy levels.

In the more common Nd:YAG, the lifetime of the upper laser energy level is relatively short. For a pulsed solid-state laser, the number of diodes required is approximately inversely proportional to the lifetime of the upper laser energy level. Thus, if a material with an upper-laser-level lifetime twice as long as that of Nd:YAG were used, about half the number of diodes would be required. For a continuous solid-state laser, the threshold is approximately inversely proportional to the lifetime of the upper laser level. Thus, such a laser could also be improved by the use of one of the proposed materials.

Cost effectiveness is the primary advantage of the solid-state laser materials that have longer upper-laser-level lifetimes. While the costs of the proposed laser materials may be somewhat higher than those of the more common ones, the number of diodes required for pumping may be reduced by factors that range from 2 to 4. Because the cost of the diodes outweighs the cost of the laser material by perhaps two orders of magnitude, the cost would be reduced significantly.

The proposed laser materials have been neglected until now, probably because of the relatively low value of the thermal-shock parameters associated with these fluoride materials. However, benefits of the use of these materials, with their long upper-laser-level lifetimes, may more than offset this disadvantage.

This work was done by Norman P. Barnes of **Langley Research Center.**

This invention is owned by NASA, and a patent application has been filed. Inquiries concerning nonexclusive or exclusive license for its commercial development should be addressed to the Patent Counsel, Langley Research Center. Refer to LAR-13807/TN.

Langley Research Ctr.
Technology Utilization
Officer John Samos
Mail Stop 139A
Hampton, VA 23665
Patent Counsel
George F. Helfrich
Mail Code 279
Hampton, VA 23665
(804) 864-3523

FOR ADDITIONAL INFORMATION: *Contact: Director, Technology Transfer Division, P.O. Box 8757, BWI Airport, MD 21240; (301) 621-0100 Ext. 241*
REFER TO THE NUMBER LISTED AT THE END OF THIS ARTICLE

NASA Tech Brief
National Aeronautics and Space Administration
NASA's Jet Propulsion Laboratory, Pasadena, California

Licensing Opportunity

Multistage Estimation of Frequency and Phase

Each stage would refine the estimate further.

A conceptual two-stage software scheme serves as a prototype of a multistage scheme for digital estimation of the phase, frequency, and the rate of change of frequency ("Doppler rate," for short) of a possibly phase-modulated received sinusoidal signal in a communication system in which the transmitter and/or the receiver is (are) traveling rapidly, accelerating, and/or jerking severely. Although the scheme was conceived for use in estimating the parameters of signals from spacecraft and the high dynamic GPS signal parameters, it is also applicable, at least in principle, to terrestrial stationary/mobile (e.g., cellular radio) and land-mobile/satellite communication systems.

The conceptual multistage estimation scheme stands in contrast to the prior single-stage schemes (phase-locked loop, conventional cross-product automatic frequency-control loop, Kalman filter, and the like). The concept embraces many variations in the number, types, and parameters of the stages. In general, the successive stages yield increasingly refined estimates (see figure), and each succeeding stage operates within a bandwidth smaller than that of the preceding stage.

In the two-stage prototype, the first-stage algorithm provides estimates of the frequency and its time derivatives that are coarse in the sense that the root-mean-square estimation errors are relatively large, but the probability that the estimated frequency exceeds one-half the sampling frequency (this phenomenon is called "cycle slip") is relatively small. This first-stage algorithm is a modified version of a prior least-squares algorithm based on a differential signal model and known as "differential least squares." The modification makes this algorithm applicable to signals that contain unknown digital modulation. The second algorithm implements a third-order extended Kalman filter, yielding an estimate of the phase and a refined estimate of the frequency.

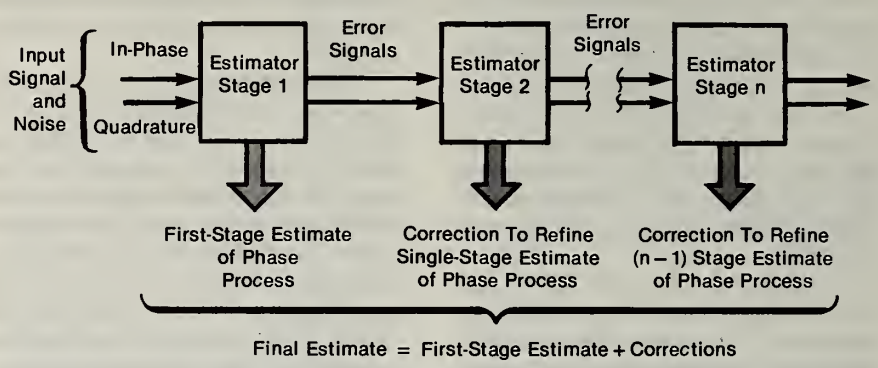

Each Additional Stage of a multistage scheme would provide an increasingly refined estimate of the frequency and phase of a signal.

One major advantage of the combination of first- and second-stage algorithms is a reduction in the threshold on the carrier-power-to-noise-power spectral-density ratio (CNR) in comparison with the threshold CNR achievable by either algorithm alone. Indeed, from computer simulations designed to test the performance of the two-stage scheme, it appears that for an unmodulated carrier, the scheme achieves the same threshold CNR as that of an almost exact and computationally intensive implementation of a maximum-likelihood estimator. The simulations also show that where digital modulation is present, the threshold CNR of this scheme is about 6 dB below that of a previous approximate maximum-likelihood-estimator (AMLE) scheme.

The overall complexity of the scheme is about twice that of a third-order Kalman filter or of a single fourth-order extended Kalman filter. Of course, one could reduce the threshold CNR and the rms estimation errors further by use of a more complicated set of algorithms that implement three or more stages of estimation.

This work was done by Rajendra Kumar of Caltech for **NASA's Jet Propulsion Laboratory**.

This invention is owned by NASA, and a patent application has been filed. Inquiries concerning nonexclusive or exclusive license for its commercial development should be addressed to the Patent Counsel, NASA Resident Office-JPL. Refer to NPO-17911/TN.

Jet Propulsion Lab.
NASA Resident Office
Technology Utilization Officer: Gordon S. Chapman
Mail Stop 180-801
4800 Oak Grove Drive
Pasadena, CA 91109
(818) 354-4849
Patent Counsel: Paul F. McCaul
Mail Code 180-801
4800 Oak Grove Drive
Pasadena, CA 91109
(818) 354-2734
Technology Utilization Mgr. for JPL: Norman L. Chalfin
Mail Stop 156-211
4800 Oak Grove Drive
Pasadena, CA 91109
(818) 354-2240

FOR ADDITIONAL INFORMATION: *Contact: Director, Technology Transfer Division, P.O. Box 8757, BWI Airport, MD 21240; (301) 621-0100 Ext. 241*
REFER TO THE NUMBER LISTED AT THE END OF THIS ARTICLE

NASA Tech Brief
National Aeronautics and Space Administration
NASA's Jet Propulsion Laboratory, Pasadena, California

Licensing Opportunity

Multiple-Quantum-Well Intersubband Infrared Detector

Bandwidth and detectivity would be increased.

A proposed multiple-quantum-well intersubband semiconductor device would detect photons over a broader range of wavelengths than present multiple-quantum-well infrared detectors can now accommodate. The structure of the detector would resemble that of other multiple-quantum-well devices reported in previous issues of *NASA Tech Briefs*, but would differ in the numbers, thicknesses, and proportions of the semiconductor elements in its layers.

The device would be a stack of multiple substacks within each of which there would be multiple barrier layers of $Al_xGa_{1-x}As$ alternating with quantum-well layers of GaAs or In_yGa_yAs (see figure). Each quantum well would support two quantum states: a lower state bound in the well, and an upper, slightly-bound state with an energy slightly above the barrier (and, therefore, in the continuum of energy levels in the conduction band). In present multiple-quantum-well devices, the upper states are below the barriers, so that the photoexcited electrons have to undergo quantum-mechanical tunneling and the consequent attenuation to leave the wells. In the proposed device, the higher energy of the upper state would enable the photoexcited electrons to cross the barriers without tunneling. In addition, the oscillator strength of the upper states would be high with respect to that of the lower states, resulting in a high probability of absorption of photon energy between the lower states and the continuum. These features would contribute to the detectivity of the device.

Within the *n*th substack, the compositions and thicknesses of the layers would be chosen so that the quantum wells in that substack would be sensitive to a certain narrow band of wavelengths around a middle wavelength of λ_n. The wide-band response would be achieved by making the quantum wells in each succeeding substack slightly wider and shallower than those of the preceding substack. By this design, the first substack would absorb the photons of highest energy (shortest wavelength, λ_1), the second substack would absorb photons of the next highest energy (slightly longer wavelength λ_2), and so on. Because the quantum efficiency of the device would decrease with an increasing number of quantum wells, this design would involve an engineering compromise between bandwidth and quantum efficiency.

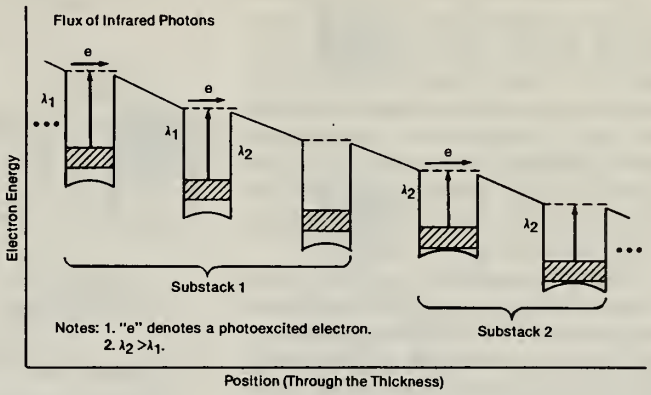

The **Proposed Multiple-Quantum-Well Device** would be a stack of substacks, each of which would contain quantum-well layers sensitive to a different narrow band of wavelengths. The energy levels shown here include the effect of the bias voltage applied to the device.

This work was done by Shmuel I. Borenstain of Caltech for **NASA's Jet Propulsion Laboratory.**

This invention is owned by NASA, and a patent application has been filed. Inquiries concerning nonexclusive or exclusive license for its commercial development should be addressed to the Patent Counsel, NASA Resident Office-JPL. Refer to NPO-17962/TN.

Jet Propulsion Lab.
NASA Resident Office
Technology Utilization Officer: Gordon S. Chapman
Mail Stop 180-801
4800 Oak Grove Drive
Pasadena, CA 91109
(818) 354-4849
Patent Counsel: Paul F. McCaul
Mail Code 180-801
4800 Oak Grove Drive
Pasadena, CA 91109
(818) 354-2734
Technology Utilization Mgr. for JPL: Norman L. Chalfin
Mail Stop 156-211
4800 Oak Grove Drive
Pasadena, CA 91109
(818) 354-2240

FOR ADDITIONAL INFORMATION: *Contact: Director, Technology Transfer Division, P.O. Box 8757, BWI Airport, MD 21240; (301) 621-0100 Ext. 241*
REFER TO THE NUMBER LISTED AT THE END OF THIS ARTICLE

NASA Tech Brief
National Aeronautics and
Space Administration
Goddard Space Flight Center, Greenbelt, Maryland

Self-Oscillating Inductive Boost Regulator

Features include optical coupling and rapid response.

An improved voltage regulator is designed for use in a solar photovoltaic dc power system utilizing a flywheel for energy storage. The voltage regulator includes a self-oscillating inductive voltage-boosting circuit, which regulates the withdrawal of energy from the flywheel and motor/generator when the output of the solar cells is insufficient to maintain the load voltage at the specified level of 150 Vdc.

The voltage-boosting circuit (see figure) increases the load voltage by supplementing it with the rectified ripple current in the boost inductor. The ripple is generated by periodically connecting the output end of the boost inductor to ground via a field-effect-transistor (FET) switch. The switching of the FET's and, therefore, the magnitude and frequency of the ripple are controlled by the current-controlling portion of the circuit, which contains a hysteretic voltage comparator. A resistive voltage-divider network feeds, to the input terminals of the comparator, a combination voltage derived partly from a shunt that senses the current in the boost inductor and partly from a control signal representative of the output voltage. The output-voltage and the FET-switching signals are transmitted to and from the current-controlling circuitry, respectively, via optoisolators, so that the isolation of relatively low control voltages from relatively high common-mode power-supply voltages presents no major problem.

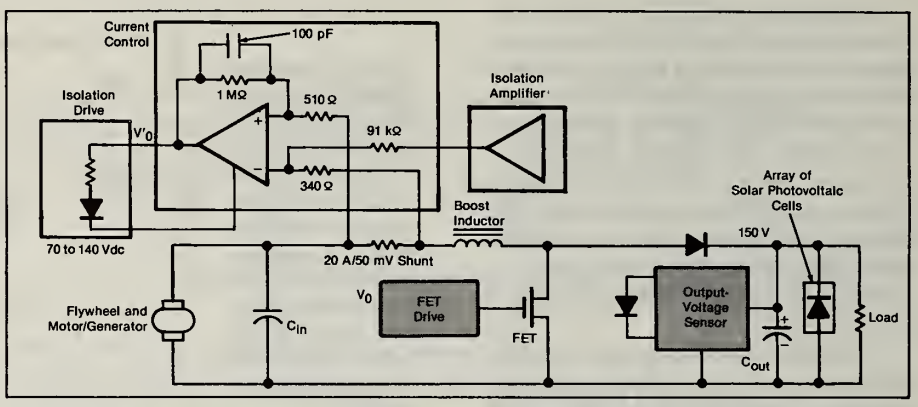

The **Self-Oscillating Boost Regulator** senses the output voltage and the current in the boost industor and accordingly turns the FET switch on and off periodically to maintain the output voltage as close as possible to 150 V.

The resistive voltage-divider network is designed to turn the FET switch off whenever the current in the boost inductor reaches a maximum safe value. Below that limit, the current-controlling circuitry continuously regulates the magnitude of the boost inductor current in response to the sensed output voltage to keep that voltage at 150 V. The circuit is self-oscillating in the sense that the FET's are turned on and off only in response to sensed current and voltage. This feature enables the circuit to respond faster to a change in the load than can a prior type of boost regulator that operates partly under control of a fixed-frequency clock signal and must wait until the next clock pulse to turn the FET switch on, no matter how much the load may change during the "off" part of the cycle.

This work was done by John Paulkovich, G. Ernest Rodriguez, and Vickie Eakin of **Goddard Space Flight Center.** *GSC-13305/TN*

FOR ADDITIONAL INFORMATION: *Contact: Director, Technology Transfer Division, P.O. Box 8757, BWI Airport, MD 21240; (301) 621-0100 Ext. 241*
REFER TO THE NUMBER LISTED AT THE END OF THIS ARTICLE

NASA Tech Brief
National Aeronautics and Space Administration
NASA's Jet Propulsion Laboratory, Pasadena, California

Licensing Opportunity

Simultaneous Detection and Estimation Amid Strong Dynamical Effects

The effective signal-to-noise ratio is several decibels greater than in previous schemes.

A proposed scheme for the digital processing of a received noisy, binary-phase-modulated radio signal provides for the simultaneous detection of the binary modulation and estimation of the Doppler phase, frequency, and frequency derivative. The scheme is intended for use where the relative motion between the transmitter and receiver can include large velocities, strong accelerations, and/or intense jerks, resulting in possibly large Doppler frequency shifts with respect to time. It could improve reception in radar, mobile/satellite communications, and navigation systems.

The scheme (see figure) starts with estimation of the local parameters (those that depend on the momentary state of the binary modulation) of the received signal, followed by detection of a possible jump in these parameters. A jump signifies a data-bit transition in the modulation and is mathematically separated from the received signal, thereby effectively demodulating the signal. The effectively demodulated signal is then processed to obtain estimates of the global parameters (those phase and frequency parameters, including the Doppler parameters, that do not depend on the modulation) of the received signal. The estimates of the global parameters are also used to improve the estimates of the local parameters during subsequent bit periods.

The scheme incorporates either of two different but equivalent algorithms for the estimation of both the local and global parameters. The algorithms are improved versions of the Kalman filter. For the local parameters, it is necessary to use a subalgorithm capable of estimating both the phase and the frequency. However, for the global parameters, it is not necessary to estimate the phase, and, therefore, a frequency-estimating algorithm can be substituted for the Kalman filter, resulting in a marginal reduction of the required P/N_o (where P = the received carrier power and N_o = the power spectral density of the noise).

Either of the two algorithms can provide an improvement of up to 3 dB (according to computer simulations) over the Kalman filter (and over a phase- or frequency-locked loop) in the estimation of phase and frequency when the signal-to-noise ratio (SNR) is low. Both algorithms are based upon the recognition of two available error signals with nearly independent noise. In conventional implementations, one of these error signals is simply ignored.

In one algorithm, the observations are reprocessed over an optimally selected period, making it possible to exploit the other error signal as well. The improvement in this scheme is not due to better linearization as in an iterated Kalman filter (where the improvement increases with the iteration interval) but, rather, is due to the fact that if the reprocessing interval is optimal, the two sets of measurements are nearly independent, resulting in an improvement of nearly 3 dB (according to computer simulations) under a low SNR. In the other algorithm, which is relevant to classical phase-locked loops, an adaptive Hilbert-transform technique results in similar improvements.

This work was done by Rajendra Kumar of Caltech for **NASA's Jet Propulsion Laboratory.**

The **Proposed Estimation/Detection Scheme** provides for the digital processing of a binary-phase-modulated, noisy sinusoid to obtain both the binary signal and estimates of the phase and frequency parameters of the sinusoid.

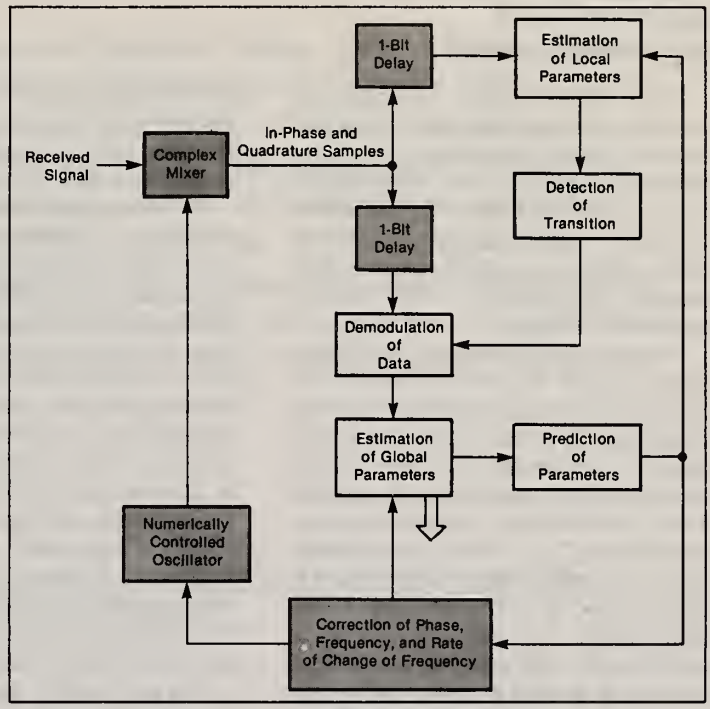

This invention is owned by NASA, and a patent application has been filed. Inquiries concerning nonexclusive or exclusive license for its commercial development should be addressed to the Patent Counsel, NASA Resident Office-JPL. Refer to NPO-17820/TN.

Jet Propulsion Lab.
NASA Resident Office
Technology Utilization Officer: Gordon S. Chapman
Mail Stop 180-801
4800 Oak Grove Drive
Pasadena, CA 91109
(818) 354-4849
Patent Counsel: Paul F. McCaul
Mail Code 180-801
4800 Oak Grove Drive
Pasadena, CA 91109
(818) 354-2734
Technology Utilization Mgr. for JPL: Norman L. Chalfin
Mail Stop 156-211
4800 Oak Grove Drive
Pasadena, CA 91109
(818) 354-2240

NASA Tech Brief
National Aeronautics and
Space Administration

Status of Imaging Radar Polarimetry

Topics include theory, equipment, and experimental data.

A report pulls together information on imaging radar polarimetry from a variety of sources. It reviews the state of the art, examines current applicable developments in radar equipment, describes the recording and processing of radar polarimetric measurements, and discusses the interpretation and application of the resulting polarimetric images.

Imaging radar polarimetry is a synthetic-aperture-radar technique in which the complete amplitude and phase response of each picture or resolution element of the target is recorded for both horizontal and vertical reflected polarizations, in response to both horizontal and vertical transmitted polarizations. Thus, the basic polarimetric data about each picture element have to be expressed as a complex-number scattering matrix. This stands in contrast to conventional radar imaging, in which polarization is ignored and each picture element is characterized by a simple scalar amplitude. In return for increased complexity, imaging polarimetry yields more detailed information about the target — for example, making it possible to distinguish between forested or treeless landscape.

The report begins with a brief history of imaging radar polarimetry. This is followed by the first section of the main text, which discusses the fundamental theory of radar polarimetry. Topics include the basic equations for back-scattering, the scattering matrix, Stokes-matrix representations of scattering matrices, polarization signatures of target areas, and development of mathematical models of polarimetric properties of different types of terrain. The modeling effort is particularly significant in that it enables the comparison of measured and predicted properties, thus providing the means for interpretation of remote-sensing data in ways that were not possible before the emergence of radar polarimetry.

The next section describes the implementation of imaging radar polarimeters. It includes a section on the radar equipment carried aboard several research airplanes and to be carried aboard future spacecraft, a section on the recording and digital processing of polarimetric measurements, a section on phase calibration of the polarimetric data, and a section on compression of the data to manageable volumes for storage and analysis.

The third section describes the experimental polarimetric scattering characteristics of several different kinds of terrain. It presents images and polarization signatures of San Francisco (including ocean, urban development, city parks, and natural terrain), the Pisgah lava flow in the Mojave desert, a forested area near Mt. Shasta, and ice floating in the Beaufort sea. The fourth and last section is a brief summary.

This work was done by Jakob J. van Zyl and Howard A. Zebker of Caltech for **NASA's Jet Propulsion Laboratory.**
NPO-17890/TN

FOR ADDITIONAL INFORMATION: *Contact: Director, Technology Transfer Division, P.O. Box 8757, BWI Airport, MD 21240; (301) 621-0100 Ext. 241*
REFER TO THE NUMBER LISTED AT THE END OF THIS ARTICLE

U.S. Navy Fact Sheet

Licensing Opportunity

Naval Surface Warfare Center

Method of Measuring Magnetic Effects Due to Eddy Currents

An eddy current magnetic field effects measurement apparatus employs a reference sensor located so that it measures an applied field and any environmental fields but does not measure eddy current effects. Then an estimate of the applied field at the locus of a plurality of measurement sensors is constructed and stored. Next, a conductive object or material to be measured is placed in the applied field near the measurement sensors away from the reference sensor, and measurements are made of the applied field, any environmental fields, and any fields caused by the effects of eddy currents induced into the conductive object or material. Finally, the stored estimates are used to compensate the applied field at the locus of the measurement sensors so that the eddy current magnetic field effects of the placement of the conductive object or material can be observed on a keyboard/display or printed by a printer or plotter.

Patent Number 4,648,041

FOR ADDITIONAL INFORMATION: Ramsey D. Johnson (Code D4), Naval Surface Warfare Center, 10901 New Hampshire Avenue, Silver Spring, MD 20903-5000; (301)394-1505.

Energy

0388 Reinforced Positive Filler Paste for Lead/Acid Batteries—Lead-coated glass fibers would extend the battery life. (Licensing Opportunity)

NASA Tech Brief
National Aeronautics and Space Administration
NASA's Jet Propulsion Laboratory, Pasadena, California

Licensing Opportunity

Reinforced Positive Filler Paste for Lead/Acid Batteries

Lead-coated glass fibers would extend the battery life.

Lead-coated glass fibers have been proposed as an additive to the positive paste used in lead/acid batteries. The fibers are expected to improve both the electrical and the mechanical properties of the positive battery electrodes, thus extending the lives of batteries during repeated charge/discharge cycles.

The positive electrode is the plate that normally fails in deep-cycle applications. As the battery is cycled, the positive paste softens and eventually causes the battery to fail. In the proposed scheme, the lead-coated glass fibers would be mixed with the paste before the paste is applied to the positive electrode. After the electrode is cured, the fibers would reinforce the electrode, somewhat like the steel rods in reinforced concrete. The fibers would also provide electrical paths in a discharged electrode, thus preventing the poorly conducting discharged active material from becoming electrically isolated.

Shown in the figure is the cross section of a typical positive battery plate pasted with a mixture of lead-coated glass fibers and active material. The fibers would be distributed uniformly throughout the 0.1-in. (2.5-mm) thickness of the plate.

The distance between the grid wires of the plate would be 0.2 in. (5 mm). The diameter of the glass fibers with lead coating would be 0.01 in. (0.25 mm), while the diameter of the glass fibers without the lead coat would be 0.004 in. (0.1 mm). The fibers, chopped to an average length of 0.1 in. (2.5 mm), would occupy about 2 percent of the volume of the active material. A pellet of active material between the grid wires would contain approximately 25 fibers.

The addition of fibers to the positive paste could be beneficial in several ways. One result could be a reduction in weight obtained by an increase in the distance between the grid wires of the positive plate. The fibers would reduce the electrical resistance of the plate so that a greater portion of the plate could be converted to lead dioxide. Because lead on the fibers would be charged during the formation of the plate, a corrosion layer of lead dioxide would form on the fibers. The corrosion layer would act to provide a good electrical and mechanical interface with the active material.

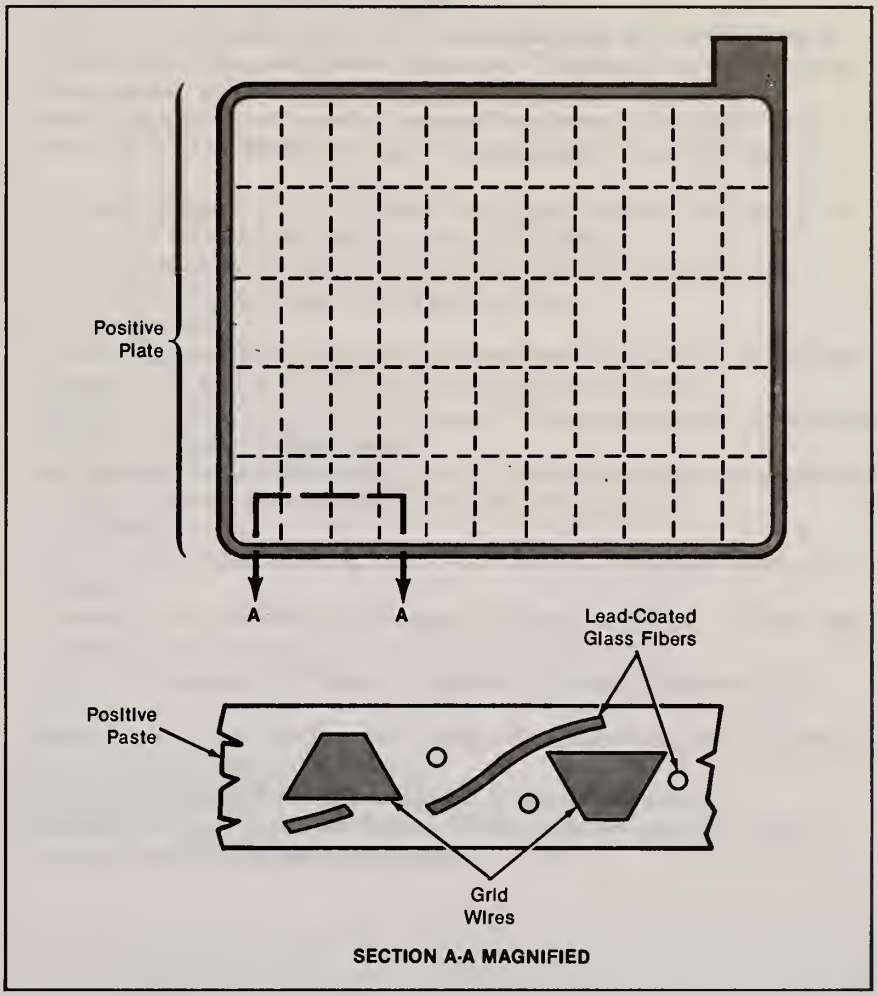

A **Mixture of Lead-Coated Glass Fibers and Positive Paste** would form pellets of active material between the grid wires of the positive battery electrode. The fibers would contribute to the charge capacity, electrical conductivity, and mechanical stability of the electrode.

This work was done by Dean B. Edwards and Wally E. Rippel of Caltech for **NASA's Jet Propulsion Laboratory.**

In accordance with Public Law 96-517, the contractor has elected to retain title to this invention. Inquiries concerning rights for its commercial use should be addressed to

Edward Ansell
Director of Patents and Licensing
Mail Stop 305-6
California Institute of Technology
1201 East California Boulevard
Pasadena, CA 91125

Refer to NPO-16991/TN.

Jet Propulsion Lab.
NASA Resident Office
Technology Utilization Officer: Gordon S. Chapman
Mail Stop 180-801
4800 Oak Grove Drive
Pasadena, CA 91109
(818) 354-4849
Patent Counsel: Paul F. McCaul
Mail Code 180-801
4800 Oak Grove Drive
Pasadena, CA 91109
(818) 354-2734

Technology Utilization Mgr. for JPL: Norman L. Chalfin
Mail Stop 156-211
4800 Oak Grove Drive
Pasadena, CA 91109
(818) 354-2240

FOR ADDITIONAL INFORMATION: *Contact: Director, Technology Transfer Division, P.O. Box 8757, BWI Airport, MD 21240; (301) 621-0100 Ext. 241*
REFER TO THE NUMBER LISTED AT THE END OF THIS ARTICLE

Engineering

0389 Robots Readied for Mapping, Removing Radioactive Wastes
0390 During a Fire, Brightness is Best for Exit Signs
0391 Design and Testing of a Balanced Air Regulator for Deep-Sea and Scuba Divers
0392 Evaporation Duct Height Calculations
0393 Naval Systems and Sciences Laboratory
0394 Test Bed for Telerobots—A versatile system keeps up with new technology.
0395 Splicing Wires Permanently With Explosives—The technique produces superior, reliable splices. (Licensing Opportunity)
0396 Making Large Suction Panels for Laminar-Flow Control—Perforated titanium panels are used to identify and resolve issues related to manufacture.

Software

0397 Program Analyzes Errors in STAGS—This program assists in scrutiny of the output of the STAGS finite-element program for plates.
0398 Program Generates Images of Solid Surfaces—Various shapes can be constructed and viewed from several perspectives.

Testing & Instrumentation

0399 Optimum Flow Noise Cancelling Hydrophone Module (Licensing Opportunity)
0400 Nondestructive Testing of Concrete with Ultrasonic Pulse-Echo
0401 Apparatus for Tests of Percussion Primers—Tests are conducted under realistic conditions. (Licensing Opportunity)
0402 Electro-optical Position-Measuring System—A nonintrusive system determines positions of models within the test section of a wind tunnel.

Other Items of Interest

0403 Design, Construction, and Evaluation of Clay Liners for Waste Management Facilities
0407 Eliminating Unbonded Edges in Explosive Bonding—A notch in the flyer plate eases removal of unbonded material. (Licensing Opportunity)
0410 Improved Computation of Dynamic Stresses—The cost of computation is reduced.
0411 Model of Bearing With Hydrostatic Damper—The model accurately represents the nonlinear aspects of the dynamics.
0414 Navy Studies Feasibility of BZS for Marine Timber Preservation
0443 Predictions of Drag in Viscous Transonic Flow—Results from the Viscous Transonic Airfoil Workshop are presented.

Sandia National Laboratory

Robots Readied for Mapping, Removing Radioactive Wastes

Researchers at Sandia National Laboratories have developed techniques that enable robots to map and remove radioactive waste from leaking underground storage tanks, such as those buried at the U.S. Department of Energy's plutonium and uranium processing plant at the Hanford Site near Richland, Washington.

Using robots to handle radioactive waste will not only make the cleanup job safer by eliminating the need for human contact, it will also allow the work to be done much faster and more efficiently - that is, more cost effectively - than by other remote means, says Pat Eicker, manager of Sandia's Computer Sciences Department. This is made possible through the development of such technologies as automatic planning and programming of robot actions.

"With current remote-control technology, it might take as long as a year to clean each one of the 149 tanks at Hanford, but with this type of intelligent system, we may be able to reduce that time to less than a month," says Ray Harrigan, supervisor of Sandia's Intelligent Machine Systems Division.

In a demonstration of the technology, a commercially available gantry robot modified with ultrasound, active computer vision, ground-penetrating radar, and metal detectors makes three-dimensional maps of the surface and subsurface contents of a simulated underground storage tank. The vision system is capable of mapping surface features to 1/1000th of an inch. After determining a safe path that prevents the robotic arm from bumping into anything, the intelligent machine uses force sensors to make controlled contact with the surface of the simulated waste deposits. Using a vacuum device, the robot then removes the tank's contents and deposits them into a storage canister.

The robot's information will comes from two sources - engineering models of the tanks stored in the computer's memory and data collected by its many sensors. For example, some of the pipes in the demonstration - set up at Sandia at DOE's request - were not part of the robot's artificial intelligence, that is, they were not included in the computer models of the tanks that were programmed into the robot's memory. Instead, the pipes were placed at unknown locations throughout the tank to test the robot, which successfully detected and mapped each one. The ability to detect and map even buried objects will be crucial in the real world, says Harrigan, where no one can initially be certain of each tank's contents.

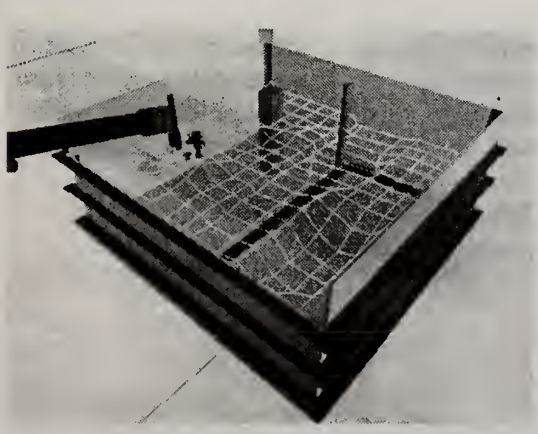

Animated graphics display, above, depicts Sandia robot detecting and mapping pipes inside simulated underground storage tank. Right, engineer Brian Christensen adjusts instruments on the robotic arm, equipped with ultrasound, active computer vision, ground-penetrating radar, and metal detectors.

The software that enables the Sandia robot to map the contents and avoid buried objects in the tanks, such as pipes, can be used with other kinds of robots as well, notes Harrigan. Though the Sandia prototype has a six-foot-long arm for mapping and removing waste, the actual cleanup project will require a robot with an extremely long arm that can reach halfway across the top of the 80-foot-wide storage tanks at Hanford from a central port. Sandia is developing damping systems to minimize vibration in the robotic arm, a problem that occurs with any long-reaching mechanical arm.

The robot will either remove the waste for transport to another storage facility or test the waste to alter its physical state, says Eicker. (One DOE suggestion has been to vitrify the waste to make it non-soluble, eliminating the threat to groundwater supplies.)

In addition to its other capabilities, the robot will assess the physical characteristics of the waste deposits, such as their consistency, level of radioactivity, chemical make-up, and density. Typically, nuclear wastes buried in underground storage tanks consist of syrupy deposits at the bottom and solid crystalline materials on top, along with pipes and other hardware. Instrumentation is being developed to characterize objects (concrete structures, pipes, cooling coils, etc.) beneath the surface.

Built-in safety features will prevent humans from executing commands that could damage the robot or the tank. The robot is manipulated in part by a human operator at a graphics workstation who oversees its motions from the safety of a central control room, where images are transmitted to a computer screen from cameras mounted inside the tank. Safety features include, for example, a sensory warning system that tells the robot to automatically avoid obstacles in its path. Human operators will not be able to override such automatic safety features, explains Harrigan.

Humans will still be in control of high-level decisions, such as the order in which various operations are executed. However, Sandia's computer science technologies will enable the robot to automatically develop its own program for moving from one point to another inside the tank, mapping the contents, and removing the waste. The human operator can approve the recommended sequence of steps or suggest something else.

The robot's motions are programmed via an animated graphics display on a computer screen. This facilitates ease of operation, allowing a human technician to view the screen and guide the robot at the same time by moving a lever. The animated display flashes red anytime the robotic arm comes within 4 inches of a solid object, such as a buried pipe.

The lead engineers on the system were project manager Sig Thunborg, Brian Christensen, and Bill Drotning of Sandia's Intelligent Machine Systems Division.

Discussions are now under way to begin transferring the new robotic technology to DOE sites in general and to the Hanford plant in particular to address concerns of leakage from underground radioactive storage tanks into the Columbia River, says Eicker.

The robotics research is part of an ongoing effort at Sandia to develop ways to clean up and protect the environment on behalf of the DOE's recently established Office of Environmental Restoration and Waste Management. Eicker headed a technical team that reported to the DOE last year on the use of robotics in removing chemical and radioactive wastes from disposal sites. Such sites have existed since the 1940s, when the DOE first began building nuclear weapons.

FOR ADDITIONAL INFORMATION: Public Information Division, Code 3161, Department of Energy, Sandia National Laboratories, Albuquerque, NM 87185-5800; (505)844-4207. Refer to announcement 25, No. 10.

NIST Technology Update

National Institute of Standards & Technology
U.S. Department of Commerce, Gaithersburg, MD 20899

During a Fire, Brightness is Best for Exit Signs

Exit signs with stenciled, brightly lit red letters on an opaque background remain visible through smoke longer than other types of signs, NIST researchers found in a recent study. The researchers used both instrumentation and 21 observers to assess the brightness and visibility of 12 exit signs in both smoky and clear conditions. The signs varied in light sources, brightness, color, and lettering. Uniform lighting was another important factor in observers being able to detect and read a sign. In addition, unlike a Canadian study that suggested that green might be a more effective color for exit markings, the observers in the NIST study preferred red. However, the NIST researchers note, the red signs were brighter and the observers were accustomed to exit signs being red.

FOR ADDITIONAL INFORMATION: A report, *Evaluation of Exit Signs in Clear and Smoke Conditions* (NISTIR 4399), is available from NTIS, Springfield, VA 22161; (703)487-4600.

NTIS order number: PB90-269523/NAC
Price code: A05

U.S. Navy Fact Sheet

Navy Diving Salvage Training Center

Design and Testing of a Balanced Air Regulator for Deep-Sea and Scuba Divers

A high-volume, low-pressure loss, balanced poppet valve was designed for use on demand type open-circuit underwater diving units. This supply valve acts as a diver's second-stage regulator providing air, on demand, to the diver with minimal breathing effort. The prototype was fabricated and tested in January 1984 by the Navy Experimental Diving Unit, Panama City, Florida. Test results showed that the unit met the U.S. Navy performance requirements for helmet-mounted second stage demand regulators. However, the valve/seat arrangement leaked excessively.

Modifications to the poppet valve and seat eliminated aerodynamic forces that were acting on the poppet valve's seating surface. Additionally, a compliant seat was used that eliminated gas leakage. Brief testing of the improved prototype on May 4, 1984 indicated that performance was equivalent or superior to performance of the best commercial second stage demand regulators available at the time of testing.

Current design modifications indicate that the regulator's performance can be further upgraded by using a newly designed cylindrical diaphragm. This will provide opening force to the poppet valve during inhalation, theoretically reducing diver breathing effort and the unit's size. Further modification of the balanced poppet valve and its seat would improve reliability and performance and reduce design complexity.

FOR ADDITIONAL INFORMATION: Lt. B. K. Miller, USN, Navy Diving and Salvage Training Center, c/o Don Wright (Code 7130T), Naval Coastal Systems Center, Panama City, FL 32407-5000; (904)235-5275.

Evaporation Duct Height Calculations

Scientists at the Naval Ocean Systems Center (NOSC), San Diego, California, funded by the Naval Oceanographic Office, have documented specifications for the evaporation duct height calculations. The evaporation ducting phenomenon, the meteorological measurements required to assess its characteristics, and the algorithms to calculate its strength are described.

The bulk meteorological measurements required for the evaporation duct calculation are wind speed, air and sea temperatures, relative humidity, and altitude of the measurements. Since gradients in the surface layer generally become small at altitudes more than a few meters, the influence of measurement altitude is neglected as long as measurements are made at least six meters above the surface. Additionally, the influence of sea waves on the measurements is usually restricted to altitudes less than three times the wave height, and the altitude of six meters or greater minimizes most wave effects.

The dominant factor in determining evaporation duct height is the difference in potential refractivity between the air at the reference height and the air at the sea surface. Errors in air temperature measurement caused by conductive and radiative heating effects have been shown to strongly affect the duct height calculation.

For Additional Information:

Backup material on this effort is available from:

Navy Domestic Technology Fact Sheet Reader Reply Service
Code E211
Naval Surface Weapons Center
Dahlgren, VA 22448-5000
(703) 663-8921

Refer to 150704/TN

U.S. Navy Fact Sheet

Naval Ocean Systems Center

Naval Systems and Sciences Laboratory

EXPERTISE: The Naval Systems and Sciences Laboratory, Naval Weapons Station, Seal Beach plays an important role in the defense of the United States by evaluating the performance, readiness, and effectiveness of naval weapons systems. Our primary mission is the quality evaluation of weapon stockpiles, quality verification of new contractor's products, and providing recommendations for implementing stockpile improvement programs. The Laboratory performs in-depth systems, subsystems, and component level evaluations of conventional ammunition, air launched and sub-surface launched weapons including Fleet Ballistic Missiles. The Laboratory also has the expertise to develop computer models of explosive separation device performance. To achieve this mission the Laboratory maintains a full compliment of professionals experienced in electronic, mechanical, chemical, and physical science disciplines.

FACILITY: Facilities include chemical analysis equipment (chromatography, spectroscopy, spectrometry, wet chemical), microwave test equipment (anechoic chamber, automated analyzer), environmental stress simulation equipment (shakers, temperature-altitude chambers, temperature-humidity chambers, salt spray chambers), nondestructive test equipment (ultrasonic, X-ray, liquid penetrant, magnetic particle), material test equipment (hardness, strength of materials, metallographic analysis), and explosive test equipment (test bays, fixtures, cutting machinery, explosive performance analysis equipment). Most of the test equipment is automated and a TEMPEST approved PC based computer network is available for the efficient storage, retrieval and analysis of test data.

FOR ADDITIONAL INFORMATION: Commanding Officer, Naval Weapons Station (53), Naval Systems and Sciences Laboratory, Seal Beach CA 90740-5000. Contact: Alan L. Armstrong (213)594-7124.

NASA Tech Brief
National Aeronautics and
Space Administration
NASA's Jet Propulsion Laboratory, Pasadena, California

Test Bed for Telerobots

A versatile system keeps up with new technology.

An assembly of electromechanical and electronic equipment (including computers) constitutes a test bed for the development of advanced robotic systems for remote manipulation. Although intended primarily for robots to be used in outer space, the test bed could be adapted to the development of advanced terrestrial telerobotic systems for handling radioactive materials, dangerous chemicals, and explosives.

The test bed serves as an interface among the human operator, the human test conductor, and the telerobot for evaluation of the ability of the telerobot to perform such tasks as mechanical assembly and disassembly, mating electrical components, in-flight and preflight inspections, refueling, removal of debris, and rescues. The test bed contains subsystems for machine vision, teleoperation, autonomous control, and planning of motions. It is designed to facilitate enhancement with such features as operation with time delay, operation in cluttered surroundings, and dexterous manipulation by incorporation of commercially available cameras, computers, robot arms, and other equipment.

The operator control station of the test bed (see figure) includes two computer workstations equipped with video monitors, a stereo vision display, two force-reflecting hand controllers, emergency-halt buttons, and computers for the maintenance of internal status and communication with other subsystems.

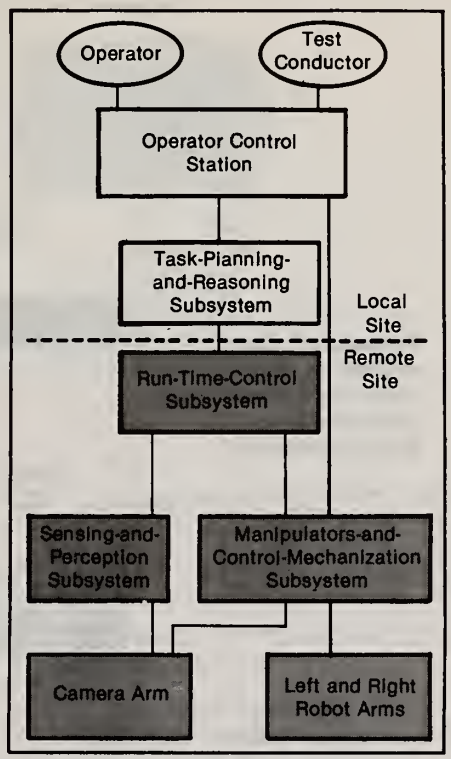

The **Test Bed Combines Features** not found in commercial systems. Its architecture allows easy growth in complexity and level of automation. The system is a national resource for the validation of new telerobotic technology.

A task-planning-and-reasoning subsystem gives the operator supervisory control over autonomous operations of the telerobot. It enables the operator to plan tasks and gross motions at a high level. It accepts task assignments and direct requests for action from the operator and translates high-level tasks into processes for remote execution by the run-time-control subsystem described in the next paragraph. It maintains a data base of objects in the workspace and the relationships between the objects and the capabilities of the telerobot.

The run-time-control subsystem provides fine-motion and grasp-planning commands for the arms of the telerobot. It detects collisions.

The sensing-and-perception subsystem furnishes the operator with up to five still or live video images. It provides machine-vision stereo images to its object calibration algorithms. It tracks moving objects, supplying estimates of the positions, orientations, translational velocities, and angular velocities of the objects to the task-planning-and-reasoning subsystem.

The manipulators-and-control-mechanization subsystem includes the robot arms and end effectors and force and torque sensors. It also includes universal control-

This work was done by Jacob R. Matijevic, Wayne F. Zimmerman, and Shlomo Dolinsky of Caltech for **NASA's Jet Propulsion Laboratory.**
NPO-17898/TN

FOR ADDITIONAL INFORMATION: *Contact: Director, Technology Transfer Division, P.O. Box 8757, BWI Airport, MD 21240; (301) 621-0100 Ext. 241*
REFER TO THE NUMBER LISTED AT THE END OF THIS ARTICLE

NASA Tech Brief
National Aeronautics and
Space Administration
Langley Research Center, Hampton, Virginia

Licensing Opportunity

Splicing Wires Permanently With Explosives

This technique produces superior, reliable splices.

An explosive joining process has been developed to splice wires by enclosing and metallurgically bonding the wires within copper sheets. Heretofore, in the manufacture of electrical equipment, small-diameter conductor wires have typically been spliced by brazing or soldering. Brazing has two disadvantages: the high temperatures locally anneal the wires and can cause wires to break, and the operators who perform the brazing operation must be highly skilled. Solder joints are not as strong as the wires. The joints made by the new explosive joining process exhibit many desirable characteristics, such as 100-percent conductivity and strength, no heat-induced annealing, no susceptibility to corrosion in contacts between dissimilar metals, and stability at high temperature. The new process could be used to join wires to terminals, as well as to splice wires.

The wires are spread in a plane in alternating fashion in the bundles to be joined (see figure). There is no limit on the number of wires and width. They are then slid into a U-shaped, prebent copper plate, wherein standoffs (any convenient material, such as tape) separate the wires from the plate. The ribbon explosive, which has previously been installed on the prebent plate and held in place by double-back tape, is then detonated by a blasting cap. The flat sections of the plate are driven into the wires in a high-velocity, angular impact, which effaces the oxide films from all surfaces to allow interatomic linkup of valence electrons.

Wires of two sizes [0.025 and 0.090 in. (0.64 and 2.3 mm)] were used with 0.030-in. (0.76-mm) copper plate, which was prebent to accommodate the different sizes and two 0.035-in. (0.89-mm) standoffs. The size of the ribbon explosive for the 0.025-in. wire was 20 grains/foot (4.2 g/m) and that for the 0.090-in wire was 30 grains/foot (6.4 g/m). The total amount of explosive used in this setup for a splice 1.5-in. (38-mm) wide is less than 1 g. After splicing, the excess copper sheet can be trimmed and the splice rolled for more convenient packaging.

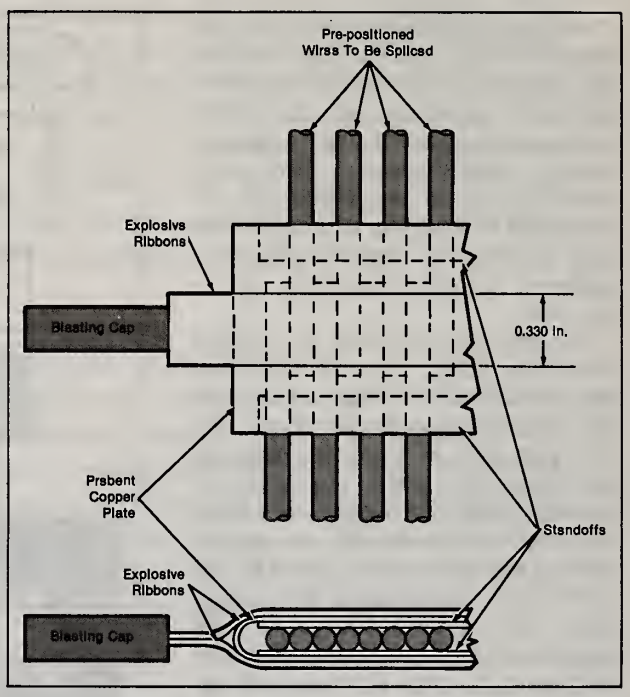

Multistrand Conductors, as well as single wires, can be readily joined with the explosive technique.

The splice produced by this technique is more reliable than are brazed or soldered splices. This technique is directly applicable to the telecommunications industry, in which literally millions of small wires are spliced annually.

This work was done by Laurence J. Bement of **Langley Research Center** *and Anne C. Kushnick of PRC Kentron.*

This invention is owned by NASA, and a patent application has been filed. Inquiries concerning nonexclusive or exclusive license for its commercial development should be addressed to the Patent Counsel, Langley Research Center. Refer to LAR-13825/TN.

Langley Research Ctr.
Technology Utilization
Officer John Samos
Mail Stop 139A
Hampton, VA 23665
Patent Counsel
George F. Helfrich
Mail Code 279
Hampton, VA 23665
(804) 864-3523

FOR ADDITIONAL INFORMATION: *Contact: Director, Technology Transfer Division, P.O. Box 8757, BWI Airport, MD 21240; (301) 621-0100 Ext. 241*
REFER TO THE NUMBER LISTED AT THE END OF THIS ARTICLE

NASA Tech Brief
National Aeronautics and
Space Administration
Langley Research Center, Hampton, Virginia

Making Large Suction Panels for Laminar-Flow Control

Perforated titanium panels are used to identify and resolve issues related to manufacture.

The attainment of laminar flow on the wings of aircraft has significant potential for reducing drag and increasing fuel efficiency. One way to maintain a large chordwise extent of laminar flow is to suck a small part of the boundary layer through the skin of a wing. This method, called laminar-flow control (LFC), can stabilize the boundary layer against small disturbances and delay the transition to turbulence. The basic theory is well established and has been verified in wind-tunnel tests and demonstrated in flight tests. Continuous suction through a porous surface is an effective means of delaying the boundary-layer transition. Until recently, however, it has been impractical to perforate airplane materials in production with holes of the small sizes required.

Recently, relatively large suction panels with aerodynamically satisfactory surface perforations and with the surface contours and smoothness characteristics necessary for LFC have been designed, fabricated, and tested. The requirements of production lines for commercial transport airplanes were carefully considered in the development of the panels. Much could be learned about the practicality of such panels for aircraft applications, inasmuch as the sizes of the panels are representative of what could be used on the wing of a commercial transport airplane. Tests of the perforated panels in a transonic wind tunnel demonstrated aerodynamic stability at flight mach numbers.

Three titanium suction panels were designed, developed, and manufactured for testing as the upper surface of a Langley 8-foot (2.4-m) Transonic Pressure Tunnel LFC model. The suction panels represent one of the largest perforated LFC structures ever built, with a chord as large as that of the wing of a general-aviation airplane. The 7- by 7-ft (2.1- by 2.1-m) titanium panels have an 0.8-percent open-area porosity ratio. The perforations are 0.0025-in. (0.064-mm) holes at 0.025-in. (0.064-cm) spacings.

The perforation was done by an electron-beam drilling process that is capable of making 1,000 holes per second. Each panel has a sandwich construction (see figure) with the titanium skin bonded to a corrugated fiberglass core (forming flutes for the subsurface transfer of airflow) and has a graphite inner face sheet. Impervious bond areas divide the surface of the panel such that suction through perforated strips occurs at the surface. Metering holes located in the bottoms of the suction flutes transfer flow to aluminum ducts, from which the flow leaves the tunnel. Ducts are attached to a wing-box support mounted on a wall of the tunnel.

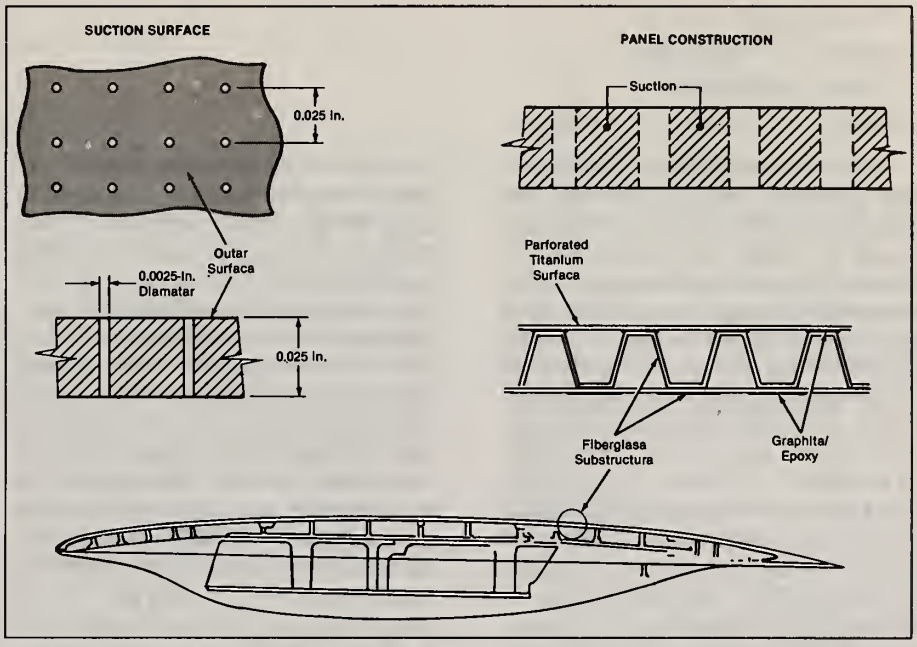

Large Titanium Suction Panels were fabricated by use of an electron-beam perforation drilling process and sandwich construction.

The distribution of pressure in the design of the airfoil incorporates the latest in the technology of supercritical flow and has a drag-divergence mach number comparable to those of modern turbulent airfoils. A significant region of supercritical flow exists on the upper surface. Features of the distribution of static pressure on the upper surface at the airfoil design point (mach number = 0.75, coefficient of lift = 0.55, Reynolds number = 20 million) include a short, steep favorable gradient near the leading edge, caused by the small nose radius, and a slightly adverse gradient over the majority of the chord, with the aft region exhibiting a Stratford-type recovery of pressure. Although the design Reynolds number for the perforated panels was 20 million, the design allows tests at Reynolds numbers as low as 8 million and as high as 40 million. Special development efforts were made to produce panels that meet LFC waviness criteria. The manufacturing tolerances of the test panels are considerably better than those attained in current production-line practice for turbulent aircraft. Critical issues related to the manufacture of large suction panels were identified and largely resolved. The techniques used to make the panels can be adapted to modern aircraft production lines.

This work was done by Dal V. Maddalon of **Langley Research Center**. *Further information may be found in NASA TM-89011 [N86-29815], "Design and Fabrication of Large Suction Panels with Perforated Surfaces for Laminar Flow Control Testing in a Transonic Wind Tunnel."*

Copies may be purchased [prepayment required] from the National Technical Information Service, Springfield, Virginia 22161, Telephone No. (703) 487-4650. Rush orders may be placed for an extra fee by calling (800) 336-4700. LAR-13844/TN

FOR ADDITIONAL INFORMATION: *Contact: Director, Technology Transfer Division, P.O. Box 8757, BWI Airport, MD 21240; (301) 621-0100 Ext. 241*

REFER TO THE NUMBER LISTED AT THE END OF THIS ARTICLE

Program Analyzes Errors in STAGS

This program assists in scrutiny of the output of the STAGS finite-element program for plates.

Estimation of the accuracies of stresses and deflections computed by the finite-element method is a common problem that arises with each new application of the method. The EAC computer program is designed for analysis of the errors in the results of the STAGS computer program (COSMIC Program HQN-10967), which is a finite-element code, for a shell unit consisting of a rectangular orthotropic plate. EAC requires input data for the geometry of the plate, the properties of the material, and a set of boundary conditions. These input data come from the STAGS code. (The specific link between the input and output data from STAGS and the input data for EAC is POSTP, the postprocessor program in the STAGS processors.) EAC computes a continuous solution from the discrete results of STAGS in order to estimate the error of the results of STAGS.

Currently, EAC can handle only one plate unit, at one load step of the execution of STAGS, using the noncorotation option. The finite-element-method solution from STAGS is assumed to be a valid zeroth approximation for starting the iterative solution of the shell equations. This solution forms the first step of execution of EAC, during the first phase of which the resulting general solution in the form of Fourier coefficients and constants of integration (generalized coordinates) are written to a temporary file. During the second phase, these data are read and are used to generate results at specified points on the plate, or over a grid defined by the user.

An option in EAC enables the user to reuse the data from this file saved from a previous execution of EAC to generate output data over a different output grid or at selected points on the plate unit. The results are written to two files. One file is used as the input data file for a contour-plotting postprocessor for EAC. The generalized coordinates allow for the computation of a continuous solution for the plate equations. The continuous solution has the obvious advantage that resultant stresses and deflections can be computed at any point on the plate and not only at grid points in STAGS. However, the main advantage of the continuous solution is that a measure of its error can be computed. The output of the code includes this measure of the error in the continuous solution, which is also an indirect measure of the error in the finite-element results in STAGS.

EAC has been implemented on a DEC MICROVAX II computer under VMS 4.7. It is written in FORTRAN 77 and has a central-memory requirement of 1369 kbytes. EAC was developed in 1988.

This program was written by Gaylen A. Thurston and Nancy Jane C. Bains of **Langley Research Center** *and Rajaram Sistla of Analytical Services & Materials. LAR-14063/TN*

FOR ADDITIONAL INFORMATION

CONTACT

COSMIC®
112 Barrow Hall
University of Georgia
Athens, GA 30602

(404) 542-3265

Program Generates Images of Solid Surfaces

Various shapes can be constructed and viewed from several perspectives.

The Solid Surface Modeler (SSM) computer program generates three-dimensional computer models of solid surfaces for use in visual analysis and animation. In addition to such basic software tools as Box and Cylinder, SSM provides advanced functions, including Constructive Solid Geometry, Skin Construction, Tube Construction, Material Property Editing, and Texture Map Tools. SSM allows a user to change such attributes as color, reflectivity, smoothing, and position of the object easily. The model can then be saved in ASCII or binary format for use in another program or saved in edit format for reloading in SSM.

When fully installed, SSM is menu-driven and can be run from any directory. The user can elect to use a mouse or a keyboard interface. Viewing choices include wire frame, solid surface, one-window orthographic, or four-window orthographic and perspective.

SSM was written in standard C with Silicon Graphic's Iris Graphics Library calls and AT&T PicLib calls. The program can be run with a minimum of 8 MB of random-access memory although 16 MB are recommended. SSM source and executable codes require a minimum memory of 3,346K bytes. The program is available for the Silicon Graphics IRIS workstation running version 3.1 of IRIX, and a Sun workstation with AT&T PXM964 running 4.2 bsd. Documentation is included on the tape. SSM was developed in 1989.

This program was written by Sharon P. Goza of **Johnson Space Center** *and Bradley Bell and David Shores of Barrios Technology.* *MSC-21630/49/TN*

FOR ADDITIONAL INFORMATION

CONTACT

COSMIC®
112 Barrow Hall
University of Georgia
Athens, GA 30602

(404) 542-3265

U.S. Navy Fact Sheet

Licensing Opportunity

Naval Underwater Systems Center

Optimum Flow Noise Cancelling Hydrophone Module

This hydrophone module rejects turbulence-induced flow noise for towed hydrophone arrays. Two adjacent hydrophones in the array are spaced less than flow noise coherence distance apart and form a flow noise cancelling module. The inverted acoustic/flow noise signal from the lead hydrophone of the pair is split. One side passes to the final state of signal processing while the other side—filtered, amplified, and inverted—is added to the combined signal from the lag hydrophone, which has been filtered and amplified. The acoustic signal components cancel, leaving only the lead hydrophone flow noise plus the lag hydrophone flow noise, which has been shifted by a factor dependent on tow vessel speed and hydrophone spacing. This flow noise signal is combined in an adder-inverter with the delayed feedback from the output stage of this same adder-inverter. The lag hydrophone flow noise cancels leaving only the flow noise of the lead hydrophone, which is then combined with the acoustic signal plus flow noise output of the lead hydrophone. The flow noise components cancel, yielding only the signal of interest, free of flow noise and undistorted by rain or phase shifts.

Patent Number 4,388,711

FOR ADDITIONAL INFORMATION: Margaret M. McNamara (Code 105), Naval Underwater Systems Center, New London, CT 06320-5594; (203)440-4590.

US Army Corps
of Engineers
Waterways Experiment
Station

Nondestructive Testing of Concrete with Ultrasonic Pulse-Echo

INTRODUCTION: Scientists at the U.S. Army Engineer Waterways Experiment Station (WES) recently developed hardware (patent pending) capable of "seeing into" concrete. Using a non-destructive, acoustic technique known as Ultrasonic Pulse-Echo or UPE, the equipment introduces ultrasonic stress waves into concrete electronically. Signal generation and detection is accomplished with piezoelectric crystals. The diagnostic capacity of this device represents a significant breakthrough for evaluating a difficult nonhomogeneous composite material such as concrete.

UPE is routinely use for metals testing, underwater detection and ranging (sonar), medical diagnosis, and testing and evaluating homogeneous and fine-grained materials. The WES developed system will work especially well on concrete walls or slabs up to 1 ft. thick. Concrete sea walls, pavements, walls, floors, parking garages, bridge decks, etc., are ideally suited for the device.

DEVELOPMENT: A literature search for nondestructive test methods for concretes revealed a need for more pulse-echo research. Commercial systems were not available. Prior pulse-echo research showed poor resolution due to long pulse lengths (high Q value) for transducers. Investigators also had problems with interfering Rayleigh waves at low frequencies, and signal-to-noise ratios (SNR) ranged from only about 2 to 6.

The WES research was part of the Repair, Evaluation, Maintenance and Rehabilitation (REMR) Research Program. Investigations resulted in the development of a pitch-catch system that operates at a center frequency of 200 kHz with a signal to noise ratio of 18. Mass and dimensions of the improved system have been reduced 90% from the prior state-of-the-art system. The WES system is able to measure thickness of portland-cement concrete floors and walls, and it can indicate the presence of voids to a depth of approximately 12 inches.

PRINCIPLE OF OPERATION: An ultrasonic (acoustic) wave is generated by exciting a piezoelectric material with a high-amplitude, transient electrical pulse from a high-voltage, high-current pulser. The short burst of ultrasonic energy from the crystal is transmitted into the concrete and impinges upon the various interfaces within. The change in acoustic impedance at the various interfaces, air voids, water-filled voids, reinforcing bars, cracks, delaminations and other interfaces or inclusions within the concrete causes a portion of the input energy to reflect (echo) back to the surface. That energy is detected by a second piezoelectric element. A larger portion of the energy continues to travel forward and strike other interfaces and return an amount of energy based on (1) the area of the reflecting surface, (2) the angle of the reflecting surface, and (3) the acoustic impedance of the reflecting material. The time for the echo to return is accurately measured by an oscilloscope.

The complete signal is stored on magnetic disc and can be retrieved at any time for further analysis. This applies especially to noisy signals, which can be brought back to the laboratory. There, digital signal processing (DSP) can be applied to recover hidden information.

It is well known that the ultrasonic pulse velocity of concrete is an indicator of its condition. For a known thickness of concrete (such as a bridge deck for example), the velocity, v, of the concrete can be determined by the equation $v = 2L/t$ where L = thickness of the concrete and $2L$ is the two-way travel distance of the ultrasonic pulse and t = time of arrival of backwall (BW) echo.

Generally, structural concrete will have a very narrow range of velocity when it is sound because structures generally consists of one concrete design mixture. When deterioration or microcracking has taken place the concrete will have a noticeably reduced velocity.

ADVANTAGES: UPE is nondestructive and can be used in the dry or underwater. Significant savings are gained by eliminating the bulk of coring that normally is needed for evaluation of concrete. UPE evaluation allows precise mapping of regions of quality concrete and regions that have deterioration. Since faulty zones can be pinpointed, repairs will be less expensive.

An important feature of UPE is the ability to monitor the condition of a structure over time. The first set of measurements (original construction and restored areas) serves as baseline data that can be compared with later measurements. The baseline data is stored on magnetic disc (fixed or floppy) and can be retrieved and plotted either over or adjacent to the new signals for comparison purposes. This ability to monitor the condition of a structure for years to come is important in investigating the causes of deterioration, the effectiveness of remedial repairs and the prevention of future problems.

LIMITATIONS: Considerable engineering judgment is needed to properly evaluate a measurement. Presently the system is limited to penetration depths of 1 ft.

FUTURE DEVELOPMENT: Research is ongoing (1) to develop a system that can penetrate to a depth of ten feet or more, (2) develop improved measurement criteria for deteriorated concrete, (3) develop new algorithms to retrieve hidden information in the signal using DSP, and (4) develop a real-time system so that DSP can be performed in the field rather than brought back to the laboratory.

POINT OF CONTACT:

Commander and Director
US Army Engineer Waterways Experiment Station
ATTN: CEWES-SC-CE/A. Michel Alexander
3909 Halls Ferry Road
Vicksburg, MS 39180-6199

Phone No.: 601-634-3237

NASA Tech Brief
National Aeronautics and
Space Administration
Langley Research Center, Hampton, Virginia

Licensing Opportunity

Apparatus for Tests of Percussion Primers

Tests are conducted under realistic conditions.

A test apparatus and method have been developed to measure the ignition capability of percussion primers. Since the 1815 invention of percussion primers, no test method has been generally accepted for measuring their output performance. Consequently, no specification, military or commercial, contains any requirements for this output.

The test method fills this technology void by providing an approach to quantify the ability of primers to ignite a small quantity of ignition material. This method closely simulates actual conditions and interfaces encountered in such applications as in munitions and rocket motors.

The figure, showing a cross section of the test chamber (bomb) illustrates the test conditions. The primer is installed into its holder, which in turn is held in place by an adapter. A 200-mg charge of FFG black powder is placed in the ignition-material holder, which is then inserted into the test cavity and held in place with a plug. A weight dropped onto the firing pin drives the pin into and ignites the primer. The primer output (heat, gas, light, and burning particles) is directed onto and ignites the black powder within the small volume of the cup in the ignition-material holder. The gas generated by the combustion of the black powder vents through six small holes from the cup into the test bomb cavity, where the resulting pressure is measured by the pressure transducers.

The firing-pin impact and pressure traces, recorded by a high-response tape deck, are analyzed to determine the function times and characterize the output performances of different types of percussion primers. The rate at which the flame spreads through, and combustion occurs in, the black powder is directly relatable to the type of primer. A "hot" output of high-pressure gases and burning particles produces a much faster burning of the black powder than does a "soft" output of low-pressure gases and no burning particles.

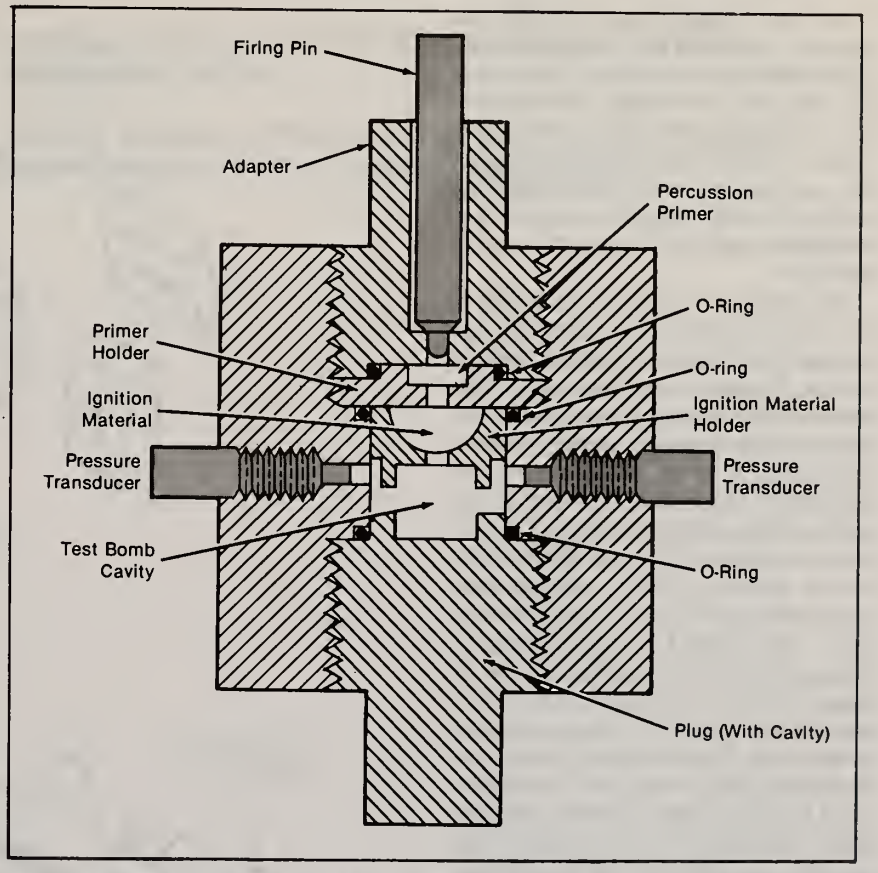

The **Ignitability-Testing Apparatus** is a small bomb instrumented with pressure transducers. The sizes, shapes, and positions of bomb components and materials under test can be selected to obtain quantitative data on ignition over a range of realistic operating conditions.

This work was done by Laurence J. Bement of **Langley Research Center** *James W. Bailey of PRC, and Morry L. Schimmel of Schimmel Co.*

This invention is owned by NASA, and a patent application has been filed. Inquiries concerning nonexclusive or exclusive license for its commercial development should be addressed to the Patent Counsel, Langley Research Center. Refer to LAR-13996/TN.

Langley Research Ctr.
Technology Utilization
Officer John Samos
Mail Stop 139A
Hampton, VA 23665
Patent Counsel
George F. Helfrich
Mail Code 279
Hampton, VA 23665
(804) 864-3523

FOR ADDITIONAL INFORMATION: *Contact: Director, Technology Transfer Division, P.O. Box 8757, BWI Airport, MD 21240; (301) 621-0100 Ext. 241*
REFER TO THE NUMBER LISTED AT THE END OF THIS ARTICLE

NASA Tech Brief
National Aeronautics and
Space Administration
Langley Research Center, Hampton, Virginia

Electro-optical Position-Measuring System

A nonintrusive system determines positions of models within the test section of a wind tunnel.

An electro-optical system has been developed to measure the five components of coordinates that represent the position and orientation of a model in the test section of a wind tunnel. This nonintrusive system, which is located entirely outside the test section, uses small lasers as sources of light and self-scanning linear photodiode arrays (LPDA's) as the sensing elements.

The optics of the system are arranged along the perimeter of the test section on adjustable rails to accommodate various models. The laser beams are shaped into sheets of light by small glass rods and collimated by plano-convex cylindrical lenses. A combination of plate beam splitters and first-surface mirrors at 45° are used in two of the optical paths, producing four sheets of light orthogonal to the test section. One pair of sheets of light is reflected from underneath the test section onto LPDA's 3 and 4 (see figure) for measurements of sideways position and yaw. Another pair of sheets is reflected across the test section onto LPDA's 1 and 5 for measurements of lift and pitch. The third sheet of light is reflected diagonally through the test section onto LPDA 2 for measurements of axial position. The LPDA's have 1-in. (2.54-cm) apertures and contain 1,024 discrete photodiodes each.

Each LPDA produces a video signal consisting of a train of recharge pulses proportional to the intensity of incident light on each of its 1,024 photodiodes. A signal conditioner converts only the pulses from saturated photodiodes into transistor/transistor-logic (TTL) form, ignoring anything below a predetermined level. Processing circuitry counts the TTL pulses and produces both binary and analog representations. The counters are updated at a rate of 256 Hz. When no model is present in the test section, all the LPDA's are fully illuminated, resulting in a count of 1,024 for each one. However, when a model obstructs the sheets of light, the locations of the resulting shadows on the LPDA's are used to determine the position of the model.

The system has been successfully installed and is currently operational in the 13-in. (33-cm) Magnetic Suspension and Balance System (MSBS) at NASA Langley Research Center. The useful full-scale ranges of the system are ±0.45 in. (±11.4 mm) and ±8° for linear and angular displacements, respectively. The system has an overall precision of ±0.002 in. (0.05 mm) and ±0.02° in linear and angular measurements, respectively. With improvements in measuring ranges, this type of electro-optical system can be adapted for use in other aerodynamic applications.

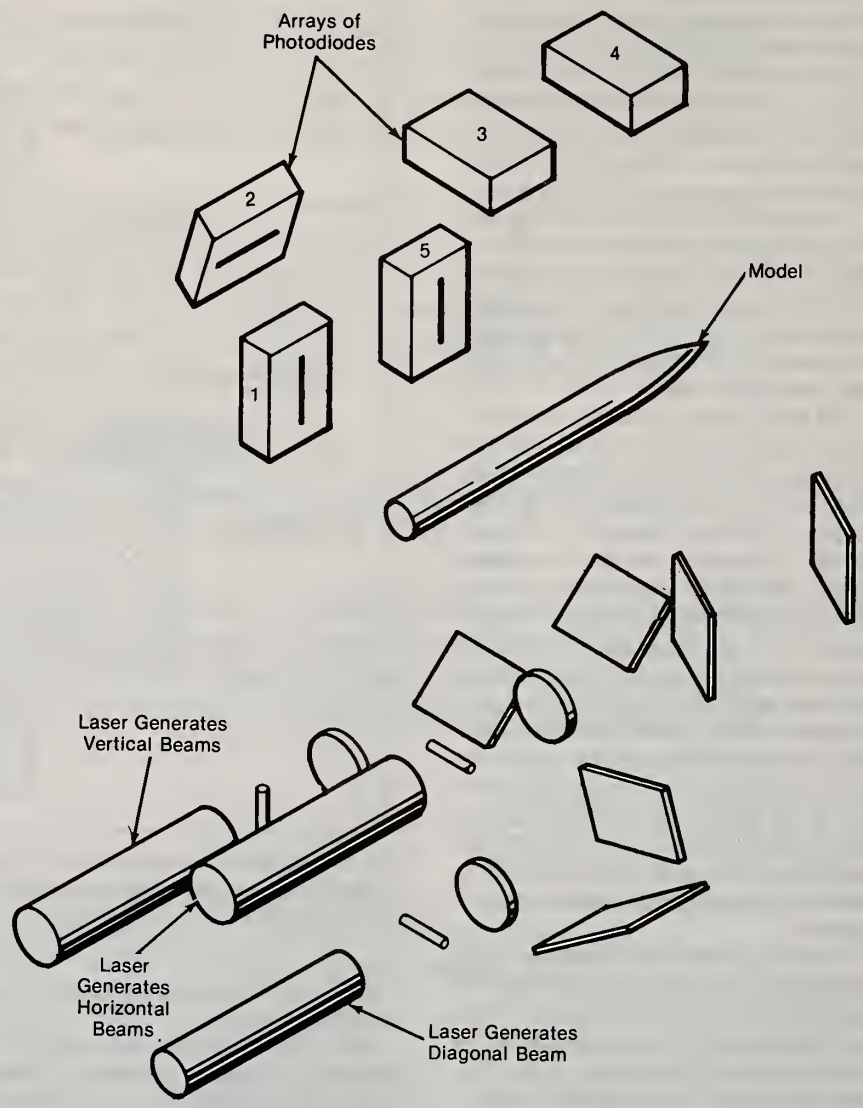

This **Electro-optical Five-Component Position-Measuring System** is used in the 13-in. Magnetic Suspension and Balance System at Langley Research Center.

This work was done by Ping Tcheng and Timothy D. Schott of **Langley Research Center.** *LAR-13840/TN*

FOR ADDITIONAL INFORMATION: *Contact: Director, Technology Transfer Division, P.O. Box 8757, BWI Airport, MD 21240; (301) 621-0100 Ext. 241*
REFER TO THE NUMBER LISTED AT THE END OF THIS ARTICLE

Environmental Science & Technology

0403 Design, Construction, and Evaluation of Clay Liners for Waste Management Facilities

0404 Treating Wastewater With Immobilized Enzymes—Urea and other contaminants are removed. (Licensing Opportunity)

United States
Environmental Protection
Agency
Research and Development

Risk Reduction
Engineering Laboratory
Cincinnati, OH 45268

EPA Project Summary

Design, Construction, and Evaluation of Clay Liners for Waste Management Facilities

This Technical Resource Document is a compilation of available information on the design, construction, and evaluation of clay liners for waste landfills, surface impoundments, and wastepiles. The information was obtained from the literature and from in-depth interviews with design and construction engineers and other knowledgeable individuals in both the private and government sectors. As a consequence, some of the information is being presented in print for the first time in this document. The broad topics covered are: clays, with emphasis on their composition, fabric, and hydraulic conductivity; the compatibility between clays and chemicals, including a discussion of the mechanisms of interaction and a comprehensive compilation of test data from the literature and private, unpublished sources; design and construction methodology and construction quality assurance; and clay liner transit time prediction models. The technical resource document also incorporates public comments received on a draft that was published in 1986.

This Project Summary was developed by EPA's Risk Reduction Engineering Laboratory, Cincinnati, OH, to announce key findings of the research project that is fully documented in a separate report of the same title (see Project Report ordering information at back).

Introduction

The U.S. Environmental Protection Agency (EPA) is developing three types of documents for preparers and reviewers of permit applications for hazardous waste facilities. These are RCRA Technical Guidance Documents, Permit Guidance Manuals, and Technical Resource Documents (TRDs).

The TRDs present state-of-the-art summaries of the technologies and evaluation techniques determined by EPA to constitute good engineering practices, designs, and procedures. They support the RCRA Technical Guidance Documents and Permit Guidance Manuals in certain areas (i.e., liners, leachate management, closure covers, and water balance) by describing current technologies and methods for designing hazardous waste facilities or for evaluating the performance of a facility design. Although emphasis is given to hazardous waste facilities, the information presented in these TRDs may be applied to nonhazardous waste facilities as well.

This is a TRD prepared by the Risk Reduction Engineering Laboratory of the Office of Research and Development at the request of and in cooperation with the Office of Solid Waste and Emergency Response. The TRD was first issued as a draft for public comment under the title, *Design, Construction, and Evaluation of Clay Liners for Waste Management Facilities* (EPA/530-SW-86-007) dated March 1986. The draft TRD was also made available through the National Technical Information Service (Order No. PB86-184496/AS). All comments received on the draft TRD have been carefully considered and, if appropriate, changes were made in this final document to address the public's concerns. With issuance of this document, all previous drafts of the TRD are obsolete and should be discarded.

The objective of this TRD was to provide, in a single document, all of the available information on the design, construction, and performance of clay lined waste management facilities. The broad topics that were covered are: clay properties and characteristics (chapter 2); geotechnical testing of soils (chapter 3); the compatibility of clays and chemical wastes (chapter 4); the design, construction, and construction quality assurance of clay liners (chapter 5); potential failure mechanisms (chapter 6); the performance of existing liner systems (chapter 7); and methods of predicting the useful life of liner systems (transit time) based on the modeling of leachate flow through soils (chapter 8).

Discussion

Chapter 2 of the TRD contains a general discussion of the structure of clay soils and continues on to a discussion of the main types of clay minerals (e.g., kaolinite, illite) and how clay soils were formed. A section on clay chemistry deals with the electrical double layer theory, cation-exchange capacity, and cation affinity. A short discussion of the significance of the double layer

theory to clay liners is also included. Other subjects discussed are related to clay soil fabric and hydraulic conductivity. These include soil porosity, macrostructure and secondary porosity, and the structure and hydraulic conductivity of compacted soils.

The third chapter presents the soil test methods currently used in the design and construction of clay liner systems. The chapter starts with a discussion of the fundamental relationships between the solid, liquid, and air phases of soil systems. The Atterberg limits and the methodology for determining them are discussed. The Unified Soil Classification System is presented in sufficient detail to provide the nontechnical reader with an understanding of how the system works. In the section on measuring density and moisture content in the field, the traditional methods are presented along with a detailed discussion of nuclear density gauges and the problems that can be encountered in their use on certain soils. Much of the chapter is devoted to describing the current methodologies employed in measuring the hydraulic conductivity of compacted clay soils in the laboratory and in the field. Included is a discussion of factors that can influence the results of permeability tests. The field permeability testing section contains descriptions of several new tests that have recently been introduced and thus have not been extensively discussed in the open literature.

In the fourth chapter, "Interactions Between Clays and Chemicals", the mechanisms of the interactions, and the effect they have on permeability are discussed. The bulk of the chapter presents the results of published and unpublished research studies, some of which are published for the first time in this document, having been obtained from the files of private soil testing firms. The studies are summarized in a large table organized on the basis of the chemical or waste stream that was tested. This table quickly references the effect that a given chemical can have on specific clays.

The fifth chapter of the document is a detailed discussion of the current practices employed in the design and construction of clay liner systems. Much of the information was obtained from interviews with design and construction professionals and appears in print for the first time in this TRD. All aspects of liner design and construction are discussed including site investigation, liner material selection, facility design, clay liner installation, and quality assurance and quality control.

Chapter 6 covers the mechanisms that potentially cause clay liner systems to fail. Mechanisms such as desiccation cracking, slope instability, freeze/thaw cycling and others are discussed theoretically, since there is little hard evidence to suggest which if any of these are consistent sources of failure in clay lined systems.

Information about the performance of clay liners is contained in chapter 7, which is a presentation and analysis of 17 case studies. The data for the sites were obtained from state and federal agencies, commercial waste disposers, clay liner design and construction firms, and the industrial sector. The information presented for each site includes geological and hydrogeological site characteristics, types of waste in the site, geotechnical characterization of the clay, leachate collection, leak detection, or groundwater monitoring data, physical description of the site, liner description, and construction methods used in building the liner.

Methods for predicting the useful life of a liner are described in chapter 8. Several mathematical models are presented for predicting the transit time of leachate through a compacted clay liner.

The full report was submitted in fulfillment of Contract No. 68-01-7310 by NUS Corporation under the sponsorship of the U.S. Environmental Protection Agency.

L.J. Goldman is with the NUS Corporation, Gaithersburg, MD 20878.
***Michael Roulier** is the EPA Project Officer (see below).*
The complete report, entitled "Design, Construction, and Evaluation of Clay Liners for Waste Management Facilities" (Order No. PB89-181 937/AS; Cost: $49.95) will be available only from:
National Technical Information Service
Springfield, VA 22161
Telephone: 703-487-4650
The EPA Project Officer can be contacted at:
Risk Reduction Engineering Laboratory
U.S. Environmental Protection Agency
Cincinnati, OH 45268

NASA Tech Brief
National Aeronautics and Space Administration
Marshall Space Flight Center, Alabama

Licensing Opportunity

Treating Wastewater With Immobilized Enzymes

Urea and other contaminants are removed.

Experiments have shown that enzymes can be immobilized on supporting materials to make biocatalyst beds for the treatment of wastewater. With a suitable combination of enzymes, the concentrations of various inorganic and organic contaminants, including ammonia and urea, can be reduced significantly.

The enzyme urease can be used to catalyze the decomposition of urea according to

$$\overbrace{NH_2CONH_2}^{\text{Urea}} + H_2O \xrightarrow{\text{Immobilized Urease}} 2NH_3 + CO_2$$

In an experiment, urease was immobilized on a 1,6-hexanediamine derivative of silica that had been activated by Ti(IV) ions. The immobilized-enzyme material was packed in a 7.1-cm^3 column. A solution of 30 mg/L urea was passed through the column at a flow of 2.5 cm^3/min, yielding a contact time of 2.8 min. Analysis of the first 29 liters of effluent showed that the column had catalyzed the reaction of nearly all measurable urea to NH_3 and CO_2.

The enzyme alcohol oxidase can be used to catalyze the decomposition of alcohols and formaldehyde. In an experiment, alcohol oxidase was immobilized on derivatized silica, and the immobilized-enzyme material was packed in a 35-cm^3 column. A solution of 50 mg/L methanol saturated with oxygen was pumped through the column at a flow of 5 cm^3/min, yielding a contact time of 7.1 min. Initially, the column removed all measurable methanol; it then began to lose activity because of degradation by H_2O_2.

To protect the alcohol oxidase, it is necessary to add enzymes that catalyze the decomposition of H_2O_2 in situ. One proposed way to do this is to coimmobilize the alcohol oxidase with catalase and superoxide dismutase on derivatized silica. When such a mixture was tested in a 30 cm^3 column at a flow of 3.4 cm^3/min (contact time 5 min), it removed 24 mg/L of ethanol from 3.2 L of 80 mg/L ethanol solution.

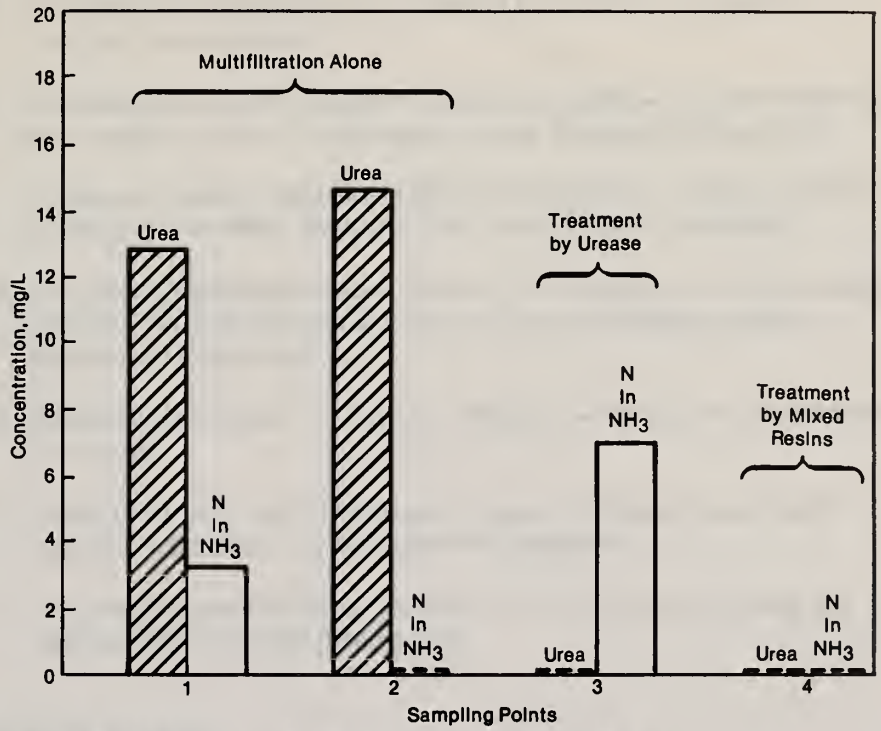

The **Concentrations of Nitrogen Bound in Ammonia and of Urea** are shown at various stages in the treatment of shower water. The limits of detection are 1.0 mg/L for urea and 0.1 mg/L for N in NH_3.

In a third experiment, a bed of immobilized urease and a bed of mixed resins were used to post-treat shower water that contained 15 mg/L urea and had been treated conventionally by multifiltration. As the figure shows, multifiltration did not remove urea from the water, but treatment by the column reduced the concentration of urea to below measurable levels. After further treatment by the bed of mixed resins, the concentrations of all of the carbon bound in inorganic compounds (principally CO_2) and of the ammonia from the decomposition of the urea were reduced below measurable levels. The total concentration of carbon bound in organic compounds in the effluent was 3.3 mg/L.

This work was done by Clifford D. Jolly of Umpqua Research Co. for **Marshall Space Flight Center.**
MFS-26090/TN

George C. Marshall Space Flight Center
Technology Utilization Officer: Ismail Akbay
Code AT01
Marshall Space Flight Center,
AL 35812
(205) 544-2223
Patent Counsel:
Leon D. Wofford, Jr.
Mail Code CC01
Marshall Space Flight Center,
AL 35812
(205) 544-0024

FOR ADDITIONAL INFORMATION: *Contact: Director, Technology Transfer Division, P.O. Box 8757, BWI Airport, MD 21240; (301) 621-0100 Ext. 241*
REFER TO THE NUMBER LISTED AT THE END OF THIS ARTICLE

Manufacturing, Machinery & Tools

0405 The One Part - One Part Number - One Drawing Standardization System

0406 Superplastic Forming/Diffusion Bonding For Low-Cost Advanced Titanium Missile Inlets

0407 Eliminating Unbonded Edges in Explosive Bonding—A notch in the flyer plate eases removal of unbonded material. (Licensing Opportunity)

0408 Electrical-Discharge Machining With Additional Axis—Benefits include enhanced flexibility of operation and reduced cost of machining.

0409 Fast, Nonspattering Inert-Gas Welding—A conceptual technique would combine the best features of three previous arc-welding methods. (Licensing Opportunity)

0410 Improved Computation of Dynamic Stresses—The cost of computation is reduced.

0411 Model of Bearing With Hydrostatic Damper—The model accurately represents the nonlinear aspects of the dynamics.

0412 Plasma Spraying Reclaims Compressor Housings—Metal coats are deposited on worn and pitted areas.

Other Items of Interest

0373 New EMPF Electronics Manufacturing Learning Center

0423 Preventing Vapor Deposition of the Backs of Substrates—This technique has been applied in the selective deposition of silicon on silicon carbide. (Licensing Opportunity)

Department of Defense Reliability Analysis Center

Rome Air Development Center, Griffiss AFB, NY 13441

The One Part - One Part Number - One Drawing Standardization System

The One Part - One Part Number - One Drawing (OPOPNOD) system combines the benefits of the Standardized Military Drawing Program (SMDP), which seeks elimination of Specification Control Drawings (SCDs) and more timely preparation of documents, with the potential availability of higher-reliability devices, as in the JAN program. The system benefits all involved. The device manufacturer will be able to provide all of the reliability levels to the same drawing. The Original Equipment Manufacturer (OEM) will have a better chance of receiving more reliable devices at the time of selection. If the highest-reliability part is not available, a non-JAN compliant device can be procured until the more reliable JAN device is available. In addition, the DoD will have only one documentation system to control.

History and Rationale

At the beginning of the Standardized Military Drawing Program in 1986 there were two levels of reliability: JAN (in accordance with MIL-M-38510) and non-JAN compliant with MIL-STD-883 paragraph 1.2.1 (primarily off-shore devices) and one government microcircuit general specification (MIL-M-38510). The non-JAN compliant parts were covered by SMDs which provided piece part replacement information for higher quality MIL-M-38510 devices. JAN devices were covered by military detail specifications. Maintaining two separate numbering and documentation systems was burdensome but controllable.

In 1989 two new microcircuit general specifications, MIL-I-38534 and MIL-H-38535, were released. Neither document contained a part numbering system. This unusual situation occurred because it was planned that the SMD would provide this system. It became apparent that a capability to easily transition from one device class to another was needed, and that this could be accomplished through use of the SMD and the part number itself.

The four military requirements documents represent different device classes. Previously when a device manufacturer upgraded military product from one class to another the benefits of the upgraded product were unavailable to the OEM due to contractual and system constraints (e. g. the parts list, assembly drawings, and bill of materials). With the establishment of the OPOPNOD system the OEM can procure the highest class level available for a given generic device without modifying the original contract parts selection criteria. For example, with one substitution statement the OEM can procure a class M level device (compliant to MIL-STD-883 1.2.1) for pre-production and procure the JAN or QML level device for production without changing applicable documentation.

New Part Number Format

The OPOPNOD numbering system is as follows:

5962	-	XXXXX	01	B	X	X
↑ Federal stock class designator	↑ RHA designator		↑ Device type	↑ Device class designator	↑ Case outline	↑ Lead finish

Figure 1: OPOPNOD part number

In transitioning between device classes, the only character in the part number that must be changed is the device class designator. This will be a single letter identifying the product assurance level, as shown below.

Device class	Device requirements documentation
B or S	Certification and qualification to MIL-M-38510
Q or V	Certification and qualification to MIL-I-38535
H or K	Certification and qualification to MIL-H-38534
M	Vendor self-certification to the requirements for non-JAN class B microcircuits in accordance with paragraph 1.2.1 of MIL-STD-883, and described by an SMD.

Figure 2: Device class designator

Benefits of the OPOPNOD system extend beyond OEMs and device manufacturers. The system combines the four different procurement specifications needed for the four requirements documents (MIL-M-38510, MIL-I-38534, MIL-H-38535, and MIL-STD-883 paragraph 1.2.1) into two

boilerplates. One covers monolithic device classes M, B, S, Q, and V; the other covers hybrid device classes H and K. This allows a device manufacturer to standardize on the MIL-STD-883/1.2.1 "off-the shelf" device immediately and to eventually qualify to higher reliability levels with little or no change to the document. This facilitates qualification of higher reliability parts, and also allows the device manufacturer to sell to all device classes on a drawing. This enables a device manufacturer to satisfy a variety of OEM requirements. The OEM, through the registered users list maintained by DESC, will have greater exposure to and control of changes made to the document involving any device class.

One device manufacturer has already taken full advantage of the OPOPNOD system. DESC is currently converting about 20 existing SMDs so that devices may be qualified under MIL-M-38510 and eventually under MIL-I-38535. The devices will then be available at all class levels (M, B, S, Q, and V) to meet OEM needs.

Generation of SMDs

Generation of an SMD is simple. DESC recommends, through the Military Parts Control Advisory Group system, the enforcement of OEM contractual obligations to prepare SMDs in lieu of SCDs. In preparing an SMD the OEM ensures that the content of the drawing satisfies their system needs. Usually the device manufacturers, who are most familiar with the device to be covered, prefer to prepare the drawing as soon as the device is available. The advantage of this is that the parts are available to the SMD when the OEM identifies a need rather than requiring the OEM to begin preparing an SMD at that time.

SMD boilerplate is available in electronic format to expedite preparation. This provides general requirements for all the device classes and the format for delineating unique requirements for a given device. Preparation time decreases further when the preparer submits an electronic copy of the drawing using the current boilerplate. This can be transmitted by modem to DESC or submitted by mail on a diskette. Preparation time is considerably longer if a drawing is not submitted electronically.

Before starting an SMD project, DESC should be contacted to determine if the device in question is a candidate for standardization. Points of contact for various device types are listed below. Once the preliminary SMD is completed and submitted to DESC the total preparation time, including the coordination and editing cycles, has averaged six months. The length of this cycle is almost totally controlled by the OEM's need and by the device manufacturer's ability to furnish complete electrical performance data to DESC on a timely basis.

The SMD boilerplate is available in electronic format 24 hours a day on the SMDP electronic bulletin board system (BBS). The phone number is (513) 296-6046. The BBS is an IBM-compatible system loaded on a Zenith 248. Logon instructions are provided upon initial access. A daily 40 minute time limit is allocated for each use. Parameter settings and other information which can be found on the bulletin board are listed in figure 3.

SMDP Electronic Bulletin Board

Phone number: (513) 296-6046

Parameter settings:	*1200 bps*	*8-bit data word*
	no parity	*1 stop bit*

Files available:

1. *Radiation Hardness Assurance, hybrid, Qualified Manufacturer's List, standard SMD boilerplates.*
2. *QPL-38510, QML-38534, QML-38535, Qualified Products List.*
3. *MIL-STD-1562 Military Standard: List of Standard Microcircuits.*
4. *Specifications and drawings in progress.*
5. *MIL-BUL-103 Military Bulletin: List of Standard Military Drawings.*
6. *MIL-M-38510 Supplement.*
7. *Personnel: name, technology area, and telephone.*
8. *MIL-STD-883 notices; MIL-M-38510 amendments.*

Figure 3: Bulletin Board Information

The OPOPNOD program was started in January 1990. To date 41 drawings have been completed and 64 drawings are currently in process. Any questions regarding this system can be directed to Monica Poelking or Greg Pitz, DESC-ECS, at (513) 296-5377.

Superplastic Forming/Diffusion Bonding For Low-Cost Advanced Titanium Missile Inlets

A program has been recently completed that demonstrated innovative fabrication techniques to produce complex titanium airframe components in a cost effective manner. The Expanded Tube Titanium Inlet With Titanium Matrix Composite Program (N60530-85-C-0071) was sponsored by the Naval Weapons Center and performed by LTV Missiles and Electronics Group, Missiles Division. The objective of the program was to demonstrate the feasibility and payoff of the use of a superplastic forming (SPF) technique, designated the Expanded Tube process, for titanium component fabrication in combination with diffusion bonding (DB) of metal matrix composite (MMC) local reinforcement. The Expanded Tube process, developed and patented by LTV, utilizes superplastic forming of low cost titanium tubular blanks to achieve near-net shapes of variable cross-sections. Titanium MMC or conventional titanium doublers can be selectively located in strategic places of the assembly and diffusion bonded in place in the assembly concurrent with the SPF forming operation to increase the structural efficiency of the final component. This technique offers the potential for economical production of missile components while the local reinforcement provides strength and stiffness improvements for valuable structural weight savings.

The program demonstrated the process by applying it to a full-scale advanced missile structural component. A study was performed to determine which specific missile component would be sufficiently complex to fabricate and show a high payoff from a cost and weight viewpoint. A fuel tank, a transition body section, and an inlet were evaluated. The inlet was selected. The inlet is a typical integral rocket-ramjet inlet that has a highly-variable rectan-

SPF/DB Missile Inlet

gular-to-circular transitioning main duct and complex by-pass air ducts coupled to the inlet body. To control deflections, a splitter is required down the centerline of the main duct. The manufacture of the baseline duct required the fabrication and assembly of numerous individual parts. The detail fabrication, machining, mechanical fastening, and welding of these parts resulted in high component costs.

The inlet was redesigned with local MMC reinforcement for the SPF fabrication process. Finite element analysis verified positive margins for stress and deflections. The local reinforcement sufficiently stiffened the main duct to permit removal of the splitter, resulting in a more efficient inlet with higher pressure recovery. Inlet contour data was fed directly to numerically controlled mills for machining of the SPF dies.

The titanium inlet was fabricated utilizing SPF/DB for the main duct, SPF for the by-pass air ducts, and SPF for the upper ramp. Other details were machined from sheet stock and subsequently welded to the assembly. The main duct utilized the expanded tube process. A tubular titanium blank was fabricated and slightly preformed to fit into the SPF dies. MMC reinforcements were located in proper locations in the SPF die. The die was then heated and the tube was pressurized (expanded). As the expanding tube filled the die, it contacted and diffusion bonded to the local reinforcement. The completed duct was then cooled and removed. Conventional single sheet SPF processes were used for the other SPF details.

The completed inlet is shown in the figure below. The inlet met the weight predictions and was lighter than the baseline duct. The successful completion of this program demonstrated the feasibility and the utility of innovative fabrication approaches to lower cost and increase performance of advanced missile components.

For further information contact:
LTV Missiles and Electronics Group
Mr. David Hunn
Program Operations Manager
(214) 266-1842

NASA Tech Brief
National Aeronautics and Space Administration
Langley Research Center, Hampton, Virginia

Licensing Opportunity

Eliminating Unbonded Edges in Explosive Bonding

A notch in the flyer plate eases removal of unbonded material.

An explosive-bonding technique eliminates the sharp unbonded notch that normally occurs between the flyer plate and baseplate. The new technique makes it possible to simply break away the unbonded outer extremity of the flyer plate; it is no longer necessary to grind away the unbonded edge to prevent the collection of corrosive contaminants in edge voids.

In the previous standard explosive-bonding method, the limit of the bonded area is not well defined; in repeated bonding cycles in the same setup, the bonded area varies, and its edge cannot be predicted precisely. To be sure that the bonded area extends at least to the prescribed limit, the flyer plate must overlap the baseplate well beyond that limit. Then, after bonding, nondestructive ultrasonic inspection is used to determine where the limit of the bonded area actually lies, and the unbonded edge of the flyer plate is ground away to that point.

In the new method, a notch is cut in the flyer plate and filled with a material that has properties similar to those of the flyer plate (see figure). The filler is held in place by an adhesive. As is usual in Langley Research Center's explosive seam-welding process, the flyer plate is prebent to give it the optimum high-velocity collision angle. Double-backed tape holds the ribbon explosive in place, centered over the bend line.

When the explosion in the ribbon is detonated, it generates a pressure wave that drives the flyer plate against the baseplate

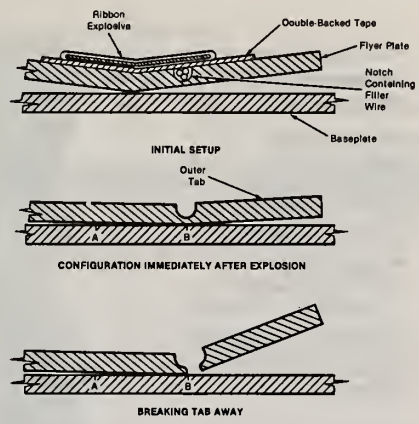

The **Bent, Notched Flyer Plate** is set up for explosive bonding (top). After detonation, thenotch is empty, and the flyer plate is bonded to the baseplate between points A and B (center). The outer part ofthe flyer plate is bent like a lever to separate it from the bonded part (bottom). The ribbon explosive (and the bond) extend perpendicularly to the plane of the paper.

so that the plates bond between edges A and B. The force of the explosion fractures the adhesive and jettisons the filler material, leaving an empty notch. The loose edge of the flyer plate can now be bent so that it breaks at the base of the notch, which coincides with the limit of the bonded area. A clean, void-free edge is thus formed.

The method has been used to bond tantalum plates 0.064 in. (1.63 mm) thick. Three strands of solid lead solder wire were used as the filler. The plate was bent to make an angle of 2.5° with the baseplate on both sides of the vertex. The notch was cut by a hemispherical end mill 0.060 in. (1.52 mm) in diameter, to a depth of 0.040 in. (1.02 mm).

Other plate materials can be similarly joined by optimizing the bonding parameters: location, shape, and depth of the notch; the filler material; bend angle and thickness of the flyer plate; and the amount and placement of explosive. For simplification, the flyer plate would not be bent, and masking tape would be applied to separate the plates outside of the notch. The explosive would be initiated as before, and the outer tab of the flyer plate would be bent as before to break it off at the notch. The method is not limited to flat surfaces.

This work was done by Laurence J. Bement of **Langley Research Center** *and Anne C. Kushnick of PRC.*

This invention is owned by NASA, and a patent application has been filed. Inquiries concerning nonexclusive or exclusive license for its commercial development should be addressed to the Patent Counsel, Langley Research Center. Refer to LAR-14096/TN.

Langley Research Ctr.
Technology Utilization
Officer John Samos
Mail Stop 139A
Hampton, VA 23665
Patent Counsel
George F. Helfrich
Mail Code 279
Hampton, VA 23665
(804) 864-3523

FOR ADDITIONAL INFORMATION: *Contact: Director, Technology Transfer Division, P.O. Box 8757, BWI Airport, MD 21240; (301) 621-0100 Ext. 241*
REFER TO THE NUMBER LISTED AT THE END OF THIS ARTICLE

NASA Tech Brief
National Aeronautics and
Space Administration
Marshall Space Flight Center, Alabama

Electrical-Discharge Machining With Additional Axis

Benefits include enhanced flexibility of operation and reduced cost of machining.

A proposed electrical-discharge-machining (EDM) apparatus would use a movable vertical wire as its electrode. The wire would be positionable horizontally along one axis as it slid vertically past the workpiece. The workpiece would be indexed in rotation about a horizontal axis.

The apparatus was proposed to make crenelated cylindrical parts, as shown in the figure. Because of the symmetry of the parts, the wire EDM process can be used to make two such parts at a time by defining the boundary between them. One advantage is that the cost of material is reduced because two such parts can be made from a forging only slightly larger than a forging used to make one such part by conventional machining with a cutting tool.

Another advantage is that wire EDM imparts less residual stress to the workpiece than conventional machining does. Yet another advantage is that less time is spent machining each part when the parts are produced in such symmetrical pairs.

This work was done by Roger M. Malinzak and Gary N. Booth of Rockwell International Corp. for **Marshall Space Flight Center.** *MFS-29630/TN*

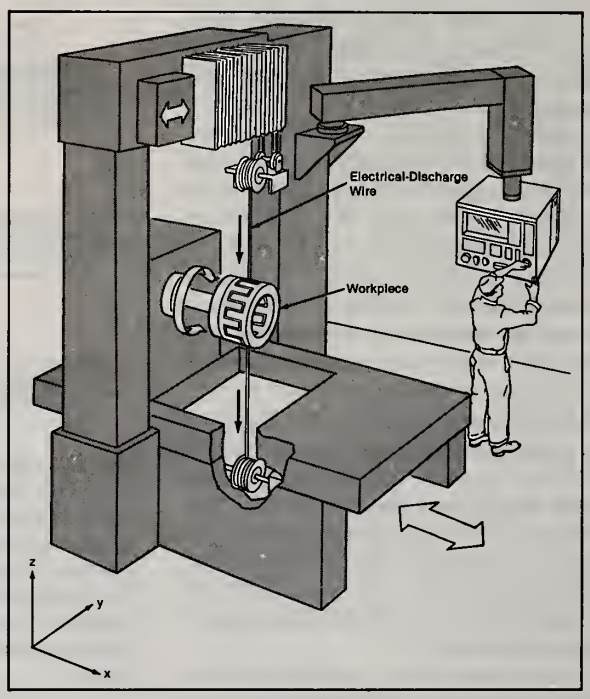

The **Upper End of the Electrical-Discharge Wire** is moved parallel to the y axis as it unrolls parallel to the z axis. Meanwhile, the workpiece is indexed in rotation about an axis parallel to the x axis and moved linearly back and forth in the x direction. The electrical discharge cuts the crenelated pattern in the workpiece.

FOR ADDITIONAL INFORMATION: *Contact: Director, Technology Transfer Division, P.O. Box 8757, BWI Airport, MD 21240; (301) 621-0100 Ext. 241*
REFER TO THE NUMBER LISTED AT THE END OF THIS ARTICLE

NASA Tech Brief
National Aeronautics and
Space Administration
Marshall Space Flight Center, Alabama

Licensing Opportunity

Fast, Nonspattering Inert-Gas Welding

A conceptual technique would combine the best features of three previous arc-welding methods.

A proposed welding technique would combine the best features of metal (other than tungsten)/inert-gas welding, plasma arc welding, and tungsten/inert-gas welding. The technique would offer these advantages:

- Wire fed to the weld joint would be preheated; it could therefore be fed at high speed without spattering.
- High-frequency energy would not have to be supplied to the workpiece to initiate welding.
- The size of the arc gap would not be critical; a power-supply control circuit would adjust the voltage across the gap to compensate for changes.
- Only a low gas-flow rate would be needed.
- The welding electrode could be replaced easily as a prefabricated assembly.
- An external wire-feeding manipulator would not be needed.
- The welding process would be relatively forgiving of operator error.

The welding electrode would be a hollow tungsten rod containing a coaxial insulating tube (see figure). A mechanism would feed wire along the inside of the tube. The wire would emerge from the chamfered tip of the rod and enter the weld puddle. An inert gas would enter the insulating tube via a porous sintered diffusing ring and flow along the tube to the welding tip. As it emerged from the tip, the gas would be ionized by a radio-frequency voltage applied across the gap between the wire and the hollow tungsten electrode. The plasma thus created would preheat the wire, provide an ionizing medium for initiation of the welding arc, and protect the wire and the hot welded metal from oxidation.

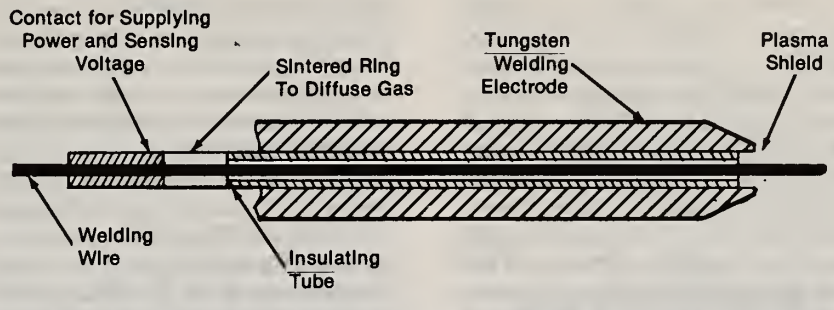

A **Welding Wire Would Pass** along the hollow core of a welding-rod assembly. The gas surrounding the wire would become ionized at the tip of the rod. The rod would be about 3/8 in. (9.5 mm) in diameter.

As in plasma welding, two power supplies would be needed. One would furnish the welding power to the wire, and the other would energize the plasma. The welding power would be applied and the welding voltage sensed via a copper contact tube integrated into the electrode structure, as in metal/inert-gas welding.

This work was done by Jeffrey L. Gilbert of Rockwell International Corp. for **Marshall Space Flight Center.**
MFS-29648/TN

George C. Marshall Space Flight Center
Technology Utilization Officer: Ismail Akbay
Code AT01
Marshall Space Flight Center,
AL 35812
(205) 544-2223
Patent Counsel:
Leon D. Wofford, Jr.
Mail Code CC01
Marshall Space Flight Center,
AL 35812
(205) 544-0024

FOR ADDITIONAL INFORMATION: *Contact: Director, Technology Transfer Division, P.O. Box 8757, BWI Airport, MD 21240; (301) 621-0100 Ext. 241*
REFER TO THE NUMBER LISTED AT THE END OF THIS ARTICLE

NASA Tech Brief
National Aeronautics and
Space Administration
Marshall Space Flight Center, Alabama

Improved Computation of Dynamic Stresses

The cost of computation is reduced.

A method that combines a modified computational procedure with a preprocessing and a postprocessing program yields additional data and reduces the time and cost of using the DYNRE1 module of the STARDYNE computer program to compute distributions of stresses in machinery under dynamic loads. The development of the method was motivated by some of the limitations of DYNRE1; namely, (1) it can compute no more than 500 components of stress in one run, (2) it does not compute von Mises stresses and (3) it does not compute frequencies.

Heretofore, because of limitation 1, it was necessary to make several relatively expensive DYNRE1 runs for each operating speed of the machine in question when the number of components of stress to be computed was large. With the modified procedure and the additional programs, only one DYNRE1 run is needed for each operating speed. The postprocessing program, which costs much less to execute, computes the additional components of stress. The new method also overcomes limitations 2 and 3 by computing von Mises stresses and the frequencies of the components of stress.

The first step of the procedure is to use the preprocessing program (called "PROGS3") to modify the dynamic-characteristics file (called "TAPE4") in the STARDYNE code. PROGS3 adds dummy nodes and the consequent dummy degrees of freedom and dummy modal displacements and stores the results in a new file (called "TAPE44").

In the second step of the procedure, one uses TAPE44 from the first step as input to DYNRE1 and runs DYNRE1 to compute the displacement history for each dummy node and degree of freedom. These displacements represent the contribution of each mode at each time point of the computation. They are used as input for the postprocessing program.

In the third step, the postprocessing program (called "PROGS4") performs matrix multiplication of the dummy displacement histories by the appropriate modal stresses to obtain stress histories. From the average number of zero crossings of each component of stress per unit time, PROGS4 computes its frequency. From the components of stress in any element at a given time, PROGS4 computes the von Mises stress history of that element.

This work was done by Tarun K. Ghosh of Rockwell International Corp. for **Marshall Space Flight Center.**
MFS-29745/TN

FOR ADDITIONAL INFORMATION: *Contact: Director, Technology Transfer Division, P.O. Box 8757, BWI Airport, MD 21240; (301) 621-0100 Ext. 241*
REFER TO THE NUMBER LISTED AT THE END OF THIS ARTICLE

NASA Tech Brief
National Aeronautics and
Space Administration
Marshall Space Flight Center, Alabama

Model of Bearing With Hydrostatic Damper

The model accurately represents the nonlinear aspects of the dynamics.

An improved mathematical model of the rotational and vibrational dynamics of a bearing package in a turbopump incorporates the effects of a hydrostatic damper. This model is part of a larger finite-element model that represents the rotational and vibrational dynamics of the rotor and housing of the pump. The previous mathematical model did not contain enough detail of the bearing package to define the effects of the hydrostatic damper explicitly. The improved model includes representations of the deadband and the nonlinear stiffness and damping of the ball bearings, the nonlinear stiffness and damping of the hydrostatic film, and the stiffness of the bearing support.

The hydrostatic damper is a stiff hydrostatic film that forms in the ~0.001-in. (~0.025-mm) radial gap between the outer surface of the cartridge and the inner backup support that holds the cartridge. There is a 0.0005-in. (0.013-mm) radial deadband between the outer races of the ball bearings and the mating inner cylindrical surfaces of the cartridge (see Figure 1). In normal operation, fixed loads on the rotor exceed the dynamic loads, and the bearing package operates fully engaged at one side of the deadband clearance.

The mathematical model of the bearing package incorporates nonlinearity through piecewise-linear representations of the coefficients of stiffness (K) and damping (C) as functions of deflections of the various components. For each segment of the piecewise-linear representation of the overall equivalent stiffness ($K_{equivalent}$), the stiffnesses of the ball bearings, hydrostatic film, and backup support are combined as though these components were springs in series (see Figure 2). The relative deflections of components of the bearing package at which changes in stiffness occur are then defined.

The amount of radial deflection between the rotor and the housing is related to the deflection of the damper via the bottom equation in Figure 2. The deflection required to "bottom out" the hydrostatic damper can be determined from this equation. For deflections greater than this value, the piecewise-linear curve of equivalent stiffness is then defined by combining only the stiffnesses of the ball bearings and backup support (that is, by treating the stiffness of the hydrostatic damper as though it were infinite).

The improved mathematical model enables the incorporation of the effects of the hydrostatic damper into the overall rotor-dynamic mathematical model without the addition of a mathematical submodel of a major substructure. The improved model was used in an analysis that led to a proposed design in which the damping of rotor vibrations was increased significantly over that of the current design. In the proposed design, the dynamic loads on the bearing would be reduced by as much as 70 percent and the worst-case stability-threshold speed would be increased from 38,200 rpm to more than 50,000 rpm.

This work was done by David G. Goggin of Rockwell International Corp. for **Marshall Space Flight Center.**
MFS-29654/TN

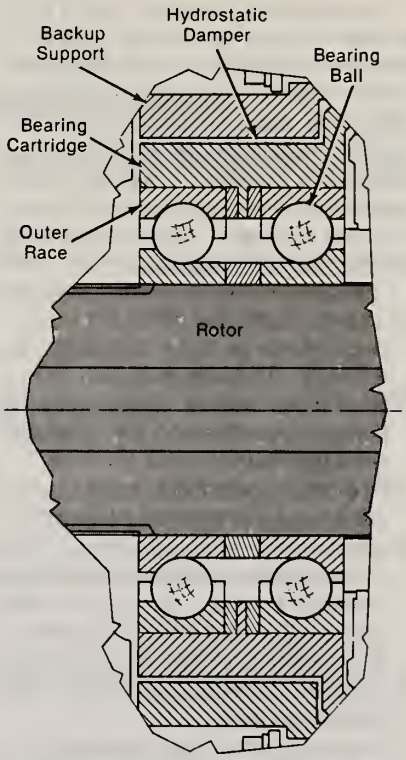

Figure1. The **Bearing Package**, shown here in simplified form, supports the rotor shaft.

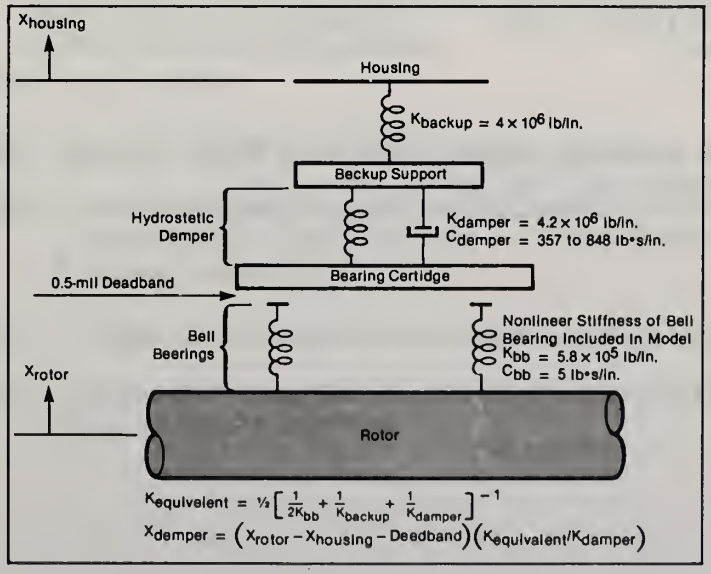

Figure 2. The **Mathematical Model of the Bearing Package** represents the stiffness, damping, and deadband characteristics of the bearing and hydrostatic damper.

FOR ADDITIONAL INFORMATION: *Contact: Director, Technology Transfer Division, P.O. Box 8757, BWI Airport, MD 21240; (301) 621-0100 Ext. 241*
REFER TO THE NUMBER LISTED AT THE END OF THIS ARTICLE

NASA Tech Brief
National Aeronautics and
Space Administration
Lewis Research Center, Cleveland, Ohio

Plasma Spraying Reclaims Compressor Housings

Metal coats are deposited on worn and pitted areas.

Plasma spraying has been found to be an effective technique for the addition of metal to out-of-tolerance magnesium-alloy turbine-engine compressor housings. Without the plasma-spraying process, the housings could not be reclaimed. The plasma-spraying process is used to build up material in worn and pitted areas. The newly applied material is then remachined to the specified surface contours.

The reclamation procedure can be summarized as follows:

1. Disassemble, clean, remove paint from, and degrease the housing.
2. Place the housing on a suitable locating fixture on a vertical turret lathe or equivalent machine tool.
3. Place a template of the desired contour in the trace section of the turret lathe.
4. Machine the affected areas of the housing to contours that provide for the subsequent plasma spraying and final machining to result in minimum plasma-spray buildups of 0.017 in. (0.43 mm).
5. Treat all machined surfaces with chromic acid solution.
6. Degrease in trichloroethylene vapor.
7. Set the plasma-spraying gun to the specified current, voltage, gas pressures and other operating parameters for the application of a Ni-5Al (parts by weight) composite bond coat.
8. Blast the affected areas with angular steel grit. Remove residual grit and foreign particles with clean, dry air.
9. Apply the specified tape or brush-on maskant to prevent deposition on the areas not to be built up.
10. Position the plasma-spray gun 5 in. (12.7 cm) from and aimed perpendicularly at the surface to be treated. Load the powder feeder with the powdered-metal ingredients of the bond coat.
11. Plasma-spray the bond coat at a rate of 0.0004 to 0.0006 in. (0.01 to 0.015 mm) per pass to obtain a buildup of 0.004 to 0.006 in. (0.1 to 0.15 mm).
12. Set the gun to the specified operating parameters for the application of a Al-12 Si alloy (parts by weight) overcoat. Load the powder feeder with the powdered-metal ingredients of this coat.
13. Plasma-spray the overcoat at 0.004 to 0.006 in. (0.1 to 0.15 mm) per pass until the final thickness is 0.015 to 0.020 in. (0.38 to 0.51 mm) greater than the specified final thickness.
14. Machine the built-up areas to the specified final dimensions.
15. Treat all reworked aluminum and magnesium surfaces with corrosion-prevention solutions.

To assess the reclamation process, tensile-strength tests were conducted on specimens that had been plasma-sprayed to coating thicknesses of 0.020 to 0.100 in. (0.51 to 2.54 mm). The specimens were also thermally cycled. The results showed that thermal cycling did not reduce tensile strength. Furthermore, compressor housings were plasma-sprayed and thermally cycled in 150-h engine tests and 200-h flight tests, during which the turbine engine was operated at a variety of loads, speeds, and torques. The plasma-sprayed coats showed no evidence of degradation or delamination from the compressor housings.

This work was done by George W. Leissler of Sverdrup Technology, Inc., and John S. Yuhas of the U.S. Army Aviation Research and Technology Activity (AVSCOM) for **Lewis Research Center**. *Further information may be found in NASA TM-101310 [N89-10156], A03 "T55-L-712 Turbine Engine Compressor Housing Refurbishment-Plasma Spray Project."*

Copies may be purchased [prepayment required] from the National Technical Information Service, Springfield, Virginia 22161, Telephone No. (703) 487-4650.
LEW-14899/TN

FOR ADDITIONAL INFORMATION: *Contact: Director, Technology Transfer Division, P.O. Box 8757, BWI Airport, MD 21240; (301) 621-0100 Ext. 241*
REFER TO THE NUMBER LISTED AT THE END OF THIS ARTICLE

Materials

0413 Model of Fiber Use Developed

0414 Navy Studies Feasibility of BZS for Marine Timber Preservation

0415 Space-Grown Protein Crystals Examined

0416 Materials for Magnetic Fusion Energy

0417 New Superconductor Polymer Composites Developed

0418 Lightweight Substrates for Mirrors—Layered structures would be made of carbon/carbon material.

0419 Polyphenylquinoxalines via Aromatic Nucleophilic Displacement—A new reaction sequence costs less and provides for a variety of molecular structures. (Licensing Opportunity)

0420 Radiographic Detection of Voids in SIC and SIN Ceramics—Projection radiography provides greater sensitivity of detection.

Testing & Instrumentation

0421 New Technique Measures Fiber Matrix in Composites (Licensing Opportunity)

0422 Measuring Adhesion and Friction Forces—The Cavendish balance is adapted to a new purpose.

0423 Preventing Vapor Deposition of the Backs of Substrates—This technique has been applied in the selective deposition of silicon on silicon carbide. (Licensing Opportunity)

Other Items of Interest

0374 Improving Contracts to High-T(c) Superconductors

0380 Long-Lifetime Laser Materials for Effective Diode Pumping—Long quantum lifetimes reduce the number of diodes required to pump. (Licensing Opportunity)

0400 Nondestructive Testing of Concrete with Ultrasonic Pulse-Echo

0406 Superplastic Forming/Diffusion Bonding For Low-Cost Advanced Titanium Missile Inlets

United States Department of Agriculture

Research Technology
Forest Products Laboratory

Model of Fiber Use Developed

The pulp, paper and paperboard industry accounts for more than a fourth of all wood products made annually in the United States. Using primarily pulpwood and recycled wood fiber, it produces such diverse products as printing and writing papers, sanitary papers, packaging papers and boxes, and construction paper and board. Manufacturing processes differ greatly by product and by region, especially in types and amounts of fiber required.

The Pulp and Paper Spreadsheet Model, developed at the Forest Products Laboratory, provides a detailed accounting of fiber requirements by product grade, manufacturing process, and region. As such, it is a detailed computer representation of fiber consumption in the U.S. pulp, paper and paperboard industry.

The model links production and fiber consumption sectors by specific conversion factors. These factors define the amount of wood pulp and recycled fiber needed per ton of product output, and the amount of pulpwood needed per ton of wood pulp. The model calculates product output and fiber consumption for ten paper and board grades, eight wood pulp grades, five recycled fiber grades, softwood and hardwood pulpwood, and three U.S. regions. Pulpwood consumption is also tracked as either roundwood or residues and by nine sub-regions.

Separate computer spreadsheets represent the industry in 1986, and in each decade from 1990 to 2040. The 1986 spreadsheet compiles all available industry data for that year. The spreadsheets for 1990 and beyond contain projections and assumptions about future production levels, regional distributions, and conversion factors.

The spreadsheet model can be used to calculate U.S. industry's pulpwood and fiber requirements in detail by region for a given level of production. The model could also be used to test alternative assumptions about wood use by product grade and region, and to determine the impact of technology changes.

The easy-to-use model was developed using a microcomputer-based spreadsheet package. The spreadsheet for each year is available as a separate computer diskette. Any of the model's data or equations can be easily changed, and results are then recalculated automatically. The model can also be enlarged in scope. Factors that could be added include exports and imports, manufacturing costs and fiber prices, wastepaper recovery, and additional manufacturing processes.

FOR ADDITIONAL INFORMATION: Contact Irene Durbak at (608)231-9377.

Navy Studies Feasibility of BZS for Marine Timber Preservation

Recent investigations of alternative chemical treatments at the Naval Civil Engineering Laboratory (NCEL), Port Hueneme, California, have focused on Basic Zinc Sulfate (BZS) pressure treatments for marine timber. Full-size piling tests in Pearl Harbor, Hawaii, that include BZS-treated pilings, conclusively demonstrated that the process renders Douglas fir borer-resistant for at least 19 years. In addition, a ground exposure test of basic zinc-treated pine stakes begun in the early 1950's has shown that the treatment imparts superior fungal protection.

The BZS treatment and testing of small pine panels were initiated in 1988 and are designed primarily to determine the effects of single- and dual-stage processes on strength and resiliency properties of wood. The examination included physical testing (static-bending and compression tests) of the variously treated small boards, as well as preliminary corrosivity testing of the solutions used to treat these panels.

It appears both single- and dual-stage BZS treatment processes are practicable, although it is likely to increase cost slightly. Also, there is some increased brittleness, but it is comparable to current ammoniacal copper arsenate (ACA) treated wood.

For Additional Information:

Backup material on this effort is available from:

Navy Domestic Technology Fact Sheet Reader Reply Service
Code E211
Naval Surface Weapons Center
Dahlgren, VA 22448-5000
(703) 663-8921

Refer to 150702/TN

Space-Grown Protein Crystals Examined

Scientists from the Naval Research Laboratory (NRL), Washington, D.C., have been analyzing protein crystals grown on the recent NASA Columbia Space Shuttle Flight. "The space-grown protein crystals have been found to be large single crystals of higher quality than those grown under similar conditions at NRL."

Protein crystal growth in space is important because of the potential applications of the unique studies of crystallization processes. The protein, porcine phospholipase A2, was crystallized onboard Columbia by mixing samples with precipitating agents and exposing the mixture to microgravity conditions available during the space shuttle mission.

The protein crystallized on the space shuttle flight is similar to ones implicated as causing such diseases as septic shock and rheumatoid arthritis in humans. The detailed understanding of the protein's molecular structure may some day lead to new drugs that could prevent or treat these diseases now suffered by millions.

For Additional Information:

Backup material on this effort is available from:

Navy Domestic Technology Fact Sheet Reader Reply Service
Code E211
Naval Surface Weapons Center
Dahlgren, VA 22448-5000
(703) 663-8921

Refer to 150604/TN

NIST Technology Update

National Institute of Standards & Technology
U.S. Department of Commerce, Gaithersburg, MD 20899

Materials for Magnetic Fusion Energy

NIST has published the 13th report in a series on research to determine the properties of materials that may be used in cryogenic structures for superconducting magnets for fusion energy power plants. *Materials Studies for Magnetic Fusion Energy Applications at Low Temperatures - XIII* (NISTIR 3944) presents research results for 1989-90 under four headings: structural alloys, welding, test standards, and technology transfer. The research is managed by NIST, sponsored by the Department of Energy's Office of Fusion Energy, and conducted at NIST and other laboratories through cooperative agreements.

FOR ADDITIONAL INFORMATION: Available from the National Technical Information Service, Springfield, Va. 22161. Order by PB91-107086 for $39.

NIST Technology Update

National Institute of Standards & Technology
U.S. Department of Commerce, Gaithersburg, MD 20899

New Superconductor Polymer Composites Developed

Composites made by mixing powdered ceramic superconducting materials with a polymer may be a practical way to fabricate a new generation of materials with the magnetic levitation properties of superconductors, even though they do not conduct electric current, say NIST researchers. The superconductor-polymer composites were developed by Aime S. DeReggi, Chwan-Kang Chiang, and George T. Davis, who have received a patent for their innovation. Laboratory work has demonstrated that a ceramic superconductor placed in a matrix of polyvinylidene fluoride displays the magnetic levitation properties of a superconductor. When a magnetic field is applied to the composite at superconducting temperatures, an electric current flows around the surface of each particle, creating a counter-magnetic field that gives the composite its levitating properties. The polymer acts as a binder and shields the particles from exposure to moisture and other chemically active substances that can destroy superconductivity.

FOR ADDITIONAL INFORMATION: For information, contact Aime S. DeReggi, B320 Polymer Bldg., NIST, Gaithersburg, Md. 20899; (301)975-6725.

NASA Tech Brief
National Aeronautics and
Space Administration
NASA's Jet Propulsion Laboratory, Pasadena, California

Lightweight Substrates for Mirrors

Layered structures would be made of carbon/carbon material.

Mirror substrates for space-based instruments are required to be lightweight, thermally and mechanically stable, and resistant to degradation from radiation. Carbon/carbon composites are ideally suited to this application, but the state of the art utilizes thick, three-dimensionally woven substrates having high areal weights.

A new substrate uses a conventional quasi-isotropic fabric laminate with a surfacing layer of carbon-fiber paper consisting of randomly oriented chopped carbon fibers. The carbon paper serves as a machinable layer, allowing the correct optical figure to be machined into the substrate. This provides the polishable surface and serves to fill in the print-through of the underlying fabric. The paper layer, being of random orientation, also removes the regular crack structure of the fabric and is therefore more readily densified into a smooth homogeneous surface layer. Substrates of this type can be made quite thin, thus keeping areal weights to a minimum. Mirrors of this type could be made faster, and would cost less, than their predecessors.

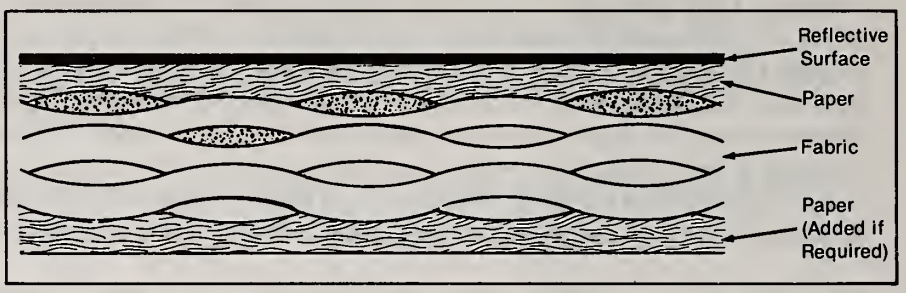

The **Layered Structure** of fabric and paper would be relatively easy to manufacture. When impregnated with carbon, the structure would be rigid and stable.

This work was done by D. Kyle Brown of Caltech for **NASA's Jet Propulsion Laboratory.**
NPO-17854/TN

FOR ADDITIONAL INFORMATION: *Contact: Director, Technology Transfer Division, P.O. Box 8757, BWI Airport, MD 21240; (301) 621-0100 Ext. 241*
REFER TO THE NUMBER LISTED AT THE END OF THIS ARTICLE

NASA Tech Brief
National Aeronautics and Space Administration
Langley Research Center, Hampton, Virginia

Licensing Opportunity

Polyphenylquinoxalines via Aromatic Nucleophilic Displacement

A new reaction sequence costs less and provides for a variety of molecular structures.

A process for the synthesis of polyphenylquinoxalines (PPQ's) involves nucleophilic displacement reactions of di(hydroxyphenyl) quinoxaline monomers with activated aromatic dihalides. The new process costs less than do other processes for the synthesis of PPQ's. In addition, because of the availability of a large variety of activated aromatic dihalides, the new process facilitates the synthesis of PPQ's of new and varied molecular structures. The new PPQ's are useful as adhesives, coatings, films, membranes, and matrices for composites.

Conventional PPQ's, prepared from bis(phenyl-α-diketones) and bis(ortho diamines), are configurationally unordered, with three possible isomers distributed randomly along the backbones of these polymers. This dissymmetry contributes to the amorphous character, high solubilities, and limited tensile moduli observed in these materials. On the other hand, the incorporation of crystallinity into the backbone of a polymer enhances its mechanical properties and its resistance to solvents. The new process can synthesize configurationally ordered semicrystalline PPQ's.

In tests of the new process, the synthesis of the PPQ's involved the use of two different types of bisphenol quinoxaline monomers; those with and those without configurational isomers. The PPQ's prepared from monomers with configurational isomers had essentially the same physical and mechanical properties as those of PPQ's prepared via the conventional process. Some PPQ's prepared from monomers without configurational isomers were semicrystalline, as evidenced by differential scanning calorimetry and wide-angle x-ray diffraction.

The top part of Figure 1 illustrates the synthesis of bisphenol quinoxaline monomers that have configurational isomers. The symbol Ar represents a radical of 1,2,4,5-tetrasubstituted benzene, 3,3′,4,4′-tetrasubstituted benzene, biphenyl, diphenylether, diphenylmethane, diphenylketone, diphenylsulfone, diphenylthioether, or any appropriate bis(ortho diamine), or a mixture of any of these compounds. The bottom part of Figure 1 illustrates the synthesis of the monomers without configurational isomers. The symbol Z represents H, Cl, Br, OCH_3, CH_3, CH_2CH_3, phenyl, or other groups. In both sequences, the catenation of the hydroxy groups can be meta meta, para para, meta para, or mixtures thereof.

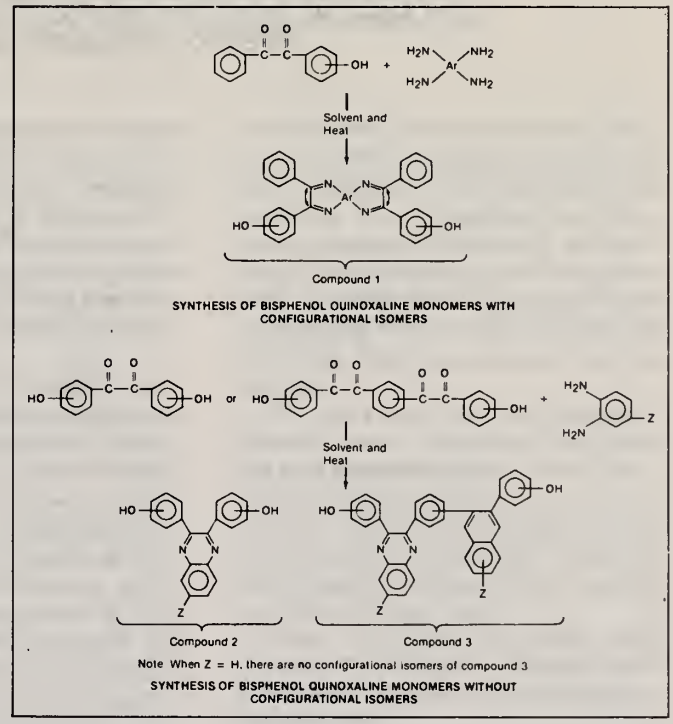

Figure 1. **Bisphenol Quinoxaline Monomers** can be synthesized with or without configurational isomers.

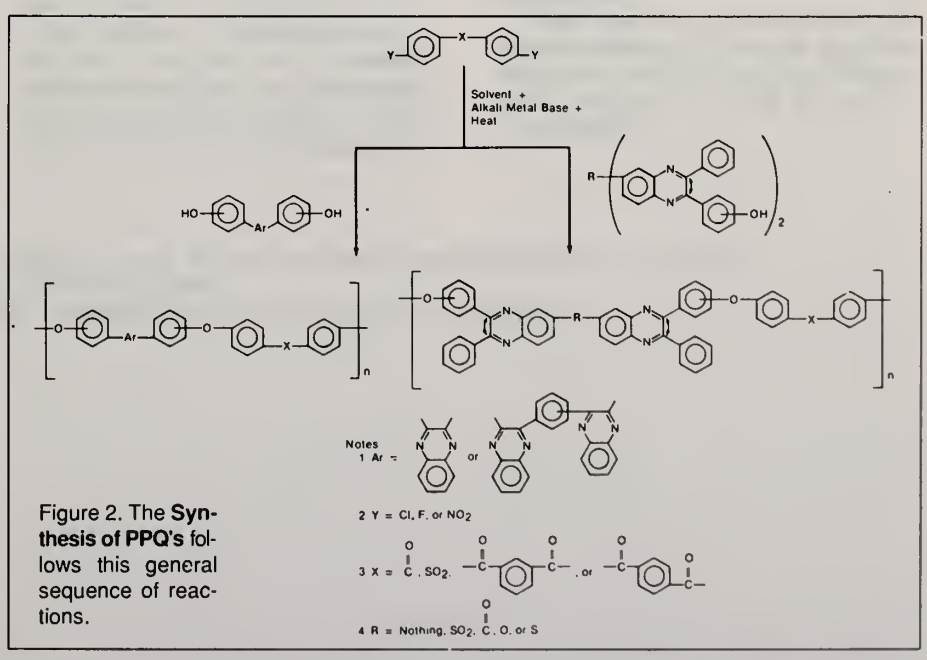

Figure 2. The **Synthesis of PPQ's** follows this general sequence of reactions.

Figure 2 illustrates the synthesis of a PPQ. The reactions are carried out in a polar aprotic solvent, possibly N,N-dimethylacetamide, sulfolane, N-methylpyrrolidone, or diphenylsulfone, using an alkali metal base, at an elevated temperature, under a nitrogen atmosphere.

This work was done by Paul M. Hergenrother and John W. Connell of **Langley Research Center.**

This invention is owned by NASA, and a patent application has been filed. Inquiries concerning nonexclusive or exclusive license for its commercial development should be addressed to the Patent Counsel, Langley Research Center. Refer to LAR-13988/TN.

Langley Research Ctr.
Technology Utilization Officer John Samos
Mail Stop 139A
Hampton, VA 23665

Patent Counsel
George F. Helfrich
Mail Code 279
Hampton, VA 23665
(804) 864-3523

FOR ADDITIONAL INFORMATION: *Contact: Director, Technology Transfer Division, P.O. Box 8757, BWI Airport, MD 21240; (301) 621-0100 Ext. 241*

REFER TO THE NUMBER LISTED AT THE END OF THIS ARTICLE .

NASA Tech Brief
National Aeronautics and
Space Administration

Radiographic Detection of Voids in SiC and SiN Ceramics

Projection radiography provides greater sensitivity of detection.

Two reports describe experimental studies of the efficacy of radiographic detection of voids in "green" (unfired) and sintered SiC and SiN ceramics. These studies were motivated by the need for a nondestructive technique to detect flaws that limit the strengths of sintered structural ceramic components.

In the experiments, solid precursors of surface and internal voids were introduced artificially by seeding green specimens of the ceramics with styrene divinyl benzene microspheres. The specimens were compacted and sintered to form the ceramics. The high sintering temperatures (above 2,100 °C) caused the microspheres to decompose, leaving the voids in the resulting ceramics.

One of the studies concentrated on the use of microfocus (magnifying projection) x-radiography to detect subsurface voids made with microspheres having diameters of 200, 321, and 528 μm. The microfocus system was operated with photon energies ≤ 20 keV and a 10-μm focal spot. Statistics were developed for the probability of detection of voids in green and sintered specimens at a 95-percent confidence level and compared with statistics obtained previously for similar specimens. It was also shown that the reliability of detection of internal voids can be inferred from the probability-of-detection curves of surface voids in the same ceramic, provided that there are no local variations in density and chemical composition.

The other study was undertaken to compare the reliabilities of the microfocus and the conventional (nonmagnifying or contact) radiography in the detection of voids. In this study, the specimens were seeded with microspheres having diameters of 50, 80, and 115 μm. The conventional x-ray system, with a tungsten target and a 400-μm focal spot, was operated at 25 to 75 kV and a beam current of 5 to 8 mA. The microfocus system, with a molybdenum target, was operated at 30 to 60 kV with a beam current of 0.25 to 0.32 mA.

The sensitivity of detection of voids by microfocus radiography at a 90-percent probability of detection and a 95-percent confidence level was found to be 1.5 percent of the thickness of the specimen in both ceramics. The corresponding figure for conventional radiography was found to be 2.5 percent of the thickness of the specimen. Thus, it appears that microfocus (projection) radiography is preferable to conventional (contact) radiography when increased sensitivity is required and the additional time and effort necessary to set up the microfocus apparatus can be tolerated.

This work was done by George Y. Baaklini, James D. Kiser, and Don J. Roth of **Lewis Research Center**. *Further information may be found in*

NASA TM-86945 [N85-21674], A02 "Radiographic Detectability Limits for Seeded Voids in Sintered Silicon Carbide and Silicon Nitride," and

NASA TM-87164 [N86-13749], A02 "Probability of Detection of Internal Voids in Structured Ceramics Using Microfocus Radiography."

Copies may be purchased from the [prepayment required] National Technical Information Service, Springfield, Virginia 22161, Telephone No. (703) 487-4650.
LEW-14881/TN

FOR ADDITIONAL INFORMATION: *Contact: Director, Technology Transfer Division, P.O. Box 8757, BWI Airport, MD 21240; (301) 621-0100 Ext. 241*
REFER TO THE NUMBER LISTED AT THE END OF THIS ARTICLE

NIST Technology Update
National Institute of Standards & Technology
U.S. Department of Commerce, Gaithersburg, MD 20899

Licensing Opportunity

New Technique Measures Fiber Matrix in Composites

NIST researcher Wen-li Wu has been awarded a patent for a new technique to estimate the strength of the bonding between polymer matrix resin and reinforcements in polymer composites. The mechanical properties of composite materials are strongly influenced by the bonding of resins and fiber reinforcements. Wu's method uses a laser to heat a very small, localized region of the sample. The thermal expansion between the fiber and resin produces an acoustical emission, which can be measured. The stronger the interface, the lower the acoustical signal. Previous methods to evaluate strength require highly trained personnel, are tedious to perform, and require special test specimens or destruction of the composite. The new technique is simple to use and nondestructive. The invention addresses one of the technical barriers to improved polymer composite processing identified by industry at two NIST workshops.

FOR ADDITIONAL INFORMATION: Contact Wen-li Wu, B320 Polymer Bldg., NIST, Gaithersburg, Md. 20899; 301/975-6839.

NASA Tech Brief
National Aeronautics and
Space Administration
Lewis Research Center, Cleveland, Ohio

Measuring Adhesion and Friction Forces

The Cavendish balance is adapted to a new purpose.

An apparatus has been developed which measures the forces of adhesion and friction between specimens of solid materials in a vacuum at temperatures from ambient to 900°C. It is intended primarily for use in studying the adhesion properties of ceramics and metals, including silicon carbide, aluminum oxide, and iron-base amorphous alloys.

The apparatus is mounted in an ultrahigh-vacuum system that also contains equipment for x-ray photoelectron spectroscopy. The portion of the apparatus that measures adhesion is based on the principle of the Cavendish balance. A pin specimen is mounted at one end of an arm that is suspended on a vertical torsion wire (see Figure 1). The other end of the arm holds the magnetic core of a linear variable-differential transformer that is used to measure the angular deflection of the arm. A flat specimen is pushed slowly against the pin specimen until it turns the beam and twists the torsion wire through a small angle. The flat specimen is then pulled back slowly until it separates from the pin specimen. The difference between the angular positions at which the specimens make and break contact gives a measure of the force of adhesion between them. If, for example, there is no adhesion, then the specimens make and break contact at the same position. If there is adhesion, then the receding flat specimen pulls the pin specimen out beyond the point of initial contact.

Inasmuch as the pulloff (adhesion) force is measured in terms of the torsion in the wire, the force can be calibrated in three ways: (1) by calculation from the length and diameter of the wire; (2) by calculation with measured values of natural periods of harmonic motions of the arm when the arm is freely oscillating; and (3) by direct comparison of microforce to standard weight when the arm and torsion wire are held horizontally. The values of pulloff force determined by all three methods of calibration have been found to be nearly the same.

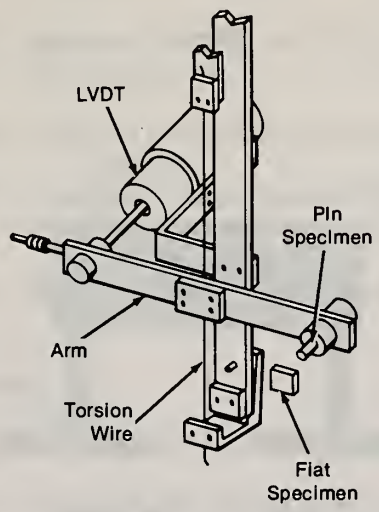

Figure 1. A **Modified Cavendish Balance** instrumented with a linear variable-differential transformer (LVDT) is used to measure adhesion between pin and flat specimens.

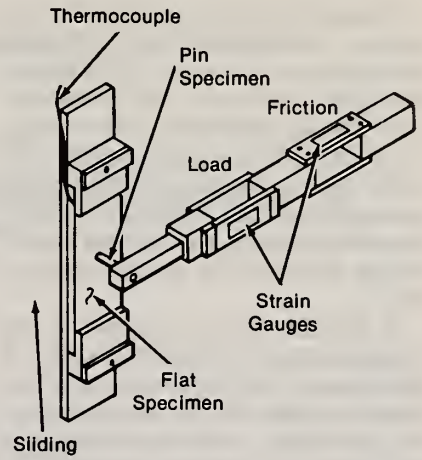

Figure 2. **Strain Gauges Measure Pressing and Sliding Forces** as pin and flat specimens are rubbed against each other.

For the measurement of friction force, a pin specimen is mounted on the end of a beam that is, in turn, mounted on a micrometer-type manipulator. The beam includes two mutually perpendicular flats instrumented with strain gauges (see Figure 2). A flat specimen is mounted on a vertical beam on another micrometer-type manipulator. The flat and pin specimens are pressed together, and the manipulators used to slide them horizontally or vertically against each other. The load (pressing) force and the sliding (frictional) force are measured by the strain gauges.

This work was done by Kazuhisa Miyoshi of **Lewis Research Center**. *Further information may be found in*

NASA TM-101959 [N89-20253], A03 "Design, Development, and Applications of Novel Techniques for Studying Surface Mechanical Properties,"
NASA TM-100799 [N88-20454], A03 "Development of a Torsion Balance for Adhesion Measurements,"
NASA TM-101377 [N89-11913], A03 "Adhesion, Friction, and Wear of Plasma-Deposited Thin Silicon Nitride Films at Temperatures to 700°C," and
NASA TP-2449 [N85-21359], A02 "Humidity Effects on Adhesion of Nickel-Zinc Ferrite in Elastic Contact With Magnetic Tape and Itself."

Copies may be purchased [prepayment required] from the National Technical Information Service, Springfield, Virginia 22161, Telephone No. (703) 487-4650.
LEW-14903/TN

FOR ADDITIONAL INFORMATION: *Contact: Director, Technology Transfer Division, P.O. Box 8757, BWI Airport, MD 21240; (301) 621-0100 Ext. 241*
REFER TO THE NUMBER LISTED AT THE END OF THIS ARTICLE

NASA Tech Brief
National Aeronautics and
Space Administration
Langley Research Center, Hampton, Virginia

Licensing Opportunity

Preventing Vapor Deposition of the Backs of Substrates

This technique has been applied in the selective deposition of silicon on silicon carbide.

A technique that prevents back-side deposition on substrates in an impinging chemical-vapor deposition (CVD) system has been developed. If not prevented, back-side deposition often results in cracking of the deposit and makes replication in a CVD reactor difficult to achieve. Also, the new technique does not require any post-deposition machining to separate the deposited substrate from the deposition fixture.

In this technique, a substrate of any shape and size is mounted on a number of pillars made of graphite or some other material compatible with the deposition process (see figure). The pillars are bonded to the substrate as close as possible to its periphery. A hollow structure, which is open on one side and closed on the other and is compatible with the substrate, is fabricated from Grafoil (or equivalent), using graphite cement to bond it together. The structure is then mounted on the pillars with the open side facing the back side of the substrate. This side is pressed against the substrate and is sealed with a bonding agent. This arrangement completely covers the back side of the substrate and prevents any vapor deposition on it. However, deposition does occur on the Grafoil body.

Typically, this approach is used when a SiC substrate is being coated with Si. Since

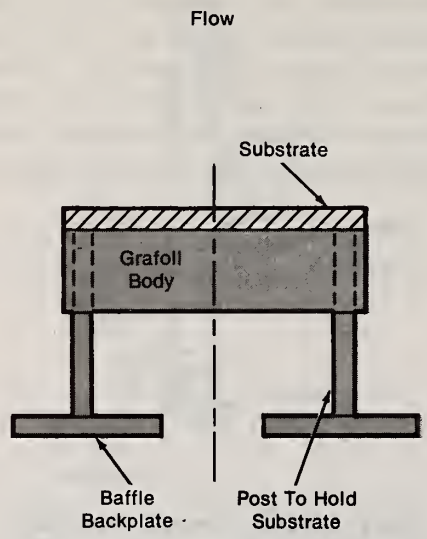

The **Back Side of the Substrate Is Covered Completely**, allowing vapor deposition only on the Grafoil body.

Grafoil is quite flexible, the Si-coated Grafoil is readily broken into small pieces for removal from the substrate by use of a piercing tool and a pair of pliers. Because the substrate is perpendicular to the Grafoil body and the flexible Grafoil deforms as stresses develop (due to growth of material and mismatch of thermal expansion), the cracks do not propagate into the substrate.

This technique is inexpensive, does not require any machining to remove excess material, and is easy to use. It has been used successfully in the selective deposition of SiC and Si in a CVD reactor.

This work was done by Jitendra S. Goela, Roy Jaworski, and Raymond L. Taylor of Morton Thiokol, Inc./CVD Inc. for **Langley Research Center**. *No further documentation is available.*

In accordance with Public Law 96-517, the contractor has elected to retain title to this invention. Inquiries concerning rights for its commercial use should be addressed to

Gerald K. White, Esq.
Director, Patents and Trademarks
Morton Thiokol, Inc.
110 North Wacker Drive
Chicago, IL 60606–1560

Refer to LAR-14071/TN.

Langley Research Ctr.
Technology Utilization Officer: John Samos
Mail Stop 139A
Hampton, VA 23665
(804) 864-2484
Patent Counsel:
George F. Helfrich
Mail Code 279
Hampton, VA 23665
(804) 864-3523

FOR ADDITIONAL INFORMATION: *Contact: Director, Technology Transfer Division, P.O. Box 8757, BWI Airport, MD 21240; (301) 621-0100 Ext. 241*
REFER TO THE NUMBER LISTED AT THE END OF THIS ARTICLE

Medicine & Biology

0424 Anesthetic Compound

0425 Defining Human Factors

0426 Ergonomics Databases

0427 Statistical Methods for Estimating Risk for Exposure Above the Reference Dose

0428 California DNA Crime Laboratory Opens

0429 Scheiner-Principle Pocket Optometer for Self Evaluation and Biofeedback Accommodation Training

0430 Scanning Tunneling Microscopy

Software

0431 Subjective Workload Assessment Technique

0432 Membrane Bioreactor With Pressure Cycle—Inhibitory reaction products and gradients of concentration are removed. (Licensing Opportunity)

0433 Rotationally Actuated Prosthetic Hand—A simple mechanism is powered by rotation of the forearm. (Licensing Opportunity)

Other Items of Interest

0434 Prosthetic Hand Lifts Heavy Loads—Features include ruggedness, simplicity, and relatively low cost. (Licensing Opportunity)

U.S. Army Fact Sheet

Anesthetic Compound

Scientists at the U.S. Army Chemical Research, Development and Engineering Center (CRDEC) have developed a new chemical compound which potentially could be an improvement over anesthetics currently used by the medical community. The compound, 4-[1-(1-Naphthalenyl)ethyl] -1H-imidazole, has been tested on swine with favorable results. It represents a possible major breakthrough as a sedative, especially for operating rooms, because it is not characterized by the cardiovascular side effects normally associated with anesthetics.

A patent application has been filed, and CRDEC is currently seeking assistance from pharmaceutical firms to cooperate on further testing and marketing.

For further information, contact CRDEC's Office of Research and Technology Applications, Mrs. Susan Luckan or Mr. Ronald Hinkle, at (301) 671-2031.

Technology Applications

Defining Human Factors

At the request of the Human Factors Committee of the National Research Council, CSERIAC analyzed existing definitions of *human factors* to aid the committee in establishing a standardized definition of the field. Although there are many definitions of *human factors,* a formally endorsed, unified definition does not exist.

CSERIAC compiled and analyzed definitions of *human factors* and related terms from a range of key reference sources and presented its findings to the committee to expedite its deliberations. Searches for appropriate resource materials were conducted at four area libraries using computerized catalogues. Definitions were extracted from 74 references, yielding a final sample of 90 verbatim definitions.

Many of the definitions had three components: the category (genus) of classification (e.g., field, discipline, profession, etc.); the domains of inclusion (e.g., biology, behavioral sciences, etc.); and the objectives (e.g., to increase system safety through application of human performance data in design). A standardized definition of *human factors* should probably incorporate all these components.

The definitions assembled for the analysis can be grouped into three general classes: *human factors, human factors engineering,* and *ergonomics.* The *human factors* definitions in our sample are characterized by a broader category of classification and broader objectives. The *human factors engineering* definitions overwhelmingly emphasize design as the medium for effecting change in end systems. Definitions of *ergonomics* stress the study of humans at work.

These differences among the terms *human factors, human factors engineering,* and *ergonomics* must be considered in developing a single, unifying definition of the field.

Our analysis reveals a chronological trend towards broadening both the domains of inclusion and the objectives of the human factors field. Originally, the focus of human factors was the design of military man-machine systems; this focus has expanded to include private industrial systems and consumer products as well. Thus, the field has moved from a discipline born in a postwar, militarily oriented engineering environment to one active in a more global manufacturing and consumer-oriented environment.

A summary report of the analysis of human factors definitions may be obtained from the CSERIAC Program Office. ●

For additional information contact:

Crew System Ergonomics Information Analysis Center
AAMRL/HE/CSERIAC
Wright-Patterson AFB
Ohio 45433-6573
(513) 255-4842

Technology Applications

Ergonomics Databases

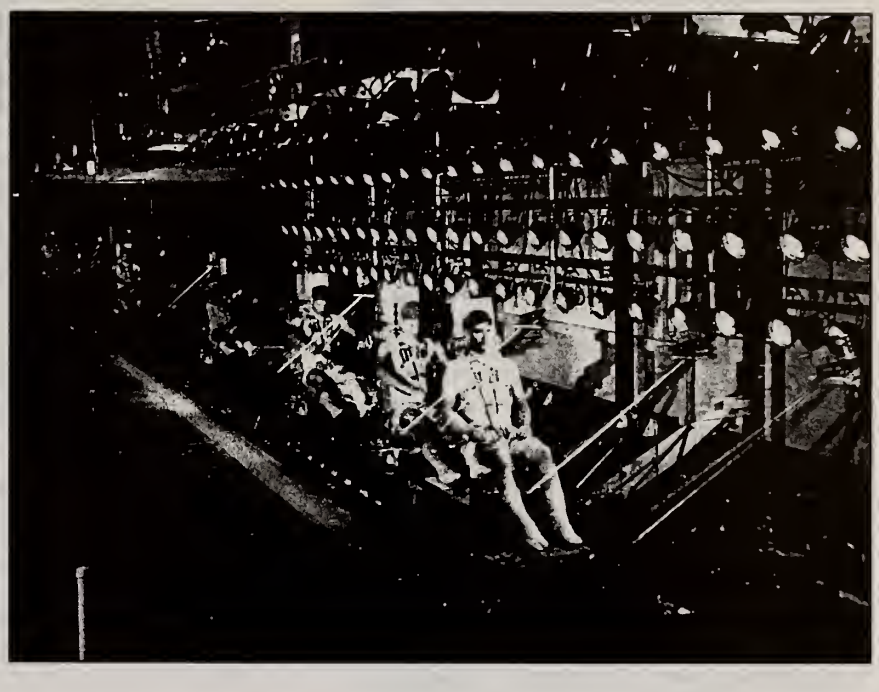

An important part of CSERIAC's mission is to manage the transfer of crew system ergonomics technical products from developers to potential users for their mutual benefit. CSERIAC can currently provide access to two ergonomics databases: the Center for Anthropometric Research Data (CARD) Anthropometric Data Base and the Biodynamics Data Bank (BDB).

Center for Anthropometric Research Data (CARD) Anthropometric Data Base

The CARD Anthropometric Data Base is operated by the Armstrong Aerospace Medical Research Laboratory (AAMRL), Workload and Ergonomics Branch, at Wright-Patterson Air Force Base (WPAFB), Ohio. An online database developed to support human engineering design activities, the CARD database contains several hundred measurements of the human body across large population samples. Users can access anthropometric data from published surveys conducted worldwide.

For example, data are available from a survey of 1,905 USAF women conducted in the spring of 1968 by the Anthropology Branch of the Aerospace Medical Research Laboratory (WPAFB), and the Anthropology Research Project (Yellow Springs, Ohio). Data for this sample include age, 123 body size measurements, and grip strength.

A relational database system is used to manage the survey data and accommodate user queries. Access to the database is through a menu-driven applications software package. Available information includes measurement frequency data and summary statistics (mean, standard deviation, etc.), measurement descriptions, and measurement classification by body region and measurement type. A glossary of anthropometric terms and abstracts of the various anthropometric surveys are also available. New surveys are integrated into the database as they are received by the Center for Anthropometric Research Data.

Anyone needing anthropometric data may obtain direct access to the CARD database.

AAMRL Biodynamics Data Bank (BDB)

The Biodynamics Data Bank, sponsored by AAMRL, Modeling and Analysis Branch, WPAFB, is a repository for

data from impact acceleration biodynamics experiments conducted by the Biomechanical Protection Branch of AAMRL (WPAFB). It is a general scientific data bank with a generic structure designed to fit the results of any scientific experiment, particularly those in the biosciences.

The BDB can hold complete raw (digital) data for smaller-scale biodynamics experiments.

For additional information contact:

Crew System Ergonomics Information Analysis Center
AAMRL/HE/CSERIAC
Wright-Patterson AFB
Ohio 45433-6573
(513) 255-4842

United States
Environmental Protection
Agency

Office of Health and
Environmental Assessment
Washington, DC 20460

Research and Development

EPA

Project Summary

Statistical Methods for Estimating Risk for Exposure Above the Reference Dose

A statistical method has been developed that provides a risk estimate for noncarcinogenic effects at a given dose. The method uses a categorical regression procedure to model severity of effect as it relates to experimental dose. Toxicity data are analyzed from multiple animal experiments that span different species, target organs, toxic effects, and exposure conditions. The data are screened for homogeneity with respect to experiment duration and route of exposure. The resulting dose-response curve provides an estimate of the risk of adverse effects that may be useful in estimating risk for exposures above the reference dose (RfD).

This Project Summary was developed by EPA's Environmental Criteria and Assessment Office, Cincinnati, OH, to announce key findings of the research project that is fully documented in a separate report of the same title (see Project Report ordering information at back).

Introduction

The U.S. Environmental Protection Agency (U.S. EPA) is charged with the responsibility of protecting public health from environmental pollutants. In this capacity, the U.S. EPA establishes a reference dose (RfD) for noncancer toxicity of individual chemicals (U.S. EPA, 1988; Barnes and Dourson, 1988). The U.S. EPA's formal definition of the RfD is:

> "An estimate (with uncertainty spanning perhaps an order of magnitude) of a daily exposure to the human population (including sensitive subgroups) that is likely to be without appreciable risk of deleterious effect during a lifetime."

The determination for the RfD for a given chemical involves several judgmental steps. First, the literature on its toxic effects is evaluated. The most scientifically sound study with the most appropriate NOAEL (no-observed-adverse-effect level) of the critical effect is then generally chosen, and that NOAEL is divided by uncertainty factors to arrive at the RfD. To date, there has been much concern regarding the risk of adverse effects for exposures above the RfD, but no reliable method for estimating this risk has been developed.

The evaluation of toxicity data for noncarcinogens is complicated by the multiplicity of possible endpoints, and the variation both in the severity of effect and in the response rate. Standard dose-response models most often assume a fixed severity (e.g., lethal) and endpoint (e.g., cancer), and would then need to be generalized into a multivariate form to be applicable to noncarcinogenic effects. Since response rates for noncarcinogenic effects are rarely reported, multivariate dose-response models are seldom developed, and "dose-response" analysis usually relates dose only to the severity of the observed effects. The approach presented here assigns the severity descriptions to ordered categories and models the "dose-category" relationship. Modeling the risk of adverse effects using categorical regression was proposed previously (Hertzberg and Miller, 1985; Hertzberg, 1987), but the statistical algorithm then used was limited.

Results and Conclusions

Several different computer programs and groupings of the data have been investigated in order to find the best approach for applying categorical regression to this dose-severity modeling. Much progress has been made: available data were put in a form conducive to such an analysis, a model was selected, a statistical algorithm was found to perform the analysis, ways of presenting the results were explored, some goodness-of-fit measures were evaluated, and a mainframe programming package was written to perform the analysis. For this document, a logistic transform was used to regress the severity of effects on the covariate, dose. Graphs displaying s-shaped dose-response curves with 95% confidence bands were then generated. The curves are statistically derived and use all of the available toxicity data in determining the risk of adverse effects at given doses.

The proposed regression procedure should be useful in risk-based decisions that can directly use animal data. For

example, the Margin of Exposure (MOE) method compares the existing exposure with the NOAEL for the critical effect. The MOE method could then be augmented by considering the estimated risk at the existing exposure and not just the MOE ratio.

The progress described above does not, however, provide a final solution to the risk problem. Some difficulties arise because of the data available for analysis. Almost all of these data are from animal studies, so the risk estimates produced by the regression are animal risk estimates that must be a manipulated further to produce human risk estimates. Thus, more research is needed to produce human risk estimates for exposures above the RfD. Also, each record in the data set represents information from an entire dose group, not from an individual animal. The interpretation of the animal risk estimate depends, then, upon the fact that the unit of input to the regression is the dose group.

Recommendations

Additional research is necessary to ensure that this categorical regression procedure is successful in estimating risk levels at specific doses. Examples of areas requiring further research are as follows:

1. Methods need to be developed that will validate the assumptions made by the model whenever the regression is performed.
2. The goodness-of-fit measures provided by the regression procedure need to be evaluated relative to their usefulness for dose-response modeling. New goodness-of-fit measures need to be developed.
3. Data should be found and analyzed that allow characterization of individual animal effects, instead of dose group effects.
4. An investigation should be made of other models that may be superior in their predictive abilities to the logistic model.
5. The enigma of the extrapolation of animal risk to human risk is thus far unsolved by this process. Ways to develop a human risk estimate need to be found.

References

Barnes, D.G. and M.L. Dourson. 1988 Reference Dose (RfD): Description and Use in Health Risk Assessment. Reg. Toxicol. Pharm-acol. 8: 471-486.

Hertzberg, R. 1987. Fitting a model to categorical response data with application to species extrapolation of toxicity. *In*: Proceedings of the 26th Hanford Life Sciences Symposium, Modeling for Scaling to Man. October 20-23, 1987. Battelle Pacific Northwest Laboratories, Richland, WA. (In press) .

Hertzberg, R. and M. Miller. 1985. A statistical model for species extrapolation using categorical response data. Toxicol. Ind. Health. 1(4): 43-57.

U.S. EPA. 1988. Reference Dose (RfD): Description and Use in Health Risk Assessments. Integrated Risk Information System (IRIS). Online. Intra-agency Re-ference Dose (RfD) Work Group, Office of Health and Environmental Assessment, Environmental Criteria and Assessment Office, Cincinnati, OH.

***Rick Hertzberg** is the EPA Project Officer (see below).*

The complete report, entitled "Statistical Methods for Estimating for Exposure Above the Reference Dose," (Order No. PB 90-261 504/AS; Cost: $.8.00 subject to change) will be available only from:

National Technical Information Service
5285 Port Royal Road
Springfield, VA 22161
Telephone: 703-487-4650

The EPA Project Officer can be contacted at:

Environmental Criteria Assessment Office
Cincinnati, OH 45268

Lawrence Berkeley Laboratory

California DNA Crime Laboratory Opens

Under the terms of a collaborative research agreement with Lawrence Berkeley Laboratory (LBL), the California State Department of Justice has opened its first DNA Crime Laboratory. Staff members for the new crime laboratory will be sharing facilities and information with LBL researchers until next August, when they move to more permanent quarters.

The DNA Crime Laboratory has been established to develop and evaluate forensic DNA testing procedures, analyze the DNA in biological evidence collected at the scene of violent crimes, and create a database that will contain DNA profiles of individuals who have been convicted of committing such acts. LBL will provide assistance in the use of the polymerase chain reaction (PCR) technique, a means of rapidly amplifying short pieces of DNA into usable quantities, and in the development of image enhancement techniques for faster and improved data analysis.

Many of the techniques and instrumentation being developed at LBL as part of the Human Genome Project--the national effort now under way to decipher the human genetic code--are expected to be applicable to the DNA Crime Laboratory.

DNA profiles were started in England in 1986 by geneticist Alec Jeffreys of the University of Lancaster, who got the idea while identifying genetic markers for inherited diseases through the use of a technique called Restriction Fragment Length Polymorphism (RFLP) analysis. Unlike conventional bio-chemical forensic techniques, which either exclude persons or limit the number of potential suspects, genetic typing is a means of identifying a specific individual, similar to fingerprinting, though not yet as precise.

The RFLP technique was first used to win a criminal conviction in this country in 1987. It involves the analysis of nuclear DNA, the genetic material inherited from both parents that forms the chromosomes inside the nucleus of every cell in the body.

At LBL, the DNA Crime Laboratory will use both RFLP analysis and PCR techniques on nuclear DNA and on mitochondrial DNA, genetic material inherited only from the mother, that is located outside the nucleus in the mitochondria (tiny organelles which convert glucose into energy).

Mitochondrial DNA does not contain as much variation as nuclear DNA. However, genetic typing using mitochondrial rather than nuclear DNA offers advantages in some situations. Whereas each cell has only one or two copies of nuclear DNA, it will have several hundred copies of mitochondrial DNA. This improves the chances of obtaining enough DNA for analysis in situations where a sample has been exposed to adverse conditions.

With mitochondrial DNA, no more than a few cells, a single hair, or even a tiny fragment of bone is needed to produce a typing. Furthermore, since mitochondrial DNA is inherited exclusively from the mother, it is identical in all persons who share the same maternal lineage, which makes the establishment of a biological relationship between two typings easier.

For further information, contact Mark Owens at (415) 486-6463.

U.S. Navy Fact Sheet

Naval Aerospace Medical Research Laboratory

Scheiner-Principle Pocket Optometer for Self Evaluation and Biofeedback Accommodation Training

Most humans tend toward myopia when presented with a visual field without sufficient detail to stimulate focusing mechanism. This means that a pilot flying in darkness, or in an ''empty field'' such as empty sky, will be likely to focus nearer the windscreen than at the optical infinity required to focus on visual targets of probable interest. Biofeedback training to counter this problem has been limited in practical application by expensive and cumbersome instrumentation.

A Scheiner-principle optometer has been developed for self-evaluation of accommodative state and biofeedback training. The specific advantages of the new invention over earlier optometers are: (a) simplicity of design; (b) handheld, portable implementation; (c) light weight; (d) small size; (e) low manufacturing cost; (f) the use of a monochromatic light source to eliminate the effects of chromatic aberrations in the subject's eye; and (g) effectiveness as a training aid.

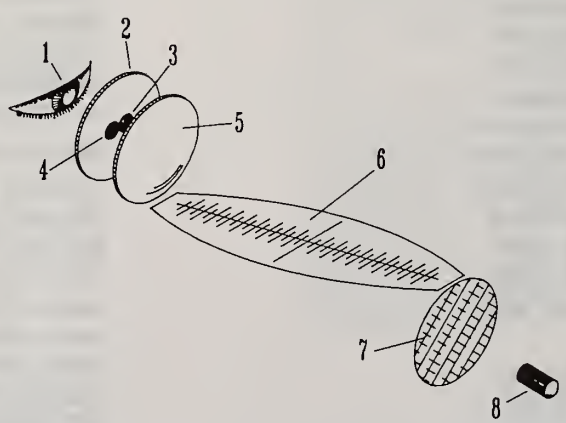

Schematic of the pocket optometer. [1] subject's eye; [2] pinhole aperture stop plate; [3] and [4] pinhole apertures; [5] Badal lens; [6] scale; [7] diffuser; [8] light emitting diodide.

Four prototypes of the pocket optometer have been built and were used to implement biofeedback training to correct night myopia in 12 Navy aviation candidates. All subjects were emmetropic in full light. Training was limited in duration because of the transient nature of subject availability but was reasonably successful in 10 out of the 12 cases.

FOR ADDITIONAL INFORMATION: LCDR T. E. Fleishman, MSC, USN, Naval Aerospace Medical Research Laboratory, Pensacola, FL 35208-5700; (904)452-3286.

NIH
Research & Technology
U.S. Department of Health and Human Services Public Health Service National Institutes of Health

Scanning Tunneling Microscopy

A Nanoscope II[R] scanning tunneling microscope has been acquired by the National Electron Spectroscopy for Chemical Analysis and Surface Analysis Center for Biomedical Problems (NESAC/BIO) at the University of Washington, Seattle, and is available to qualified biomedical researchers for use in collaborative projects.

Scanning tunneling microscopy (STM) can provide images of biological macromolecules such as DNA, RNA, and proteins that rival the details of those obtained by other available methods.

"It's very different from any other tool," says Dr. Buddy D. Ratner, director and principal investigator of NESAC/BIO.

Unlike other high-resolution microscopic techniques, STM and atomic force microscopy, its related technique, can operate in liquid and air as well as in a vacuum. This ability is significant for biomedical studies because it allows investigators to observe proteins and polymers interacting with biological and nonbiological surfaces under physiological conditions, Dr. Ratner says.

NESAC/BIO was established in 1984 and is funded by the Biomedical Research Technology Program of the National Center for Research Resources. The resource provides contemporary surface analysis tools for biomedical researchers.

"The resource is devoted to taking ideas from the physics community and introducing them to the biomedical community," Dr. Ratner explains.

The Nanoscope II[R], acquired about 2 years ago, is one of the newest surface analysis tools available at NESAC/BIO. Other surface analysis methods offered by NESAC/BIO include electron spectroscopy for chemical analysis, secondary ion mass spectrometry, and scanning electron microscopy.

Dr. Buddy Ratner

Dr. Buddy Ratner and laboratory manager Deborah Leach-Scampavia examine a sample being prepared for analysis.

STM, which won a Nobel Prize in physics for its inventors in 1986, obtains its information through a phenomenon called quantum or electron tunneling. A sample is scanned with the STM probe, which is a sharp metal tip or needle terminating in a single atom. Electron tunneling occurs when the tip of the needle is brought to within approximately 10 angstroms of the sample being examined.

"At that distance the electron cloud of the atoms from the sample surface overlaps with the electron cloud of the atoms from the needle tip, starting quantum tunneling in which a current of electrons moves be-

tween the sample surface and the needle tip," explains Dr. Ratner. A computer linked to the microscope measures the tunneling current as the needle is scanned over the sample. Small irregularities on the sample surface cause corresponding variations in the tunneling current.

"What we do is set up the apparatus to raise and lower the tip so that the tunneling current remains constant as the tip follows the electronic topography of the surface," Dr. Ratner says. STM provides "a three-dimensional image of the surface," he says. "One can easily image individual atoms and investigate their arrangements and geometries."

STM has significant biomedical applications because it allows scientists to examine how proteins react and change in response to the surface on which they are adsorbed. "We want to see what proteins and other biomolecules look like when they are adsorbed on a surface," Dr. Ratner explains. "If the needle tip encounters a protein molecule when it is scanned along the surface we can get the tip to trace a contour of the molecule.

"Our motivation for using STM is to study medical implants such as artificial hearts, blood vessel replacements, and intraocular implants," Dr. Ratner says. "These materials adsorb a layer of protein, and the way the body responds to these materials seems to be related to what happens to the protein layer at the surface.

"There aren't a lot of good ways to look at proteins on surfaces, but STM is a great way to do it," he says. To date many different proteins including albumin, collagen, and fibrinogen have been imaged.

NESAC/BIO has a project under way to sequence DNA using STM. "We think it may have the potential for reading the genetic code, for reading the base pairs," Dr. Ratner says.

NESAC/BIO accepts proposals for collaborative research projects, and there is no cost to outside investigators.

For more information about NESAC/BIO or the Nanoscope II contact:

Dr. Buddy D. Ratner
Director
NESAC/BIO
BF-10
University of Washington
Seattle, Washington 98195
Telephone: (206) 685-1005
FAX: (206) 543-3778

Department of Defense Fact Sheet

Subjective Workload Assessment Technique

High technology systems can, at times, place an overwhelming demand on information processing, decision making, and other mental abilities of human operators. Mental workload is a concept that describes the degree to which an operator's non-physical capacities are taxed by a system while the person is attempting to maintain adequate performance.

Measures to quantify workload (both mental and physical) have been developed to provide operations analysts, system designers, and training designers with tools to ensure that missions and equipment are designed within the capabilities of operators.

The Subjective Workload Assessment Technique (SWAT) is a procedure for measuring mental workload which was developed at the Workload and Ergonomics Branch of the Air Force Harry G. Armstrong Aerospace Medical Research Laboratory. It is a workload measure with known metric properties and is useful in operational or "real-world" environments.

The workload model defined for SWAT includes three dimensions: time load, mental effort load, and psychological stress load.

Mental effort load refers to the amount of attentional capacity or effort required by the task, without regard to time. This includes functions such as retrieving information from memory, performing calculations, and making decisions.

Psychological stress load refers to anything that makes the task more difficult by producing anxiety, frustration, and/or confusion. This includes factors such as fatigue, vibration, g-loading, and heat. The effects of the stressors that are included occur prior to their direct interference with task performance.

SWAT has an easily administered subjective scaling method which can be used in cockpits and other operator stations. Relatively unintrusive data collection techniques were chosen for SWAT because of its intended use in the "real-world" environments.

Through conjoint scaling, responses made using simple descriptors for each of the three workload dimensions are converted into scale values for workload. The amount of time required to make responses is minimized because operators need only memorize a limited number of non-complex descriptors.

SWAT uses a two-step procedure to quantify the mental workload associated with various events. In the first step, the scale development phase, hypothetical activities are rank-ordered according to perceived workload. Each activity is specified in terms of a particular distribution of load across the three dimensions. These data are transformed, by means of conjoint measurement, into an interval scale of workload ranging from 1 to 100.

In the second step, the event scoring phase, an activity or event is rated by assigning a value of 1 to 3 on each of the three dimensions. The scale value associated with this combination (obtained from the scale development phase) is then assigned as the workload value for that activity.

SWAT is implemented on an IBM PC or compatible system with a minimum of 512K internal memory, and two floppy disk drives (or one fixed and one floppy drive). An 8087 math coprocessor will speed up the program, but is not necessary for execution. The program can analyze scale development data for up to 30 subjects.

SWAT exists in English, German, and French versions. Copies of the "User's Guide" and Scale Development software are available from CSERIAC for a cost-recovery fee.

FOR ADDITIONAL INFORMATION: A copy of the report is available from NTIS, Springfield, VA 22161; (703)487-4600. For further information, contact AAMRL/HE/CSERIAC, Wright Patterson AFB, OH 45433-6573.

NASA Tech Brief
National Aeronautics and Space Administration
NASA's Jet Propulsion Laboratory, Pasadena, California

Licensing Opportunity

Membrane Bioreactor With Pressure Cycle

Inhibitory reaction products and gradients of concentration are removed.

An improved class of multilayer membrane bioreactors uses convection forced by differences in pressure to overcome some of the diffusional limitations of prior bioreactors. The problem is to provide nutrients to the biocatalyst in a bioreactor and to remove the products (including both the product and the undesired gaseous or other byproducts), which can inhibit the activity of the biocatalyst and thereby slow or stop production. Prior bioreactors have relied largely on diffusion to effect these transfers of materials to and from the biocatalyst. In a reactor of the new class, a flow of nutrient solution reduces adverse gradients of concentration, keeps cells supplied with fresh nutrient, and sweeps away the products faster than diffusion alone can. As a result, the overall yield and rate of reaction are increased.

The principle of operation is illustrated with the simple bioreactor shown schematically in the figure. As in some prior bioreactors, the biocatalyst can be a layer of immobilized cells, (e.g., *Saccharomyces cerevisiae*, which takes up glucose and produces ethanol and carbon dioxide). The biocatalyst is held below a hydrophobic membrane and above a hydrophilic membrane. The nutrient liquid is supplied through the hydrophilic membrane from below. The desired product (e.g., ethanol) is dissolved in the nutrient liquid and transferred to a solvent or extractant liquid through a lower hydrophobic membrane at the bottom of the nutrient layer. The undesired gaseous byproduct (e.g., carbon dioxide) is removed by a sweeping gas (e.g., air) that flows in the space above the upper hydrophobic membrane.

The pressures in the sweeping gas and nutrient liquid are controlled cyclically to obtain the desired cyclical convection of nutrient liquid into and out of the biocatalyst layer. During one phase of the cycle, the pressure in the nutrient layer is made higher than the pressure in the sweeping gas, so that the nutrient liquid is forced through the hydrophilic membrane into the biocatalyst layer and the sweeping and byproduct gases are forced out of the cell layer through the upper hydrophobic membrane. The difference between the pressures is not, however, made so great as to force the nutrient liquid through the upper hydrophobic membrane into the sweeping-gas layer.

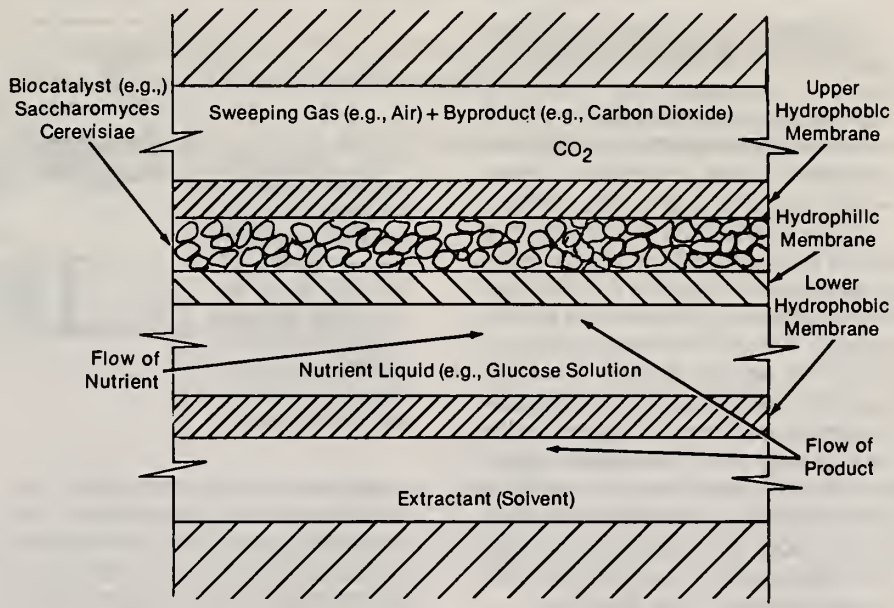

The **Pressures in the Sweeping Gas and Nutrient** are alternated to force nutrient liquid into and out of the biocatalyst layer through the hydrophilic membrane.

During the opposite phase of the cycle, the pressure in the sweeping-gas layer is made greater than the pressure in the nutrient layer, so that the nutrient, containing the desired product (e.g., ethanol), is forced out of the biocatalyst layer into the nutrient layer. Thus, the product dissolved in the nutrient is brought more rapidly into contact with the extractant in the lowest layer. The cycle is then repeated.

This work was done by George S. Efthymiou and Michael L. Shuler of Cornell Research Foundation, Inc., for **NASA's Jet Propulsion Laboratory.**

In accordance with Public Law 96-517, the contractor has elected to retain title to this invention. Inquiries concerning rights for its commercial use should be addressed to

H. Walter Haeussler, V.P.
Dir. Patents and Tech. Marketing
Cornell Research Found., Inc.
20 Thornwood Dr., Ste. 105
Ithaca, NY 14850
Refer to NPO-17974/TN.

Jet Propulsion Lab.
NASA Resident Office
Technology Utilization Officer: Gordon S. Chapman
Mail Stop 180-801
4800 Oak Grove Drive
Pasadena, CA 91109
(818) 354-4849
Patent Counsel: Paul F. McCaul
Mail Code 180-801
4800 Oak Grove Drive
Pasadena, CA 91109
(818) 354-2734
Technology Utilization Mgr. for JPL: Norman L. Chalfin
Mail Stop 156-211
4800 Oak Grove Drive
Pasadena, CA 91109
(818) 354-2240

FOR ADDITIONAL INFORMATION: *Contact: Director, Technology Transfer Division, P.O. Box 8757, BWI Airport, MD 21240; (301) 621-0100 Ext. 241*
REFER TO THE NUMBER LISTED AT THE END OF THIS ARTICLE

NASA Tech Brief
National Aeronautics and Space Administration
Marshall Space Flight Center, Alabama

Licensing Opportunity

Rotationally Actuated Prosthetic Hand

A simple mechanism is powered by rotation of the forearm.

A prosthetic hand includes two pincerlike fingers that are actuated by rotation of the forearm. In comparison with "bionic" devices and body-powered artificial limbs that include cable controls, the prosthetic hand is simpler in design, is simpler to operate, weighs less, and takes up less space.

The prosthetic hand (see figure) is attached to the affected arm of an amputee at two places: (1) a plastic cuff slips over the end of the remaining part of the forearm, and (2) a flexible band with hook-and-pile (Velcro™ or equivalent) straps is wrapped around the upper arm just above the elbow. A pair of braces jointed at the elbow restrain the main body of the hand against rotation about the axis of the forearm. However, the forearm is free to rotate about its own axis, and as it does so it rotates the cuff, which is mounted at one end of a shaft supported by roller bearings in the main body.

An oval cam is mounted at the other end of the shaft; it rotates with the cuff and shaft. Two fingers attached to the main body are pressed toward each other and onto the cam by a rubber band. The cam pushes the fingers apart by an amount that depends on its rotational position. When the forearm and cuff are rotated to a position at which the long dimension of the oval lies along the gap between the fingers, the fingers are spread apart to the maximum extent; when the forearm and cuff are rotated 90° from the foregoing position, the ends of the fingers are pressed together. Intermediate separations are obtained at intermediate rotational positions.

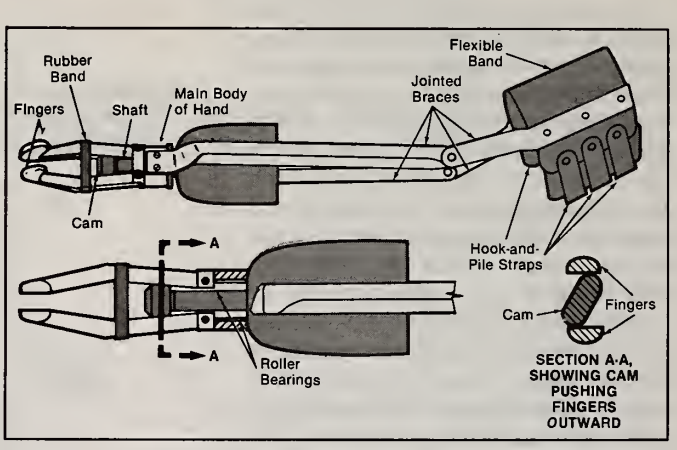

The **Prosthetic Hand** is attached to the end of the remaining part of the forearm and to the upper arm just above the elbow. The pincerlike fingers are pushed apart to a degree that depends on the rotation of the forearm.

This work was done by William E. Norton, Jewell G. Belcher, Jr., and James R. Carden of **Marshall Space Flight Center** *and Thomas W. Vest of Management Services, Inc.*

Inquiries concerning rights for the commercial use of this invention should be addressed to the Patent Counsel, Marshall Space Flight Center. Refer to MFS-28426/TN.

George C. Marshall Space Flight Center
Technology Utilization Officer: Ismail Akbay
Code AT01
Marshall Space Flight Center,
AL 35812
(205) 544-2223
Patent Counsel:
Leon D. Wofford, Jr.
Mail Code CC01
Marshall Space Flight Center,
AL 35812
(205) 544-0024

FOR ADDITIONAL INFORMATION: *Contact: Director, Technology Transfer Division, P.O. Box 8757, BWI Airport, MD 21240; (301) 621-0100 Ext. 241*
REFER TO THE NUMBER LISTED AT THE END OF THIS ARTICLE

Natural Resources Technology & Engineering

0434 Prosthetic Hand Lifts Heavy Loads—Features include ruggedness, simplicity, and relatively low cost. (Licensing Opportunity)

0435 Estimating the SNR of AVIRIS Data—Improved estimates of noise are better suited to the needs of investigators.

0436 Measuring Wildfires From Aircraft and Satellites—Remote sensing systems yield a wealth of data.

Software

0437 Microcomputer Weather Model

NASA Tech Brief
National Aeronautics and
Space Administration
Marshall Space Flight Center, Alabama

Licensing Opportunity

Prosthetic Hand Lifts Heavy Loads

Features include ruggedness, simplicity, and relatively low cost.

A prosthetic hand is designed to enable an amputee to lift diverse heavy objects like rocks and logs. The device is both simple and rugged. In addition, it costs less than do many other prosthetic hands, which are often awkward, bulky, heavy, and otherwise not well suited to strenuous lifting.

The new prosthetic hand (see figure) has no moving parts other than flexible straps that hold it in place. It includes a simple L-shaped metal end effector that is serrated to help prevent the lifted object from slipping off. The end effector is bolted into the end of a reinforced fiberglass cuff, which is fitted onto the remaining part of the forearm. A sock of cotton or similar material is placed over the remaining part of the forearm before inserting it in the cuff.

Hook-and-pile straps hold a flexible band on the upper arm. An inner strap and an outer strap extend downward from this flexible band to hold the cuff on the forearm. A loop strap, a front shoulder strap, and a back strap (hidden in the figure) keep the flexible band and, therefore, the prosthetic hand from being pulled off by heavy loads. The back strap and the front shoulder strap are anchored by a ring to a front strap, which anchors the system of straps under the shoulder opposite that of the amputated hand.

A steel strip on the side of the cuff that faces the body protects the cuff against damage by the lifted object. A rubber sheath could be placed over the cuff for additional protection.

This work was done by James R. Carden, William Norton, and Jewell G. Belcher of **Marshall Space Flight Center** *and Thomas W. Vest of Management Services, Inc.*

Inquiries concerning rights for the commercial use of this invention should be addressed to the Patent Counsel, Marshall Space Flight Center. Refer to MFS-28465/TN.

George C. Marshall Space Flight Center
Technology Utilization Officer: Ismail Akbay
Code AT01
Marshall Space Flight Center,
AL 35812
(205) 544-2223
Patent Counsel:
Leon D. Wofford, Jr.
Mail Code CC01
Marshall Space Flight Center,
AL 35812
(205) 544-0024

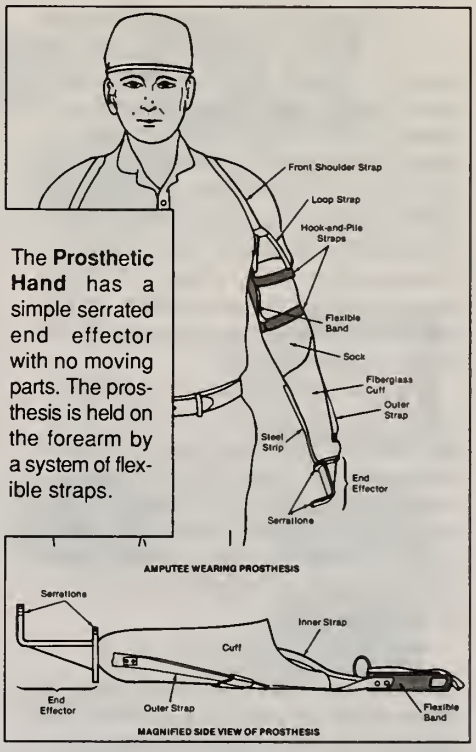

The **Prosthetic Hand** has a simple serrated end effector with no moving parts. The prosthesis is held on the forearm by a system of flexible straps.

FOR ADDITIONAL INFORMATION: *Contact: Director, Technology Transfer Division, P.O. Box 8757, BWI Airport, MD 21240; (301) 621-0100 Ext. 241*
REFER TO THE NUMBER LISTED AT THE END OF THIS ARTICLE

NASA Tech Brief
National Aeronautics and
Space Administration
Ames Research Center, Moffett Field, California

Estimating the SNR of AVIRIS Data

Improved estimates of noise are better suited to the needs of investigators.

A combination of established statistical and filtering techniques yields improved estimates of the signal-to-noise ratio (SNR) of multispectral imagery produced by the Airborne Visible/Infrared Imaging Spectrometer (AVIRIS). The three methods used heretofore to estimate the SNR have been inadequate: the "laboratory" method inflates the SNR, while the "dark-current" and "image" methods deflate the SNR. The new method yields a more accurate estimate of the random variability in AVIRIS imagery.

The new combination of techniques is called the "geostatistical" method. In the first step of this method, periodic noise is removed by notch filtering in the frequency domain. In the subsequent steps, sensor noise and variability within picture elements are isolated by use of the the semivariance of picture elements. This function is defined as follows:

$$\gamma(h) = (1/2)E[z(x_i) - z(x_i + h)]^2$$

where $\gamma(h)$ denotes the semivariance for all pairs of picture elements in which the members of each pair are a distance h (called the "lag") apart, x_i is the applicable coordinate of the ith picture element, E denotes the expectation operator, and z denotes the signal at a picture element. The function $\gamma(h)$ or the plot thereof is called the "semivariogram" (see figure).

An unbiased estimate of $\gamma(h)$ is obtained from a transect of m pairs of picture elements separated by the same lag distance, as follows:

$$\bar{S}^2 = (1/2m)\sum_{i=1}^{m} [z(x_i) - z(x_i + h)]^2$$

This is a useful measure of the difference between the signals at spatially separate picture elements. The larger $\bar{S}^2$ and, therefore, $\gamma(h)$ is, the less similar the picture elements are.

Three aspects of the semivariogram are of interest here: the sill, which is the asymptotic upper-bound value of $\gamma(h)$; the nugget variance (so named because it is reminiscent of a statistical measure used in prospecting for gold) C_o, which is the limit of $\gamma(h)$ when h approaches 0; and the spatially dependent structural variance, C, which is the sill minus the nugget variance. By definition $\gamma(h)$ equals zero when $h = 0$. In practice, the limit of $\gamma(h)$ when h approaches 0 has a positive value because the nugget variance represents variability at scales smaller than a picture element. This phenomenon is a characteristic of the "regularized" semivariogram calculated for plot rather than point data.

The key argument upon which the geostatistical method is based is that the nugget variance is a sound estimate of the spatially-independent noise variance relevant to the investigator. This argument is intuitively acceptable because at the limit of $\gamma(h)$, when h approaches 0, the nugget variance does not have a spatial component and is composed almost entirely of random sensor noise and variability within picture elements. The statistical justification for this argument requires consideration of a one-dimensional mathematical model in which x is a continuous parameter giving the location along a linear transect. The observed signal $z(x)$, comprises both radiance $r(x)$ (assumed to be stationary) and noise $n(x)$, which is assumed to be stationary, uncorrelated with $r(x)$, and not autocorrelated. It can be shown that the square root of the nugget variance can be used to estimate the standard deviation of the random noise and the variability within picture elements and, thereby, the SNR of AVIRIS data, via the equation

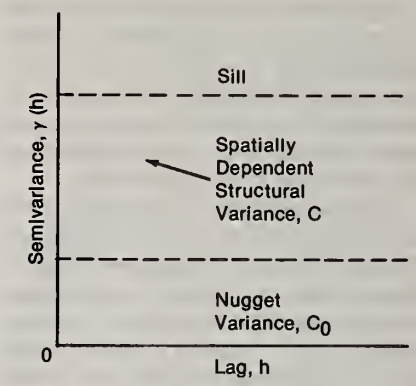

The **semivariogram** of an image gives a measure of the difference between the signals at spatially-separate picture elements.

$$\text{SNR} \simeq \bar{z}/\sqrt{C_o}$$

where $\bar{z}$ = the average of the z_i. Because $\bar{z}$ and $\sqrt{C_o}$ depend on wavelength, this calculation should be done for the data in each spectral band sensed by the AVIRIS.

This work was done by Paul J. Curran of **Ames Research Center** *and Jennifer L. Dungan of TGS Technology, Inc. Further information may be found in NASA TM-101035 [N89-15443], "Estimating the Signal-to-Noise Ratio of AVIRIS Data."*

Copies may be purchased [prepayment required] from the National Technical Information Service, Springfield, Virginia 22161, Telephone No. (703) 487-4650. Rush orders may be placed for an extra fee by calling (800) 336-4700.
ARC-12361/TN

FOR ADDITIONAL INFORMATION: *Contact: Director, Technology Transfer Division, P.O. Box 8757, BWI Airport, MD 21240; (301) 621-0100 Ext. 241*
REFER TO THE NUMBER LISTED AT THE END OF THIS ARTICLE

NASA Tech Brief
National Aeronautics and
Space Administration
Ames Research Center, Moffett Field, California

Measuring Wildfires From Aircraft and Satellites

Remote sensing systems yield a wealth of data.

Data about wildfires, collected remotely from satellites and aircraft, provides valuable information both for the management of wildfires and for research on the causes and effects of fires. Aircraft and satellite systems yield wide-area views, providing total coverage of the affected areas. Moreover, they collect data at a variety of wavelengths in the electromagnetic spectrum. The digital transmission of the data makes it easy to enhance images so that the combustion characteristics of biomass can be identified.

A system developed for use aboard the ER-2 aircraft (see figure) includes a digital scanner that records data in 12 channels at wavelengths from 0.42 to 12.5 μm. The data from the system have been used to correlate the characteristics of fires and fuels with reflected and emitted energies. In addition, the system transmits data to a ground station for immediate use in fighting fires.

The advanced very-high-resolution radiometer (AVHRR) on the TIROS polar-orbiting satellite provides images and radiance data at 1- and 4-km resolutions. It collects data in five channels at wavelengths from 0.58 to 12.5 μm. It gives synoptic views for regional and global monitoring of fires and for extension of the knowledge of biotic and abiotic responses of ecosystems to larger scales.

The ability to collect digitally encoded information from a multispectral scanner enables researchers to estimate gaseous and particulate emissions from the fires. The data provide information on the temperatures of flame fronts and soils, the intensities and rates of spread of fires, the characteristics of fuels and smoke plumes, energy-release rates, and concentrations and movements of trace gases. These data can be related to the heating and cooling of soils, the loss of nutrients, and the effects on atmospheric, terrestrial, and aquatic systems.

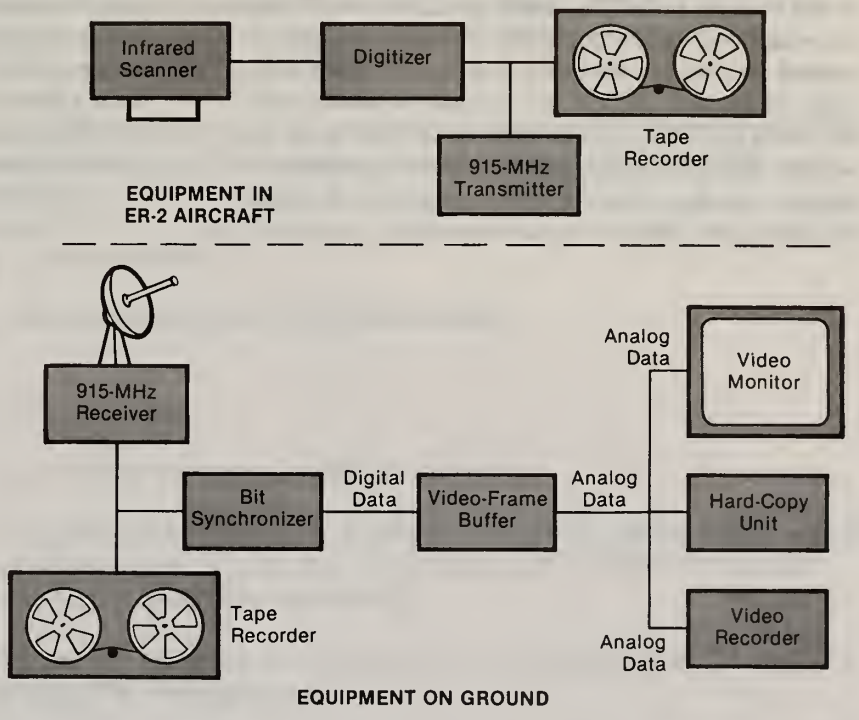

The **Airborne Imaging System** records data in 12 wavelength channels and sends digitized data in 2 of these channels to a station on the ground for immediate use in monitoring fires.

This work was done by J. A. Brass and J. C. Arvesen of **Ames Research Center**, *V. G. Ambrosia of TGS Technology, Inc., P. J. Riggan of the U.S. Department of Agriculture Forest Service, and J. S. Meyers of ATAC, Inc. Further information may be found in AIAA paper 87-A24933, "Aircraft and Satellite Thermographic Systems for Wildfire Mapping and Assessment."*

Copies may be purchased [prepayment required] from AIAA Technical Information Service Library, 555 West 57th Street, New York, New York 10019, Telephone No. (212) 247-6500.

ARC-12132/TN

FOR ADDITIONAL INFORMATION: *Contact: Director, Technology Transfer Division, P.O. Box 8757, BWI Airport, MD 21240; (301) 621-0100 Ext. 241*

REFER TO THE NUMBER LISTED AT THE END OF THIS ARTICLE

Microcomputer Weather Model

No, it's not the latest pop-rock radio station, but WGEN is still a big hit around the world. WGEN—for "Weather Generator"—is a computer model that considers past weather patterns in calculating what the future weather might be like at a specific site. It could be used by farmers, but WGEN is most often put to work developing the weather data that's an integral part of other computer models, including those for farm management decisions. WGEN's users already include universities, agricultural chemical companies and researchers from Europe, Africa, Australia and Central and South America. Historical weather information locally is plugged into the model. In return, it reports on likely daily rainfall, temperatures and solar radiation for any period in the future. A personal computer can pour out 50 year's worth of calculations in about 5 minutes.

Grassland, Soil and Water Research Lab, Temple, TX
C.W. Richardson, (817) 770-6500

Physical Sciences

0438 Recovery of Carboxylic Acids from Solvents (Licensing Opportunity)

0439 Adhesion Between Particles and Surfaces in a Vacuum—Factors that could affect contamination are studied.

0440 Monolithic Unidirectional Nonplanar Ring Laser—A design concept provides for narrow-linewidth operation in relatively inexpensive Nd:glass. (Licensing Opportunity)

0441 Real-Gas Properties of Air and Air-Plus-Hydrogen Mixtures—Properties related to chemical reactivity are calculated from first principles.

Testing & Instrumentation

0442 Wavefront Dividing Infrared Interferometer

Other Items of Interest

0415 Space-Grown Protein Crystals Examined

0419 Polyphenylquinoxalines via Aromatic Nucleophilic Displacement—A new reaction sequence costs less and provides for a variety of molecular structures. (Licensing Opportunity)

0422 Measuring Adhesion and Friction Forces—The Cavendish balance is adapted to a new purpose.

Department of Energy

Technology Application

Lawrence Berkeley Laboratory

Recovery of Carboxylic Acids from Solvents

A new technique for the recovery of carboxylic acids from solution in organic solvents has been invented by LBL scientists. The approach is easy to execute and consumes less energy than current recovery methods. It is particularly well suited for low- to moderate-solubility carboxylic acids, such as adipic, succinic and fumaric acids. The invention also enhances the recovery of carboxylic acids from aqueous solutions, such as fermentation broths. LBL's new technique offers a definite economic advantage over present recovery methods: it saves energy and reduces waste products.

A solvent extraction recovery process requires a means of regeneration in which the product, carboxylic acid, is isolated from the solvent-phase extract and the extractant (solvent) is made ready for recycle and reuse. Recovering carboxylic acids from organic extracts or other solvents has been a challenging task because most carboxylic acids have low-volatility and are therefore non-distillable. Yet solvent extraction offers an attractive method for recovering low-volatility acids like dicarboxylic acids and hydroxycarboxylic acids. In solving the problem of recovery and regeneration, LBL's invention exploits a remarkable property of carboxylic acids: in many solvents, carboxylic acids have solubilities that are substantially increased in the presence of co-extracted or co-dissolved water. For example, solubilities of dicarboxylic acids in cyclohexanone are increased by as much as a factor of eight when water is also present in the solution.

LBL's invention uses solvent extraction to remove carboxylic acid from aqueous solution. The addition of an organic solvent allows carboxylic acid and a small amount of water to co-extract from the aqueous phase into the solvent. Water, having a high volatility in organic media, is then easily stripped, distilled, or otherwise removed from the solvent extract. The removal of the co-extracted water lowers the solubility of the carboxylic acid, causing it to precipitate in product form. Once the water and precipitated carboxylic acid are removed, the remaining solvent is ready to recycle and recover more carboxylic acid from aqueous solution. LBL's invention is energy-efficient. It removes the small amount of co-extracted water without substantially evaporating the solvent phase.

Carboxylic acids have many commercial applications, such as raw material for manufacturing nylon and biodegradable plastics, builders in detergents, acidulents and buffers in food, and chemical intermediates for the pharmaceutical industry.

Technology highlights include the recovering of low-volatility and low- to moderate-solubility carboxylic acids, such as adipic and succinic acids; working simply, inexpensively, and with low energy consumption; the removal of co-extracted water by stripping; the lessening of the solubilities of carboxylic acids, allowing precipitation and recovery of most of the dissolved acid; being successful with commonly used solvents, such as ketones, esters, alcohols, and ethers; the recovering of carboxylic acids from fermemtation broths and other industrial streams; and effective removal and recovery of carboxylic acids from effluent streams.

Development Status: Transfer-ready, ready for pilot scale processing, patent pending.

FOR ADDITIONAL INFORMATION: The recovery technique is available for licensing from Lawrence Berkeley Laboratory. For further information contact: Mark Owens, Technology Transfer Office, Lawrence Berkeley Laboratory, 1 Cyclotron Road, Mail Stop 90-1076, Berkeley, CA 94720; (415)486-6463.

NASA Tech Brief
National Aeronautics and
Space Administration

Adhesion Between Particles and Surfaces in a Vacuum

Factors that could affect contamination are studied.

A report discusses an experimental study of the adhesion between several kinds of particles and solid surfaces. The purpose of this investigation was to extend the available data on the adhesion of contaminant particles; in particular, to contribute to an understanding of the ways in which acceleration can redistribute contaminant particles, thereby causing increases or decreases in contamination. The investigation was motivated by concern over the contamination of optical instruments resulting from the transfer of dust from nearby equipment during the launch of the Space Shuttle.

The adhesion between a surface and particles of a given type was measured via observation of the fraction of particles removed from the surface by acceleration in a centrifuge. The particle/surface combinations tested were glass beads on glass, road dust on glass, glass beads on aluminum, and road dust on aluminum. The particle/surface specimens were placed in the centrifuge tube, which was evacuated before it was spun. Tests were also done at ambient pressure; that is, without evacuating the centrifuge tube. The accelerations were calculated from the speed and dimensions of the centrifuge. For each type and size range of particles tested, the fraction removed by centrifugation as a function of size was matched via a least-squares best fit to a two-parameter log-normal probability distribution and to a related mathematical model of the acceleration (or, equivalently, the force of adhesion) as a function of size and density.

In comparing the results for glass beads on aluminum with those for glass beads on stainless steel in a previous study, the author drew the tentative conclusion that continuous acceleration could remove particles more effectively than brief impulses could. From the results of these experiments, the author concluded that glass beads did not adhere as well as dust did to either glass or aluminum, either at ambient pressure or in the vacuum. Dust appeared to adhere more strongly to glass than to aluminum, at both ambient pressure and in the vacuum. No statistical difference between the adhesions of glass beads or dust to either substrate at ambient pressure and in the vacuum was found. However, the dust adhered more weakly to glass at the intermediate pressure of 10 torr (1.3 kPa) than at the ambient pressures or in the high vacuum. This result was the only evidence for a dependence on pressure.

This work was done by Jack B. Barengoltz of Caltech for **NASA's Jet Propulsion Laboratory.** *"Particle Adhesion to Surfaces Under Vacuum."*
NPO-17743/TN

FOR ADDITIONAL INFORMATION: *Contact: Director, Technology Transfer Division, P.O. Box 8757, BWI Airport, MD 21240; (301) 621-0100 Ext. 241*
REFER TO THE NUMBER LISTED AT THE END OF THIS ARTICLE

NASA Tech Brief
National Aeronautics and Space Administration
Langley Research Center, Hampton, Virginia

Licensing Opportunity

Monolithic Unidirectional Nonplanar Ring Laser

A design concept provides for narrow-linewidth operation in relatively inexpensive Nd:glass.

In typical previous work with a monolithic nonplanar ring laser, four reflecting surfaces defined the ring light path. A new design has six reflecting surfaces. With this design, the differential loss that is required to achieve unidirectional oscillation can be 100 times as great as with four reflecting surfaces.

Unidirectional oscillation occurs in a ring laser if there is a sufficiently large differential loss between the polarization eigenmodes of the two directions of propagation around the ring. The most important criterion for producing large differential loss is that the sum of the relative phase shifts produced by the total internal reflections must slightly exceed 180°. In a conventional design with four reflecting surfaces, it is impossible to satisfy this criterion for a laser material that has an index of refraction smaller than $\sqrt{3}$ because the index of refraction determines the upper limit of the amount of relative phase shift produced by a single total internal reflection.

Since most laser glasses have indices of refraction substantially smaller than $\sqrt{3}$, the new six-reflector geometry was conceived to design monolithic glass resonators with large differential loss, overcoming the index-of-refraction limitations associated with the four-reflection resonator. The new design calls for a monolithic ring laser with five total internal reflections and one reflection from a partially transmitting multilayer dielectric-coated output coupler. Preliminary analysis of the six-reflection resonator shows that the differential loss can be at least 100 times as great as the largest differential loss available in a four-reflection design, assuming that the same magnetic field is applied to each resonator. This design should enable unidirectional operation.

Laser glasses differ from such cystalline host media as yttrium aluminum garnet (YAG) in several important ways. For example, the intrinsic scatter and absorption loss in well-engineered laser glass promise to be several orders of magnitude lower than those of Nd:YAG. The implication of this difference is that the fundamental limit on the width of the spectral line of a free-running Nd:glass laser can be many orders of magnitude smaller than that of a comparable Nd:YAG laser. Narrow-linewidth Nd:glass master oscillators based on this design could find immediate applications as the seed lasers for large Nd:glass laser systems. The very-narrow-linewidth lasers made possible with this concept have potential applications in metrology and spectroscopy.

This work was done by Alan C. Nilsson and Robert L. Byer of Stanford University for **Langley Research Center**. *No further documentation is available.*

In accordance with Public Law 96-517, the contractor has elected to retain title to this invention. Inquiries concerning rights for its commercial use should be addressed to

Mr. Jon Sandelin
Office of Technology Licensing
Stanford University
857 Serra Street, 2d Floor
Stanford, CA 94305-6225

Refer to LAR-14146/TN.

Langley Research Ctr.
Technology Utilization
Officer: John Samos
Mail Stop 139A
Hampton, VA 23665
(804) 864-2484
Patent Counsel:
George F. Helfrich
Mail Code 279
Hampton, VA 23665
(804) 864-3523

FOR ADDITIONAL INFORMATION: *Contact: Director, Technology Transfer Division, P.O. Box 8757, BWI Airport, MD 21240; (301) 621-0100 Ext. 241*
REFER TO THE NUMBER LISTED AT THE END OF THIS ARTICLE

NASA Tech Brief
National Aeronautics and
Space Administration

Real-Gas Properties of Air and Air-Plus-Hydrogen Mixtures

Properties related to chemical reactivity are calculated from first principles.

The report presents some calculated chemical, physical, and spectroscopic properties of nitrogen, oxygen, hydrogen, and compounds thereof. The data are needed particularly in numerical simulations of the heating, radiative properties, and chemical reactions of molecular species in the air flowing through jet engines and around spacecraft. These real-gas properties (as distinguished from the ideal-gas properties used in simplifying assumptions) are often difficult or impossible to measure and are best obtained via state-of-the-art quantum-chemical calculations on advanced computers.

The report includes three main sections and an appendix. Section I discusses the electronic-transition moments (proportional to the probabilities of radiative transitions) of 13 molecular species found in air. For each species, there is a brief narrative summary of the literature, the status of calculations to date, and the recommended values. The transition moments of some species are plotted as functions of bond lengths. An appendix discusses the relationships between transition moments and other quantities that appear in quantum-mechanical calculations of radiative intensities and lifetimes.

Section II discusses the constants of proportionality to the rates of selected chemical reactions among some of the species. Calculations of these constants are continuing, and values available thus far are presented. Each such calculation requires a three-step process: (1) The potential-energy surface that represents the energy of interaction between the species in question at any geometrical arrangement of the atoms must be calculated. This surface is related to a map of the forces between the species during a collision that leads to the reaction in question. (2) The data generated in step 1 must be fitted to an equation that can be used to calculate the interaction energy of the system for any geometrical arrangement of the atoms. (3) A large number of collisions between reactants is simultated by classical mechanics, using the equation derived in step 2. The results are averaged to obtain cross sections and rate constants.

Section III discusses the use of potential-energy curves and collision integrals to calculate the transport properties of hot air. Potential energies of O_2, N_2, NO, N_2^+, and O_2^+ are plotted as functions of intermolecular separations. Some viscosities, thermal conductivities, and diffusion coefficients are plotted as functions of temperature.

This work was done by David M. Cooper, Richard L. Jaffe, Stephen R. Langhoff, and Harry Partridge, III of **Ames Research Center.** *ARC-12275/TN*

FOR ADDITIONAL INFORMATION: *Contact: Director, Technology Transfer Division, P.O. Box 8757, BWI Airport, MD 21240; (301) 621-0100 Ext. 241*

REFER TO THE NUMBER LISTED AT THE END OF THIS ARTICLE

Brookhaven National Laboratory

Wavefront Dividing Infrared Interferometer

Researchers at Brookhaven National Laboratory have developed a novel instrument that opens up a new class of experiments with synchrotron radiation. Known as a wavefront dividing infrared interferometer, the instrument is installed at Brookhaven's National Synchrotron Light Source (NSLS), the world's largest synchrotron radiation center. An interferometer splits light from a source into two beams, one of which then passes through a sample. When the beams are recombined, an interference pattern results, thereby giving information about the sample.

At the NSLS, the BNL interferometer is coupled to the new infrared beam line, which is the brightest broadband Infrared source available today. As a point of reference, the infrared beam line produces radiation that is over 300 times hotter than the surface of the sun. This extreme intensity enables the interferometer to perform efficiently in the spectral region from the mid-infrared to millimeter wavelengths. In the past, this particular region has been difficult to work in because it is an area of low photon energy and, hence, weak signals. The BNL interferometer has a signal-to-noise ratio as much as 1,000 times better than that of conventional instruments. As such, it can measure highly absorbing samples such as high-temperature superconductors, newly discovered materials that have promising applications in such areas as electronics and transportation.

The interferometer can also detect small signals from dilute systems, such as molecules on metal surfaces, which makes possible catalysis and corrosion studies at the molecular level. Further, the spectral region covered by the instrument is of great interest to the chemical, oil, and gas industries, particularly for research on environmental control and monitoring.

When measuring a sample, the BNL interferometer covers in a single scan a wavelength region from 10 micrometers to 1 centimeter. Even though it functions over such a broad wavelength range, the instrument can operate with no change in components, a significant advantage over conventional instruments. In addition, it can completely characterize the optical activity of solids, liquids, and gases. A future refinement of the instrument will enable it to scan samples rapidly, thereby eliminating low-frequency noise.

The instrument was developed by Gwyn Williams, Peter Siddons, and Carol Hirschmugl, all of BNL, along with K. Dieter Möller, a collaborator from Fairleigh Dickinson University in New Jersey.

Literature: G. P. Williams, The Initial Scientific Program at the NSLS Infrared Beam Line, Nuclear Instruments and Methods, vol. A291, pp. 8-12, 1990.

Patent Status: No patent, none pending.

Applications/Spinoffs: The instrument will perform with any synchrotron or other diffraction limited source.

FOR ADDITIONAL INFORMATION: Contact William Marcuse, Technology Transfer Office, Bldg. 902C, Brookhaven National Laboratory, Upton, NY 11973; (516)282-2103 or FTS 666-2103. BNL/AA-53.

Transportation & Components

0443 Predictions of Drag in Viscous Transonic Flow—Results from the Viscous Transonic Airfoil Workshop are presented.

NASA Tech Brief
National Aeronautics and
Space Administration

Predictions of Drag in Viscous Transonic Flow

Results from the Viscous Transonic Airfoil Workshop are presented.

A NASA technical memorandum summarizes the results of computations of viscous, transonic flow reported at the Viscous Transonic Airfoil Workshop held in January, 1987. The results are reexamined and analyzed with special emphasis on drag. They are compared with each other and with data from experiments. Test cases include attached and separated transonic flows about a NACA 0012 airfoil. A total of 23 sets of numerical results from 15 different groups of authors are included.

The methods of computation used by the various authors vary from momentum-integral boundary-layer methods coupled with transonic potential inviscid codes to full Navier–Stokes methods. The majority of methods (a total of 16) utilize the Navier–Stokes equations. This suggests a strong trend toward the Navier–Stokes formulation, even though it can be computationally expensive. The remaining formulations are split between several categories: two are Euler/boundary-layer methods, and five are potential/boundary-layer methods. The boundary-layer methods are divided between the momentum-integral approach and the full boundary-layer-equation approach.

The computed and measured data are presented as graphs showing the coefficients of pressure as functions of position on the upper and lower surfaces of the airfoil, coefficients of lift as functions of the angle of attack and the coefficient of drag, coefficients of drag as functions of the free-stream mach number, the derivative of the coefficient of lift with respect to the angle of attack as a function of the free-stream mach number, and the effect of grid refinement on the computed coefficient of drag.

The author draws the following conclusions: Methods for the computation of viscous, transonic, attached flows about airfoils have reached a sophisticated level of development. Most methods are capable of producing valuable results in the design environment, including the prediction of lift to within ±3 percent and drag to within ±5 percent. Other computed flow field data, including velocity boundary-layer profiles and skin-friction distributions, are in good agreement with each other and with experiment. Levels of scatter in computed and experimental zero-lift drag-rise characteristics are comparable, provided that proper levels of refinement of the computational grid are used.

On the other hand, methods for the computation of separated viscous, transonic flows about airfoils are not as well developed as are those for attached flows. This is largely due to the lack of accurate mathematical modeling of turbulence in regions of separated flow. Inadequacies in turbulence models are the most important physical-model errors associated with the results contained in the report. Despite this major defect, recent progress in this area suggests hope for the future.

This work was done by Terry L. Holst of **Ames Research Center**. *Further information may be found in NASA TM-100095 [N88-22009], Price Code: A03 "Computational Fluid Dynamics Drag Prediction — Results from the Viscous Transonic Airfoil Workshop."*

Copies may be purchased from the National Technical Information Service, Springfield, Virginia 22161, Telephone No. (703) 487-4650. Rush orders may be placed for an extra fee by calling (800) 336-4700. *ARC-12252/TN*

FOR ADDITIONAL INFORMATION: *Contact: Director, Technology Transfer Division, P.O. Box 8757, BWI Airport, MD 21240; (301) 621-0100 Ext. 241*
REFER TO THE NUMBER LISTED AT THE END OF THIS ARTICLE

U.S. DEPARTMENT OF COMMERCE
National Technical Information Service
Springfield, VA 22161

NTIS ORDER FORM

Use this form ONLY to order reports designated as available from NTIS.

TELEPHONE ORDERS (703) 487-4650 FAX (703) 321-8547 TELEX 89-9405

For Subscription Questions
(703) 487-4630

For Tracing an Order
(703) 487-4660

For Editorial Questions
(703) 487-4805

Postage:
NTIS uses First Class Delivery, or equivalent service, on all shipping. For information about one day RUSH ordering, call (800) 553-6847 or (703) 487-4650.

NTIS PRICE SCHEDULE *

This schedule converts into actual prices the price codes cited in those Tech Notes having a report available from NTIS.

Price Code	*Price*
A01	$8.00
A02	11.00
A03	15.00
A04 through A05	17.00
A06 through A09	23.00
A10 through A13	31.00
A14 through A17	39.00
A18 through A21	45.00
A22 through A25	53.00
A99	Contact NTIS for price

These prices are for customers in United States, Canada, and Mexico. Other addresses should write for the price listing, number PR-360-4.

Prices effective January 1, 1991

† Purchase Order Service: There is a $7.50 charge for this service. It is restricted to customers in the United States, Canada, and Mexico. A late payment charge will be applied to all billings more than 30 days overdue.

If your address lable on this Tech Notes is NOT correct, call the NTIS Subscriptions Department on (703) 487-4630.

1 ADDRESS INFORMATION

Last Name .....

Title .....

Company/Organization .....

Address .....

.....

City/State/ZIP .....

Telephone Number .....

2 METHOD OF PAYMENT

☐ Charge my NTIS Deposit Account .... – .....

☐ Check/Money order enclosed payable to NTIS for $ .....

☐ Purchase order **ADD $7.50 per order** (see below for restrictions)†

Purchase order number .....

Charge my ☐ American Express ☐ VISA ☐ MasterCard

Account Number..... Exp. .....

Signature .....
(Required to validate order)

3 ORDER SELECTION (Use only for reports stated as available from NTIS)

NTIS Order Number	*Price**	*Quantity*	*Total Price*
..... /NAC	.....	.....	.....
..... /NAC	.....	.....	.....
..... /NAC	.....	.....	.....
..... /NAC	.....	.....	.....
..... /NAC	.....	.....	.....
		Handling fee	$3.00
		Total	.....

U.S. DEPARTMENT OF COMMERCE
National Technical Information Service
Springfield, VA 22161

NTIS ORDER FORM

Use this form ONLY to order reports designated as available from NTIS.

TELEPHONE ORDERS (703) 487-4650 FAX (703) 321-8547 TELEX 89-9405

If your address lable on this Tech Notes is NOT correct, call the NTIS Subscriptions Department on (703) 487-4630.

For Subscription Questions
(703) 487-4630

For Tracing an Order
(703) 487-4660

For Editorial Questions
(703) 487-4805

Postage:
NTIS uses First Class Delivery, or equivalent service, on all shipping. For information about one day RUSH ordering, call (800) 553-6847 or (703) 487-4650.

NTIS PRICE SCHEDULE *

This schedule converts into actual prices the price codes cited in those Tech Notes having a report available from NTIS.

Price Code	*Price*
A01	$8.00
A02	11.00
A03	15.00
A04 through A05	17.00
A06 through A09	23.00
A10 through A13	31.00
A14 through A17	39.00
A18 through A21	45.00
A22 through A25	53.00
A99	Contact NTIS for price

These prices are for customers in United States, Canada, and Mexico. Other addresses should write for the price listing, number PR-360-4.

Prices effective January 1, 1991

† Purchase Order Service: There is a $7.50 charge for this service. It is restricted to customers in the United States, Canada, and Mexico. A late payment charge will be applied to all billings more than 30 days overdue.

1 ADDRESS INFORMATION

Last Name .....

Title .....

Company/Organization .....

Address .....

.....

City/State/ZIP .....

Telephone Number .....

2 METHOD OF PAYMENT

☐ Charge my NTIS Deposit Account .... – .....

☐ Check/Money order enclosed payable to NTIS for $ .....

☐ Purchase order **ADD $7.50 per order** (see below for restrictions)†

Purchase order number .....

Charge my ☐ American Express ☐ VISA ☐ MasterCard

Account Number..... Exp. .....

Signature .....
(Required to validate order)

3 ORDER SELECTION (Use only for reports stated as available from NTIS)

NTIS Order Number	*Price**	*Quantity*	*Total Price*
..... /NAC	.....	.....	.....
..... /NAC	.....	.....	.....
..... /NAC	.....	.....	.....
..... /NAC	.....	.....	.....
..... /NAC	.....	.....	.....

Handling fee ... $3.00

Total .....

- Agriculture & Food
- Computers
- Electrotechnology
- Energy
- Engineering
- Environmental Science & Technology
- Manufacturing, Machinery, & Tools
- Materials
- Medicine & Biology
- Natural Resources Technology & Engineering
- Physical Sciences
- Transportation & Components

Route To:

PENN STATE UNIVERSITY LIBRARIES
A000072010327

EPARTMENT OF COMMERCE
al Technical Information Service
ld, Va. 22161

L BUSINESS
or Private Use, $300

AN EQUAL OPPORTUNITY EMPLOYER

BULK RATE
POSTAGE & FEES PAID
NTIS
Permit No. G-292